


AN ABSTRACT OF THE THESIS OF

Thomas Harding Massey for the M. S. in Chemistry  
(Name) (Degree) (Biochemistry)  
(Major)

Date thesis is presented August 27, 1966

Title A COMPARATIVE STUDY OF THE IN VITRO LOCALIZATION  
OF MERCURY FROM PHENYL MERCURIC ACETATE AND  
MERCURIC SALT IN RAT KIDNEY AND LIVER SUB-  
CELLULAR FRACTIONS AND THEIR EFFECT ON  
ALKALINE PHOSPHATASE

Abstract approved

  
(Major professor)

Studies were undertaken to determine the extent and rate of binding of Hg-203 labeled phenylmercuric acetate and mercuric acetate in rat kidney and liver slices and their subcellular fractions after 37°C incubation of the slices in Krebs-Ringer-phosphate solutions containing the mercurials at 10<sup>-4</sup> molar. A fast and parallel rate of uptake of both mercurials in kidney slices between 1 to 3 hour periods was observed. The uptake of the two mercurials into liver slices was much less than that found in kidney slices. The binding rate of phenylmercuric acetate was almost double the rate of inorganic mercury.

The subcellular fractions (nuclear, mitochondrial, microsomal, and soluble) of the tissue slices were prepared by homogenizing in

0.25 molar sucrose with subsequent differential centrifugation. Even though the two mercurials showed similar binding in kidney slices, it was found that phenylmercuric acetate was bound to almost twice the extent that of inorganic mercury in the mitochondria, microsomal, and soluble fractions, with the preponderate of the inorganic mercury being bound in the nuclear.

Phenylmercuric acetate was also bound to twice the extent of inorganic mercury in the mitochondrial, microsomal, and soluble fractions from incubated liver slices; however, the binding of the two mercurials in the liver nuclear fraction was similar during the first hours. Also, there was a decrease of the binding of inorganic mercury in the soluble fraction from incubated liver slices as the incubation time increased.

Sephadex G-100 elution patterns of the soluble protein fractions from incubated kidney and liver slices were determined. The mercury binding patterns in the elution fractions were also determined. There was found to be three main peaks in the elution pattern from liver and kidney soluble proteins. The first peak represents proteins with molecular weights of 100,000 or greater. The second peak consists of 15,000 to 30,000 molecular weight proteins followed by a trough or dip in the pattern representing large polypeptides (molecular weights of 2,000 to 3,000). The last peak consists of small polypeptides.

The specific binding of phenylmercuric acetate in the proteins of the elution pattern corresponding to a molecular weight of 100,000 or larger is greater than inorganic mercury by as much as two-fold. The 15,000 to 30,000 molecular weight proteins in the Sephadex G-100 elution patterns show 2.5 to five times as much specific binding of phenylmercuric acetate as compared to mercuric ion. There was no other area in the patterns in which the mercurials were bound to any significant extent.

The binding patterns of the two mercury compounds in the soluble proteins of incubated kidney slices filtered through Sephadex G-100 columns, were similar to those of the liver soluble proteins, except for a very high specific binding of both in the region of the elution pattern corresponding to large polypeptides (2,000 to 3,000 molecular weight).

Sephadex G-100 filtration of the incubation soluble proteins leached from liver slices indicated that phenylmercuric acetate caused a greater loss of large molecular weight proteins as compared to the control or inorganic mercury incubated slices.

The migration characteristics of soluble proteins from kidney slices with and without mercurial treatment were measured by disc electrophoresis on polyacrylamide gel columns. The results indicated that phenylmercuric acetate caused a possible loss of large molecular weight proteins from the soluble fraction as compared to

control or inorganic mercury incubated kidney slices.

There was found to be no correlation between the specific binding of the two mercurials with the enzymatic activity of alkaline phosphatase in the soluble and microsomal fractions. It was found that kidney slices incubated in solutions of inorganic mercury resulted in approximately 83 percent enhancement of alkaline phosphatase activity in the soluble fraction as compared to control. Phenylmercuric acetate caused about a 40 percent increase. The microsomal fractions from inorganic mercury treated kidney slices showed a greater decrease in the alkaline phosphatase activity than did phenylmercuric acetate as compared to that of control. Twenty to 30 percent of the alkaline phosphatase activity of the 35,000 X G soluble fraction was removed by ultracentrifugation at 150,000 X G. It is possible that the apparent activation of alkaline phosphatase in the soluble fraction was due to a solubilization of the enzyme, with its genesis possibly being in the microsomes.

Addition of phenylmercuric acetate to the reaction mixture at concentrations up to  $10^{-3}$  molar caused no significant decrease in the activity of alkaline phosphatase from kidney soluble proteins, while inorganic mercury showed 20 percent inhibition at  $10^{-5}$  molar and almost 75 percent inhibition at  $5 \times 10^{-5}$  molar. There was no significant stimulation of the enzyme when either of the mercurials was added to the reaction mixture.

A COMPARATIVE STUDY OF THE IN VITRO LOCALIZATION  
OF MERCURY FROM PHENYL MERCURIC ACETATE AND  
MERCURIC SALT IN RAT KIDNEY AND LIVER  
SUBCELLULAR FRACTIONS AND THEIR  
EFFECT ON ALKALINE PHOSPHATASE

by

THOMAS HARDING MASSEY

A THESIS

submitted to

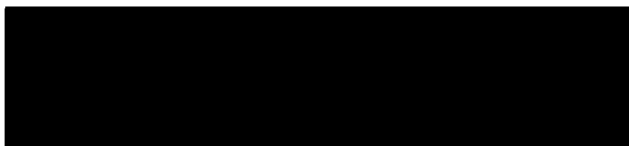
OREGON STATE UNIVERSITY

in partial fulfillment of  
the requirements for the  
degree of

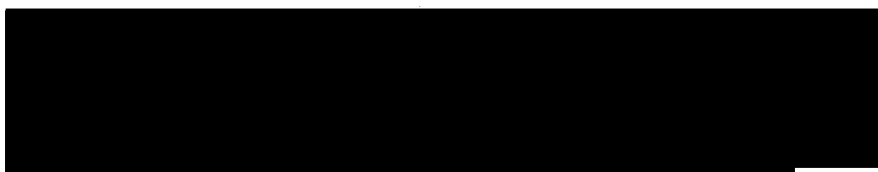
MASTER OF SCIENCE

June 1967

APPROVED:



Associate Professor of Agricultural Chemistry  
In Charge of Major



Head of Department of Chemistry



Dean of Graduate School

Date thesis is presented August 29, 1966

Typed by Kay Smith

## ACKNOWLEDGMENT

The author wishes to express his sincere appreciation to Dr. S. C. Fang for his patience and suggestions during the progress of this thesis. The research was made possible by funds from a Public Health Service grant, PHS EF00574-01-03. Acknowledgment is extended to Dr. R. O. Morris and R. L. Tucker for their kind help in the disc electrophoresis experiments. Thanks is extended to Dr. I. J. Tinsly, Dr. S. D. Lu, and Dr. J. W. Gillett for making available much needed equipment and instruments during many of the experiments.

The author acknowledges Dr. F. Staver for help in reviewing the thesis and Mrs. Kay Smith for the typing.

Last, but not least, the author wishes to express his most sincere appreciation and thanks to his wife, Mrs. Judy L. Massey, for her help in preparing the figures and especially for her patience and understanding during much of the course of this work.

## TABLE OF CONTENTS

	<u>Page</u>
INTRODUCTION	1
SURVEY OF THE LITERATURE	4
The Binding of Mercury to Sulfhydryl Groups	4
<u>In Vivo</u> Experiments: Absorption, Localization, Excretion	6
<u>In Vitro</u> Experiments: Effects on Membrane Function and Enzymes	13
Alkaline Phosphatase in Relation to Mercury Toxicity	18
MATERIALS AND METHODS	21
Preparation of the Liver and Kidney Slices	21
Preparation of the Subcellular Fractions	22
Determination of the Sephadex G-100 Elution Patterns of the Soluble Proteins	23
Determination of the Sephadex G-100 Elution Patterns of the Incubation Solutions from Liver Slices	26
Method for the Determination of Nitrogen in the Subcellular Fractions	27
Determination of Hg-203 Labeled Phenylmercuric Acetate and Mercuric Ion Bound to the Tissue Slices, Subcellular Fractions, and the Proteins in the Sephadex Elution Patterns	30
Method of Separation of the Soluble Proteins from Kidney Slices by Disc Polyacrylamide Gel Electrophoresis	38
Quantitative Determination of the Gel Electrophoresis Patterns of the Kidney Soluble Proteins	43
Method for the Determination of the Alkaline Phosphatase Content of the Microsomal and Soluble Fractions	46
RESULTS	48
The Uptake of Phenylmercuric Acetate and Mercuric Acetate by Rat Kidney and Liver Slices	48
The Incorporation of Phenylmercuric Acetate and Mercuric Acetate into the Subcellular Fractions of Rat Kidney and Liver Slices	51



	<u>Page</u>
The Nitrogen Content of the Subcellular Fractions in Control and Mercury Treated Kidney and Liver Slices	58
Sephadex G-100 Elution Patterns and the Mercury Binding of the Soluble Proteins from Liver and Kidney Slices	62
Sephadex G-100 Elution Patterns and the Mercury Binding of the Incubation Solution Proteins Leached from Liver Slices	72
Poluacrylamide Gel Electrophoresis Patterns of the Soluble Proteins from Control and Mercury Incubated Kidney Slices	75
The Effect of Incubation of Kidney Slices in Phenyl- mercuric Acetate and Mercuric Acetate on the Alkaline Phosphatase Activity in the Microsomal and Soluble Fractions	80
SUMMARY AND CONCLUSIONS	87
BIBLIOGRAPHY	95

## LIST OF TABLES

<u>Table</u>		<u>Page</u>
1	Reaction mixture for alkaline phosphatase assay.	47
2	Major peak intensities, relative to peak no. 2, of the disc polyacrylamide gel electrophoresis patterns for control and mercury treated kidney soluble proteins.	77
3	Alkaline phosphatase activity of soluble and microsomal fractions from control and mercury treated kidney slices.	81

## LIST OF FIGURES

<u>Figure</u>		<u>Page</u>
1	Activity of a radioactive Hg-203 solution, counted in a well-type solid scintillation gamma detector.	33
2	Correction curve for the sample volume of $^{203}\text{Hg}$ gamma activity counted on a well-type solid scintillation gamma detector.	33
3	Beta activity from Hg-203 labeled mercuric ion bound to precipitated and filtered protein. Activity counted by liquid scintillation.	35
4	Correction curve for self-absorption of $^{203}\text{Hg}$ beta activity bound to precipitated and filtered protein. Activity counted by liquid scintillation.	35
5	Uptake of mercury by rat kidney slices.	49
6	Uptake of mercury by rat liver slices.	50
7	Uptake of PMA in subcellular fractions of rat kidney on the basis of wet weight of tissue.	52
8	Uptake of inorganic mercury in subcellular fractions of rat kidney on the basis of wet weight of tissue.	52
9	Uptake of PMA in subcellular fractions of rat liver on the basis of wet weight of tissue.	53
10	Uptake of inorganic mercury in subcellular fractions of rat liver on the basis of wet weight of tissue.	53
11	Subcellular binding of PMA in rat kidney slices as percent of total uptake.	54
12	Subcellular binding of inorganic mercury in rat kidney slices as percent of total uptake.	54

<u>Figure</u>		<u>Page</u>
13	Subcellular binding of PMA in rat liver slices as percent of total uptake.	55
14	Subcellular binding of inorganic mercury in rat liver slices as percent of total uptake.	55
15	Subcellular binding of PMA in rat kidney slices on the basis of nitrogen weight.	56
16	Subcellular binding of inorganic mercury in rat kidney slices on the basis of nitrogen weight.	56
17	Subcellular binding of PMA in rat liver slices on the basis of nitrogen weight.	57
18	Subcellular binding of inorganic mercury in rat liver slices on the basis of nitrogen weight.	57
19	The nitrogen content in the subcellular fractions of control liver slices.	59
20	The nitrogen content in the subcellular fractions of control kidney slices.	59
21	The nitrogen content in the subcellular fractions of PMA treated liver slices.	60
22	The nitrogen content in the subcellular fractions of PMA treated kidney slices.	60
23	The nitrogen content in the subcellular fractions of inorganic mercury treated liver slices.	61
24	The nitrogen content in the subcellular fractions of inorganic mercury treated kidney slices.	61
25	Sephadex G-100 O. D. elution pattern of control rat liver soluble proteins.	64
26	Sephadex G-100 O. D. elution pattern of PMA bound rat liver soluble proteins.	64

<u>Figure</u>		<u>Page</u>
27	Sephadex G-100 O. D. elution pattern of inorganic mercury bound rat liver soluble proteins.	65
28	The O. D. specific binding of PMA and inorganic mercury in rat liver soluble proteins.	65
29	Sephadex G-100 precipitable protein elution pattern of control rat liver soluble proteins.	66
30	Sephadex G-100 precipitable protein elution pattern of PMA bound rat liver soluble proteins.	67
31	Sephadex G-100 precipitable protein elution pattern of inorganic mercury bound rat liver soluble proteins.	68
32	The precipitable protein specific binding of PMA and inorganic mercury in rat liver soluble proteins.	68
33	Sephadex G-100 O. D. elution pattern of control rat kidney soluble proteins.	70
34	Sephadex G-100 O. D. elution pattern of PMA bound rat kidney soluble proteins.	70
35	Sephadex G-100 O. D. elution pattern of inorganic mercury bound rat kidney soluble proteins.	71
36	The O. D. specific binding of PMA and inorganic mercury in rat kidney soluble proteins.	71
37	Sephadex G-100 O. D. elution pattern of control proteins leached from rat liver slices.	73
38	Sephadex G-100 O. D. elution pattern of PMA bound proteins leached from rat liver slices.	73
39	Sephadex G-100 O. D. elution pattern of inorganic mercury bound proteins leached from rat liver slices.	74
40	The O. D. specific binding of PMA and inorganic mercury in proteins leached from rat liver slices.	74

<u>Figure</u>		<u>Page</u>
41	Disc polyacrylamide gel electrophoresis pattern of soluble proteins from control treated kidney slices.	78
42	Disc electrophoresis patterns of soluble proteins from mercury treated kidney slices.	79
43	Disc electrophoresis patterns of soluble proteins from mercury treated kidney slices.	79
44	The effect of pH on the activity of alkaline phosphatase from rat liver soluble proteins.	83
45	The effect of PMA and inorganic mercury at various concentrations in the reaction mixture on the activity of alkaline phosphatase in the soluble proteins of rat kidney.	83
46	Sephadex G-100 O. D. elution pattern and the distribution of alkaline phosphatase activity after Sephadex G-100 filtration of soluble proteins from control kidney slices.	85

A COMPARATIVE STUDY OF THE IN VITRO LOCALIZATION  
OF MERCURY FROM PHENYL MERCURIC ACETATE AND  
MERCURIC SALT IN RAT KIDNEY AND LIVER  
SUBCELLULAR FRACTIONS AND THEIR  
EFFECT ON ALKALINE PHOSPHATASE

INTRODUCTION

The toxicity of mercurial compounds has been known for many centuries. It was found that elemental mercury vapors as well as mercuric salts were poisonous and that their symptoms, in many cases, differed. Battigelli (2) points out that the rate of absorption determines not only the length of time of intoxication, but also the organs which are most affected. For example, acute intoxication usually results in damage to the kidneys and the gastrointestinal tract if the dose is taken orally. Pulmonary changes will occur if the air contains a high concentration of mercury. Chronic mercurialism is usually associated with changes in the nervous system.

The increasing use of organic mercurials as fungicides in agriculture for the treatment of fruit trees and vegetable crops has brought to the attention of the tolerance hearings under the Federal Food, Drug, and Cosmetic Act the need to know more about their toxicity levels. It had been generally assumed that the organic mercurials are less toxic than mercuric salts when taken orally (8). However, there has been mounting evidence that the organic mercurials are just as toxic as inorganic mercury and some sources assert

them to be much more toxic.

Battigelli (2) lists the important factors that determine the degree of intoxication produced by mercury and its derivatives:

1. Rate and amount absorbed
2. Individual susceptibility
3. Physicochemical properties of the absorbed compounds.

Each of these factors will have an effect on the intoxication mechanism, and the result will be modified by the other factors acting simultaneously. These factors will operate throughout the complete spectrum of study of the intoxication mechanism in biological systems ranging from oral dosages of the toxic substances in a live animal to the determination of the sulfhydryl character of a pure enzyme.

The literature on the investigation of mercurial intoxication in animals does, indeed, range throughout the entire spectrum of methodology. There has been extensive work on the localization of mercury compounds in the different organs of animals. Much was done in conjunction with rates of absorption, binding, and excretion. The effects of mercurials on enzymes have received much attention, ranging from respiration of live animals to activities of highly purified enzyme systems.

There has been, however, very little attempt to localize mercury compounds in the subcellular components of different organs



and especially little attention given to the correlation of enzymatic activities in these components to the concentration of mercury. Because of the interest in comparing the toxicity of mercuric salts to that of phenyl mercuric acetate used in agriculture, it was decided to investigate the localization of the two mercurials in the subcellular components of these two organs of the rat that show the highest concentration of mercury after oral feeding or intravenous injection-- the liver and kidney. It was also decided to attempt to correlate the mercury binding with some effects on enzymes and membrane permeability.

It was important in this study that the exposure of the organs to the mercury compounds be of the same concentration, the same form (i. e. , unbound to any other molecule), and the same time duration. In vivo experiments in which the mercury would be absorbed from the gastrointestinal tract, carried in the blood stream (bound to any of a large number of different components of the blood), and deposited in the organs of the body in possibly different concentrations would not satisfy the above requirements.

It was decided that in vitro incubation of liver and kidney slices in solutions containing the concentration of salts found in extracellular fluids plus known concentrations of mercuric acetate and phenylmercuric acetate would provide adequate control over concentration, form, and duration of exposure.

## SURVEY OF THE LITERATURE

The Binding of Mercury to Sulfhydryl Groups

The toxicity of mercury is based on the high affinity of mercury for sulfhydryl groups. Hughes (18) develops the concept that the principle reaction of mercury is with thiol groups. A very important point is that all but traces of the mercurial will be bound to thiols, assuming there is an excess of thiol groups in the biological system. Mercury also has some affinity for other organic ligands such as amines, carbonyls, and hydroxyls, although this is less than for sulfhydryl groups.

Shaw has correlated the inhibition of urease by various metal ions with the insolubility of the metal sulfides. The metals with the most insoluble sulfides are the strongest inhibitors (39). He has also shown a correlation with the magnitude of the sum of the first and second ionization potentials and the chelation stability of the metal ions. He concludes that inhibition may occur through chelation of electron donor groups on the enzyme, as well as binding of the sulfhydryl groups. However, the chelation with electron donor groups is relatively small as compared to mercaptide formation, and these groups can only direct mercury compounds toward a certain mercaptide and not away from it.

The effects of mercurials on living processes, by the binding

of mercury to sulfhydryl groups, is easily demonstrated in bacterial cultures and purified enzyme systems. Pershin and Shcherbakova (34), working with Escherichia coli, decided that the bacteriostatic action of mercuric chloride was due to its interference of biochemical reactions favored by sulfhydryl groups.

Shaechter and Santomassino (38) have shown the effect of p-chloromercuribenzoate (p-CMB) on the stability of cell envelopes of E. coli. Treatments of growing cultures of E. coli with p-CMB, at concentrations ranging from  $10^{-3}$  to  $5 \times 10^{-6}$  molar, all caused lysis in hypotonic solutions. Non-growing cell cultures were not affected by the mercurial. The loss in cell integrity and viability can be partially reversed by an excess of cystine, if treated early in the experiments. It is hypothesized that disulfide bonds play an important role in maintaining the bacterial-cell structural integrity and that p-CMB inhibits the formation of the disulfide bridges.

The effects of mercurials can also be demonstrated on purified enzymes. When an organic mercurial contains a charged group, the binding capacity for some thiols is modified or reduced. Nygaard (33) titrated lactic dehydrogenase from ox heart amperometrically with mercuric chloride and spectrophotometrically with p-chloromercuribenzoate and found that the lactic dehydrogenase activity was inhibited slowly with the p-CMB and rapidly with silver and mercuric ions. After incubation of lactic dehydrogenase with acetic

anhydride, which blocked  $\text{NH}_2$  groups on the protein, there was an increased reactivity of the sulfhydryl groups to p-CMB which caused strong inhibition. A similar reaction was found for acetylated liver alcohol dehydrogenase.

Frisell and Hellerman (14), working with d-amino acid oxidase, found that phenylmercuric acetate (PMA) inhibits irreversibly after treatment with a twenty-fold molar excess of reduced glutathione. The phenylmercuric ion lacks the benzoate configuration and its primary interaction with d-amino acid oxidase should involve, uniquely, the protein sulfhydryl groups.

The text of this report is to discuss the effects of mercurials on mammalian systems with reference to their interference with cellular processes assumed to be correlated with sulfhydryl groups.

#### In Vivo Experiments: Absorption, Localization, Excretion

Elemental mercury is usually taken into the body as vapor (2, 18), with resulting absorption into the blood, and being dissolved in blood lipids, is transported to the body tissues. Metallic mercury, because of its lipid solubility, is easily distributed to all parts of the body and is subsequently oxidized to the reactive mercuric salts. Because elemental mercury is quickly oxidized in water (42), the formation of ionized salts impairs the egress of mercury back across cell membranes through which it had formally entered

as the lipid soluble elemental mercury. Battigelli (2) says that the well-tolerated dose of elemental mercury can be directly inferred from the air concentration of 0.1 milligram of mercury per cubic meter. Assuming that 25 percent of the elemental mercury or mercury compounds in inhaled air is absorbed through the lungs and that intake and excretion of mercury are at equilibrium, a daily dose of 2 to 4 micrograms per kilogram resulting from this exposure is well tolerated. High acute doses of mercury resulting from absorption in the lungs caused lung irritation and possible nephro-gastrointestinal effects. Chronic mercurialism is characterized mainly by neurological involvement, regardless of the method of intoxication of the mercury or of the mercury compound present.

The mercurous salts are generally considered to be much less toxic than other mercury compounds. In studying the acute, dermal, subacute, and chronic toxicity, Lehman (24) has shown that, while mercuric chloride, ethylmercuric phosphate, and phenylmercuric triethanolammonium lactate all resulted in LD<sub>50</sub> values of 30 to 37 milligrams of mercury per kilogram, calamel required 210 milligrams mercury per kilogram for an LD<sub>50</sub> dose.

Swensson, Lundgren, and Lindström (45) found, after injection of 100 micrograms per kilogram of mercury (mercuric nitrate, phenylmercuric acetate, and methylmercuric hydroxide) in the femoral vein of white rats, that the mercuric salts were transported

mainly in the plasma. The two organic compounds were to a large extent bound to the erythrocytes. The mercuric nitrate and phenylmercuric acetate were deposited chiefly in the kidneys, whereas the methylmercuric hydroxide appeared to be distributed more uniformly throughout the body. The supply of mercuric nitrate gave a high content of mercury in the colon wall. A later paper by Lundgren and Swensson (25) reported similar results. They determined that the toxicities of the organic mercury compounds were roughly the same.

Berlin and Gibson (4) found that 50 percent of the mercuric salts infused into the jugular vein of rabbits at a rate of 0.2 milligrams of mercury per hour were bound to the erythrocytes and that the turnover rate between the plasma and blood cells was quite low. The urinary excretion of mercury was found to correlate with the concentration in the blood. However, there was no correlation between the amount of mercury accumulated in the kidney and in the urinary excretion. Berlin (3), in a later paper, reports that methyl- and phenylmercuric salts infused into the jugular vein of rabbits at a rate of 0.2 milligrams of mercury per hour showed considerably less accumulation of mercury in the kidneys after the first hour, with a much lower rate of excretion as compared to mercuric salts.

The renal extraction of all three of the mercury compounds

(mercuric chloride, methylmercuric dicyandiamide, and phenylmercuric acetate) as reported by Berlin (3) and Berlin and Gibson (4) did not exceed 10 percent of the amount of mercury in the blood passing through the kidneys. About 50 percent of the total dose of infused mercuric nitrate (0.1 to 1.0 milligrams), over a four-hour period, accumulated in the kidney. This compares with about 30 percent for phenylmercuric acetate (total dose ranged from 0.1 to 8.0 milligrams of mercury) and about 10 percent for the methylmercuric dicyandiamide (total dose was about 4 milligrams of mercury). The PMA (phenylmercuric acetate) excreted in the urine was a small percentage of the infused mercury, whereas the methylmercuric dicyandiamide excretion did not exceed a few parts per thousand of the infused dose, after a four-hour period. These findings can be compared to mercuric nitrate in which less than 10 percent of the mercury was excreted in the first four-hour period. Berlin concludes that urinary excretion of PMA as inorganic mercury indicates a decomposition of PMA in the body.

Prickett, Laug, and Kunze (36) found that adult rats (250 to 300 milligrams) injected intravenously with 120 micrograms of mercuric acetate and phenylmercuric acetate showed four times as much inorganic mercury in the kidney as compared to PMA. After a similar dose of the mercury compounds given orally, it was found that PMA was absorbed much more readily from the

gastrointestinal tract than was the mercuric salt and that there was five to six times as much PMA excreted in the urine. After intravenous injections, it was found that PMA was excreted mainly through the intestinal tract via the bile, and the mercuric acetate was excreted mainly from the kidney. The excretion of mercuric ion in the urine was 17 percent of the dose in 48 hours as compared to 3 percent after intravenous injections of PMA.

Miller, Klavano, and Csonka (30) state that phenylmercuric acetate is decomposed in both the kidney and liver. After administering PMA at the rate of 3 milligrams of mercury per kilogram of body weight, orally, intravenously, or intramuscularly, slightly over half the urinary mercury was in a form other than PMA. Less than 10 percent of the initial dose of PMA was excreted unchanged in the urine of rats in the first 48 hours. The decomposition in the body was fairly rapid, with detectable amounts of PMA occurring only for approximately 96 hours.

Suzuki, Miyama, and Katsunuma (44) compared the localization and excretion of several mercury compounds (ethylmercury chloride, methylmercury chloride, merthiolate, phenylmercuric acetate, and mercuric nitrate). After a subcutaneous injection of subtoxic doses into rats, mercuric nitrate had the longest continuance of excretion. The excretion of phenylmercuric acetate was intermediate in rats, while the alkyl mercury compounds were



excreted faster. The mercury in the kidney was much higher than in the liver after administration of PMA and mercuric nitrate. The alkylmercuric compounds showed a level of mercury in the kidney about equal to or slightly smaller than that in the liver. The muscles and the blood were the main depot of mercury 24 hours after the injection of the alkyl mercury compounds. The mercury content of the brain after alkyl mercury treatment was greater than that from PMA or mercuric nitrate treatment.

Surtshin and Yagi (43) found that there was an increase in resistance to the toxicity of mercuric chloride in rats fed on high sucrose diets. Most rats fed on a diet of sucrose and vitamins for three or more weeks survive intravenous injections of mercuric chloride up to doses of 3 milligrams per kilogram, a dose usually lethal to rats with normal diets. It was found that the sulfhydryl content of the soluble proteins of the kidney is higher in rats fed on sucrose diets. Kidney analyses were done three hours after injection of Hg-203 labeled mercuric chloride into the femoral vein of rats on diets of sucrose and rats with diets of Purina chow. It was found that the total mercury content in the kidney was the same. However, there was a much higher content of mercury in the soluble fraction and a much lower content of mercury in the nuclear and granular fractions with rats fed with sucrose as compared to rats fed on normal chow diets. Surtshin and Yagi believe that the

decreased mercury binding in the nuclear and granular fractions, after sucrose diets, is the cause of increased resistance to mercuric chloride.

Martin and Reid (27) found that hypoproteinemia in dogs caused an increased resistance to mercuric chloride poisoning. A dose of 3 milligrams of mercuric chloride per kilogram given intravenously was lethal to dogs on normal diets. The normal dogs did not excrete as much as half of the mercuric chloride load and all died 2.5 to 4.5 days after administration of the mercury. The hypoproteinemic dogs showed essentially no toxic symptoms. Some symptoms were observed only after the third or fourth doses of mercury. In each case, each dog excreted more than half the mercuric ion within three days. Martin and Reid suggest that the increase in resistance to mercuric ion poisoning is due to an increased extracellular volume which would dilute the mercury and, also, that a relatively small binding of mercuric ion by protein permits more rapid excretion and diminished cell susceptibility.

Tadatomo (46) injected Hg-203 labeled mercuric nitrate intramuscularly in sub-lethal doses into guinea pigs and determined the activity after 24 and 48 hours in subcellular components of various organs. The kidney and liver homogenates were differentially centrifuged and the amount of mercury in the various fractions was determined. The binding is shown in decreasing order of amounts found

in the fractions:

<u>Kidney</u>	<u>Liver</u>
Soluble proteins	Soluble proteins
Microsomes	Nucleus
Mitochondria	Microsomes
Nucleus	Mitochondria

In Vitro Experiments: Effects on Membrane Function and Enzymes

Kleinzeller and Cort (22) found that rabbit kidney cortex slices, when incubated at 0°C in  $1.45 \times 10^{-3}$  molar Esidron,  $4-5 \times 10^{-4}$  mercuric chloride, and  $10^{-4}$  molar p-chloromercuribenzoate, with 0.154 molar sodium chloride, brought about a greater loss of protein nitrogen into the medium than did controls without mercury treatment. They also found an increase of sodium and a loss of potassium from the kidney slices. Similar results were obtained with brain cortex and myocardium. Striated muscle and liver slices did not give the effect when incubated in the mercurial solutions. Kleinzeller and Cort suggested that mercurials change the permeability of the basal membrane of renal tubular cells, thus increasing the passive movement of sodium, chloride, and water back into the cells.

Hunter (19) found that increasing concentrations of mercury ( $6.25 \times 10^{-7}$  to  $2.5 \times 10^{-6}$  molar) progressively decreased the rate at which glucose moves across the membranes of human erythrocytes. The effect of mercury can be completely or partially reversed by

cysteine, depending on the concentration of cysteine used. Piedrafeta, Trull, and Alemany (35) have also found that concentrations of  $2 \times 10^{-4}$  to  $10^{-4}$  molar mercuric ion inhibits intestinal absorption of sugars. The effect was thought to be intracellular.

Maizels and Remington (26), working with several types of mercurial diuretics, found that incubation of rat kidney cortex slices at  $10^{-3}$  molar caused an increase in the sodium content of the slices as compared to the controls. They also found that the swelling of the cortex slices (uptake of water) was largely determined by the increase in the cell sodium. Their findings are consistent with the view that the mercurial diuretics act mainly on active transport with slight increases of the membrane permeability to sodium.

Demis and Rothstein (10) incubated rat diaphragm in various concentrations of mercuric chloride with Krebs-Ringer-phosphate solutions and determined the effect on glucose absorption and respiration. At concentrations of mercuric ion of  $2 \times 10^{-4}$  to  $5 \times 10^{-5}$  molar the absorption of glucose was almost completely blocked. The inhibition of respiration by mercuric chloride solutions required much higher concentrations and prolonged time periods.  $2 \times 10^{-4}$  molar mercuric salt had no effect on oxygen consumption for over 30 minutes, but eventually, after 2 hours, there was 30 percent inhibition. With concentrations of mercury approaching  $2 \times 10^{-3}$

molar, 90 percent inhibition was observed after 1.5 hours. The inhibition of glucose uptake develops very rapidly, whereas respiration inhibition requires a lag time.

Reversal of the inhibition of glucose uptake was achieved by adding cysteine into the incubation medium at a concentration of  $2 \times 10^{-3}$  molar when the mercury concentration was  $2 \times 10^{-4}$ . Within 30 minutes the rates of glucose uptake returned almost to normal. Reversal of inhibition of respiration was not found to a measurable extent. Diaphragms incubated in  $10^{-3}$  molar mercury developed an inhibition of respiration of 60 percent within one hour. The addition of  $4 \times 10^{-3}$  molar cysteine gave no reversal within the next half hour. The results were compatible with the hypothesis that certain reactions necessary for glucose uptake are located in the periphery of the cell or on the cell surface, whereas enzymes for respiration are located within the interior of the cell.

Hirade (17), using rat kidney homogenates, found that both respiration and esterification of phosphate were inhibited by mercuric ion concentrations of  $2-5 \times 10^{-5}$  and PMA concentrations of  $2 \times 10^{-4}$  molar. Glutathione (reduced) restored oxygen uptake, especially in the case of mercuric inhibition. Inorganic phosphate esterification was restored only slightly.

The effects of mercury compounds on the kidney have been categorized by Dzurik and Krajci-Lazary (11) into two types.

The cytoplasmic effect is that in which mercury reduces the activity of the tricarboxylic acid cycle. The effect is possessed by mercury compounds lacking a diuretic effect and mercurial diuretics in toxic doses. It is assumed that this effect is responsible for the toxicity of mercury. The membrane effect is that in which compounds of mercury having a diuretic action, act by increasing the membrane permeability of the proximal tubule cells. Both PMA and mercuric ion possess diuretic potency, but they are more toxic than the mercurial diuretics. The general action of mercurial diuretics is to increase the sodium concentration and urine volume (13).

Mudge (32) found that the diuretic effect occurs at concentrations of mercury significantly lower than concentrations required to depress oxygen consumption. Cohen (7) found that intravenous injection of mersalyl at a rate of 8.1 micromoles per 100 grams of body weight of rats caused death, and that the oxygen consumption of the kidney slices were less than for the controls. With diuretic doses (2.1 micromoles per 100 grams of body weight) there was no difference in the oxygen consumption of the kidney slices as compared to those of the controls. However, there was more inorganic phosphate taken up in the control kidney slices as compared to the mersalyl treated slices. Cohen believes that the effect is probably due to a change in the permeability of cell membranes for inorganic phosphate, thereby impeding the generation of high energy phosphate esters.

This change would cause a lack of these esters required for the reabsorption of water in the tubules.

Clarkson and Magos (5), using equilibrium dialysis of mercuric ion against one percent homogenates of rat kidney or liver in the presence of penicillamine, found two classes of mercury binding. The binding capacities occurred at concentrations of mercury of  $1.0 \times 10^{-7}$  and  $30 \times 10^{-7}$  moles of mercury per gram wet weight of tissue. The same binding sites were found in both kidney and liver homogenates. They explain that the preferential uptake by kidney of inorganic mercury may be coupled to metabolism. Clarkson, Rothstein, and Sutherland (6) determined that Chlormerodrin breaks down to mercuric ion in the rat kidney and that  $2 \times 10^{-7}$  moles of mercury per gram wet weight of kidney induces diuresis in rate.

Taylor (47) approached the problem of mercurial diuresis from the standpoint of the sodium transport mechanism being closely associated with certain adenosine triphosphatase systems in rabbit kidney. The ATPase (adenosine triphosphatase) of kidney cell debris was found to resemble that of erythrocyte and nerve in its cation requirements. Also, the activity of the ATPase in kidney cell debris could be stimulated with sodium and potassium. It was found that organic mercurial compounds (some diuretics and p-CMB) preferentially inhibited the sodium and potassium stimulated portion of the kidney ATPase activity at concentrations of  $5 \times 10^{-5}$  molar. There was

very little effect of the organic mercurials on the unstimulated portion of ATPase activity at concentrations greater than  $10^{-5}$  molar. However, mercuric ion inhibited both the stimulated and unstimulated ATPase activity. Concentrations of mercuric ion greater than  $10^{-5}$  M inhibited the unstimulated portion of the activity.

#### Alkaline Phosphatase in Relation to Mercury Toxicity

Much work has been done in attempting to correlate the changes in the activity of enzymes in blood serum proteins or subcellular fractions after mercury treatment in order to indicate the toxicity of mercury. For example, Tuci, Cenacchi, and Lodi (48) dosed rats with intraperitoneal injections of mercuric chloride (0.8 milligrams per day for 50 days) and performed histological analysis on the liver, kidney, myocardium, and spleen at different time intervals. Pathological manifestations were observed on the 30th day of intoxication. However, serum aldolase, lactic dehydrogenase, and malic dehydrogenase were increased in comparison to the controls by the 10th day.

Some work has been done with mercury on alkaline phosphatase; however, there has been no comparative study with regard to different types of mercury compounds.

Kosmider, Zurkowski, and Wegiel (23) found that mercuric chloride in a final concentration of  $10^{-3}$  molar caused a 95 percent



fall in the activity of alkaline phosphatase in the cytoplasm of neutrophilic granulocytes. Sachs and Dulskas (37), using histochemical studies, found a decrease in the phosphatase activity of kidney after chronic mercury poisoning, with an appreciable survival time. Acute poisoning with mercury generally does not cause a decrease in the phosphatase activity. A study of 50 workers exposed to mercury vapors in industrial plants showed that alkaline phosphatase was slightly activated in the serum (20).

Agus, Cox, and Griffin (1), working with alkaline phosphatase from human kidney, rat bone, rat liver, Escherichia coli, and other sources, found that cysteine inhibited the activity at a pH range above 10.1. The inhibition was caused by a chelation of the zinc at the active center of the enzyme. The inhibiting species was of the type  $-S-R-NH_2$ . The species  $HS-R-NH_3^+$  found below a pH of 8.20 does not combine effectively with the enzyme. They ascribed the inhibition to be a result of chelation in situ rather than a removal of the zinc from the enzyme. Mercuric ion caused a partial reversibility of the inhibition, as did the addition of divalent zinc.

Mathies (28) points out that alkaline phosphatase from swine kidney requires the presence of both divalent manganese and divalent zinc. He showed a direct correlation between the activity of the enzyme and the zinc content and that divalent zinc was essential to the enzyme. It is also generally accepted that magnesium is essential

for the activation of alkaline phosphatase, but its optimum concentration is of the order of  $10^{-3}$  molar when the enzyme concentration is of the order of  $10^{-8}$  molar. The magnitude of the magnesium concentration is similar to that of the substrate, and it is postulated that a magnesium salt of the phosphate ester is the substrate for the enzyme.

Because the nature of this paper is to correlate the subcellular localization of inorganic mercury and phenylmercuric acetate in rat kidney and liver with its effect on alkaline phosphatase, it is important to understand the subcellular localization of the enzyme.

Griffin and Cox (15) found that 98 percent of the alkaline phosphatase from rat kidney is sedimented by centrifugation at 105,000 X G, which indicated its close association with cell particles. The microsomes contained the highest specific activity of any of the subcellular fractions. When the microsomes were treated with 0.26 percent deoxycholate at pH 7.4, three fractions were obtained upon centrifugation: ribonucleoprotein particles, microsomal membranes, and a microsomal supernatant. When the microsomal supernatant was centrifuged at 130,000 X G for three hours, a pellet of light microsomal membranes was obtained. The specific activity of alkaline phosphatase was by far the highest in the light microsomal membranes.

## MATERIALS AND METHODS

Preparation of the Liver and Kidney Slices

Rats were placed in a closed container and suffocated with  $\text{CO}_2$ . The abdominal and thoracic cavities were opened immediately while the heart was still beating. The posterior vena cava between the heart and diaphragm was cut to bleed the liver. The color of the liver changed from dark red to light red, indicating that most of the blood was removed.

The liver and kidneys were excised and placed in crushed ice. The fat and connective tissue were removed and the organs were sliced in the cold on a tissue slicer number 140 from the Havard Apparatus company. The thickness of the slices averaged about one millimeter. These slices were immediately placed in a beaker containing cold Krebs-Ringer-phosphate solutions. The slices were then divided into three groups and placed into beakers containing  $10^{-4}$  molar  $\text{P}^{203}\text{MA}$  and Krebs-Ringer solution,  $10^{-4}$  molar  $^{203}\text{Hg}(\text{oAc})_2$  and Krebs-Ringer solution, and Krebs-Ringer solution for the control. The volume of the incubation solutions was 50 to 100 milliliters but was the same for all three sample solutions in any particular experiment. The slices were incubated in these solutions at  $37^\circ\text{C}$  in a water bath.

Samples of tissue slices were removed from the beakers,

washed with cold tap water, and patted dry with paper towels at 0.5, 1.0, 2.0, and 3.0 hour intervals. These were immediately placed in plastic vials and frozen in dry ice. While frozen, the slices were weighed. The weight for the liver slices was from one to two grams, and the kidney slices weighed about 0.5 grams.

#### Preparation of the Subcellular Fractions

The frozen slices were weighed and thawed slowly in the cold. The slices were homogenized in nine volumes of 0.25 molar sucrose with a glass tissue grinder and teflon pestle and centrifuged at 700 X G in 50 milliliter centrifuge tubes for 10 minutes. The supernatant was decanted and the pellet was resuspended and washed twice with 2.5 milliliters of 0.25 molar sucrose solution. The final pellet was called the nuclear fraction.

The supernatant and washings from the isolation of the nuclear fraction were centrifuged at 5000 X G for 20 minutes. The supernatant was decanted and the pellet was resuspended and washed once in the 0.25 molar sucrose solution. The final pellet was called the mitochondrial fraction.

The supernatant and washings from the isolation of the mitochondria fraction were diluted with 0.25 molar sucrose to 40 milliliters and centrifuged at 35,000 X G (maximum) for 1.5 hours. The supernatant was decanted and called the soluble protein fraction,

and the pellet was called the microsomal fraction. This method was based on a procedure described by Umbreit, Burris and Stauffer (49, p. 194).

#### Determination of the Sephadex G-100 Elution Patterns of the Soluble Proteins

The incubation of liver and kidney tissue slices and the preparation of the homogenates were the same as for the subcellular fractions, except that the time of incubation was 1.5 hours, and the tissue was homogenized in only 3 to 4 volumes of 0.25 molar sucrose. Fifteen milliliter centrifuge tubes were used. The homogenate was centrifuged at 35,000 X G for 1.5 hours. Three to five milliliters of the supernatant were introduced into a G-100 Sephadex column (23 X 62 mm) in the cold and eluted with 0.1 molar NaCl and 0.01 molar NaOAc buffer solution (pH 6.0).

The Sephadex columns were prepared according to the method described by Whitaker (50). Fifteen grams of dry Sephadex G-100 granules were soaked in a one percent NaCl solution for 3 to 4 days at 3 to 5°C. A stopcock was sealed to the bottom of a two-foot piece of 23 millimeter inside diameter glass tubing, and a piece of glass wool was placed in the bottom of the column with glass beads layered on top to a height of two centimeters. After the column had been filled with the buffer solution, the soaked Sephadex slurry was introduced into a funnel fitted to the top of the column with a rubber stopper. Upon opening the stopcock, the buffer flowed out at the

bottom and the Sephadex slurry passed into the column at the top. Because the flow rate was fast during the packing of the first 10 or 15 centimeters of the column, the stopcock was almost turned off. This reduced flow rate prevented too tight packing of the Sephadex granules in the lower end of the column which was found to result in a slight decrease in flow rate. A spun glass filter disc was placed on top of the gel to prevent its disturbance when a sample was introduced into the column.

After the sample was added, it was allowed to enter the top of the gel until there was no sample fluid showing above the gel. At this time buffer solution was added to the column, and a rubber stopper fitted with a small teflon tube was attached at the top. The teflon tube was connected to a reservoir containing the buffer solution. The reservoir was designed to maintain a constant hydrostatic head in relation to the column to insure a constant flow rate throughout the filtration process. The flow rates of the column were between 0.5 and 1.0 milliliters per minute.

Since three samples were incubated (control, PMA treated, and inorganic mercury treated), there were three Sephadex columns used. All samples were filtered through the columns at the same time and at 3 to 5°C. The fractions were collected in test tubes mounted in a fraction collector, and the volumes averaged about 4 to 6 milliliters.

The elution patterns of the soluble proteins filtered through the Sephadex columns were determined by reading the optical density of each fraction at 260 millimicrons on a Beckman DU model 2400 spectrophotometer. Dilutions of some of the fractions were made with buffer due to the high protein concentrations resulting in high optical density readings. The values for the optical density of the elution fractions were divided by the net wet weight of the incubated tissue slices, and the elution pattern was plotted as the optical density per gram wet weight as a function of the elution volume. The net wet weight of the incubated tissue slices was determined by multiplying the fraction of the total volume of the soluble fraction introduced into the column times the total weight of the incubated tissue slices.

The elution pattern for the soluble proteins was also determined by precipitating the proteins in a steam bath and treating with one milliliter of 10 percent trichloroacetic acid. The precipitated proteins were filtered onto glass fiber filters, washed with distilled water, and dried with acetone. The weight of the dried protein was divided by the net wet weight of the incubated tissue slices and the volume of the fraction. The elution pattern was expressed as the milligrams protein per gram wet weight per milliliter. The dimensions of the optical density is a measurement of concentration. Therefore, the precipitated protein elution patterns must contain

the same units (1/milliliters.)

It was found that the glass fiber filters lost 0.16 milligrams when washed and dried. The precipitated protein weight data were corrected for this amount.

#### Determination of the Sephadex G-100 Elution Patterns of the Incubation Solutions from Liver Slices

It was noticed that protein was being leached out into the incubation solution during the incubation of the liver and kidney slices. Liver slices seemed to release much more protein into the incubation solution as compared to kidney slices. This observation was based on the turbidity of the incubation solutions. It was decided to determine the filtration pattern for these proteins and to see where the mercury compounds were bound.

After incubation of liver slices for 1.5 hours, the incubation solutions were placed in 0.5 liter polyethylene bottles and dipped into a dry ice and acetone mixture. The solution was frozen on the sides and the bottom of the bottles by swirling them around in the acetone bath. These bottles were then placed in a VirTis model freeze drying apparatus and lyophilized in a vacuum of 0.050 millimeters of mercury.

When the samples were completely dry, the vacuum was slowly released, the bottles were removed, and a portion of the dried



material was weighed out and dissolved into about five milliliters of distilled water. The samples were then introduced into the Sephadex columns, and the filtration fractions were collected as described in the section on Sephadex filtration of soluble proteins.

The protein patterns were expressed as the optical density per gram of the net wet weight of tissue leached as a function of the elution volume. The net wet weight of tissue leached was determined as the fraction of the dried incubation solutions placed into the columns multiplied times the weight of the incubated slices.

#### Method for the Determination of Nitrogen in the Subcellular Fractions

The centrifuged cellular fractions in the form of pellets were resuspended in distilled water with the aid of the glass tissue grinder and teflon pestle and diluted in volumetric flasks. Aliquots of 10 to 40 micrograms were taken for the nitrogen assay. The samples were pipetted into 18 X 150 mm pyrex test tubes. To each of the tubes was added one milliliter of 2 normal sulfuric acid containing 0.2 grams per liter of  $\text{CuSeO}_3$ . The tubes were placed in a heated sand bath with a temperature of 110 to 140°C.

Evaporation of the sample usually took about six to twelve hours. When the water from the digestion mixture was evaporated, it was usually black due to the carbon in the sample. The color in

the samples was cleared up by adding drops of 30 percent of  $H_2O_2$ . The test for complete digestion was to wait for half an hour after adding the hydrogen peroxide. If the digestion mixture remained clear, the digestion was complete.

To the tubes after digestion were added (in order) two milliliters of water, two milliliters of color reagent, and three milliliters of 2 normal NaOH. The color reagent contained four grams of potassium iodide, four grams of mercuric iodide, and 1.75 grams of gum ghatti. The gum ghatti (in powder form) was placed in about 500 milliliters of boiling water and allowed to reflux until dissolved. The potassium iodide and mercuric iodide were dissolved in 20 to 50 milliliters of water. The two solutions were added together and diluted to one liter. Due to some insoluble residues in the gum ghatti, the color reagent was centrifuged at 2,000 X G for five minutes. The clear supernatant was decanted off and used without further treatment.

Full color development was obtained after 15 minutes. Each sample was diluted to 10 milliliters in a Klett type photometer tube with distilled water, and the optical density at 490 millimicrons was determined on a Baush and Lomb model Spectronic 20 spectrophotometer.

The nitrogen assays were done in triplicate including blanks and standards. The blanks contained about one milliliter of distilled

water. The standards were made by pipetting one, two, and three milliliters of a standard ammonium chloride solution (10 micrograms of nitrogen per milliliter) into three test tubes. The blanks and standards were carried throughout the digestion procedure and color development with the other samples.

The number of micrograms that gave an optical density rating of 0.10 was calculated. After subtracting the optical density of the blanks from that of the samples, the nitrogen present was determined. The nitrogen present was determined by multiplying the resultant optical density times the extinction coefficient. Nitrogen in the total sample was calculated according to the dilution and aliquot taken for the determination.

The nitrogen content of the subcellular fractions was determined in liver and kidney slices incubated in Krebs-Ringer-phosphate solution alone. The samples of slices were removed at 0.5, 1.0, 2.0, and 3.0 hour intervals. The nitrogen content was expressed as the milligrams of nitrogen per gram wet weight of tissue that was incubated. These values were used as the control nitrogen content of the subcellular fractions to compare to the values for the inorganic mercury and PMA incubated slices.

Determination of Hg-203 Labeled Phenylmercuric Acetate  
and Mercuric Ion Bound to the Tissue Slices, Subcellular  
Fractions, and the Proteins in the Sephadex Elution Patterns

The PMA and  $\text{Hg}(\text{oAc})_2$  used in the incubation solutions were labeled with  $^{203}\text{Hg}$  which emits gamma and beta radiation. The content of  $\text{P}^{203}\text{MA}$  and  $^{203}\text{Hg}(\text{oAc})_2$  in the subcellular fractions was determined with the aid of a Tracerlab Superscaler with a Tracerlab NaI Thallium activated scintillation detector number 455 for counting the gamma activity. The centrifuge tubes, with the pellets (subcellular fractions) at the bottom, or plastic vials containing the tissue slices were placed on the detector and the activity was counted. The detector was mounted upside down. The amount of mercury ( $\text{PMA}$  or  $\text{Hg}(\text{oAc})_2$ ) present was determined from the inverse specific activity of the two mercury compounds used in the incubation solutions. Five milliliters of the soluble fraction was pipetted into plastic vials and placed on the detector. The total activity in the soluble fraction was calculated.

The inverse specific activity of the mercury was found by pipetting five milliliters of the standard solutions used to make up the incubation solutions ( $2 \times 10^{-4}$  molar  $\text{PMA}$  and  $\text{Hg}(\text{oAc})_2$ ) into plastic vials, placing them on the detector and determining the number of millimicromoles of mercury per 100 counts per minute (mumoles/100cpm). This figure was multiplied times the activity in

the subcellular fractions to give the amount of PMA and mercuric salts present. There was found to be no significant difference in geometry when counting the activity in the samples and in the standard solutions.

The radioactive PMA and inorganic mercury in the elution fractions was determined by transferring the fractions to plastic counting tubes and counting the gamma radiation in a well-type Packard Auto-Gamma Spectrometer, series 410 A. The inverse specific activity of the mercury was found by pipetting 3 milliliters of the standard solutions used to make up the incubation solutions ( $2 \times 10^{-4}$  molar PMA and  $\text{Hg}(\text{oAc})_2$ ) into two plastic counting tubes and counting them with the rest of the samples. One or two empty tubes were counted to obtain the background activity on the spectrometer.

Because the samples in the elution fractions from Sephadex filtration were usually in volume different from the volume of the standard solutions used to determine the inverse specific activity, it was necessary to establish a correction curve for the difference in geometry in the well-type detector.

A three milliliter sample resulted in about 89 percent efficiency in counting. From the volumes of the elution fractions, the percent efficiencies of counting of the standard solutions and the samples was used to correct the sample determinations.

Figure 1 shows the activity of a radioactive mercury solution counted in a well-type gamma detector as a function of the volume of the sample. Figure 2 shows the percent of the maximum activity that is determined at different volumes of the sample.

Wang and Jones (50) have determined the radioactivity in proteins in paper chromatograms immersed in suitable scintillator solutions. A method similar to Wang and Jones was used to determine the mercury activity in the precipitated protein fractions of the soluble protein elution patterns from Sephadex G-100 filtration.

The glass fiber filters on which the precipitated proteins were filtered were placed in glass vials used for liquid scintillation counting, and 4 milliliters of liquiflour solution (4 grams of 2, 5-diphenyl-oxazole and 50 milligrams of 1, 4-bis-2(5 phenyloxazolyl)-benzene dissolved in one liter of toluene) were added. The beta radiation was determined in a Tri-Carb Liquid Scintillation Spectrometer, series 314 E.

A correction curve for self-absorption was determined by precipitating various amounts of radioactive mercury labeled soluble proteins. These were filtered as described, and the logarithm of the counts per minute per milligram weight of protein was plotted against the weight of the protein which was corrected for the loss of weight of the filter (Figure 3). Extrapolation to zero weight of the protein gave the true counts per minute per milligram protein.

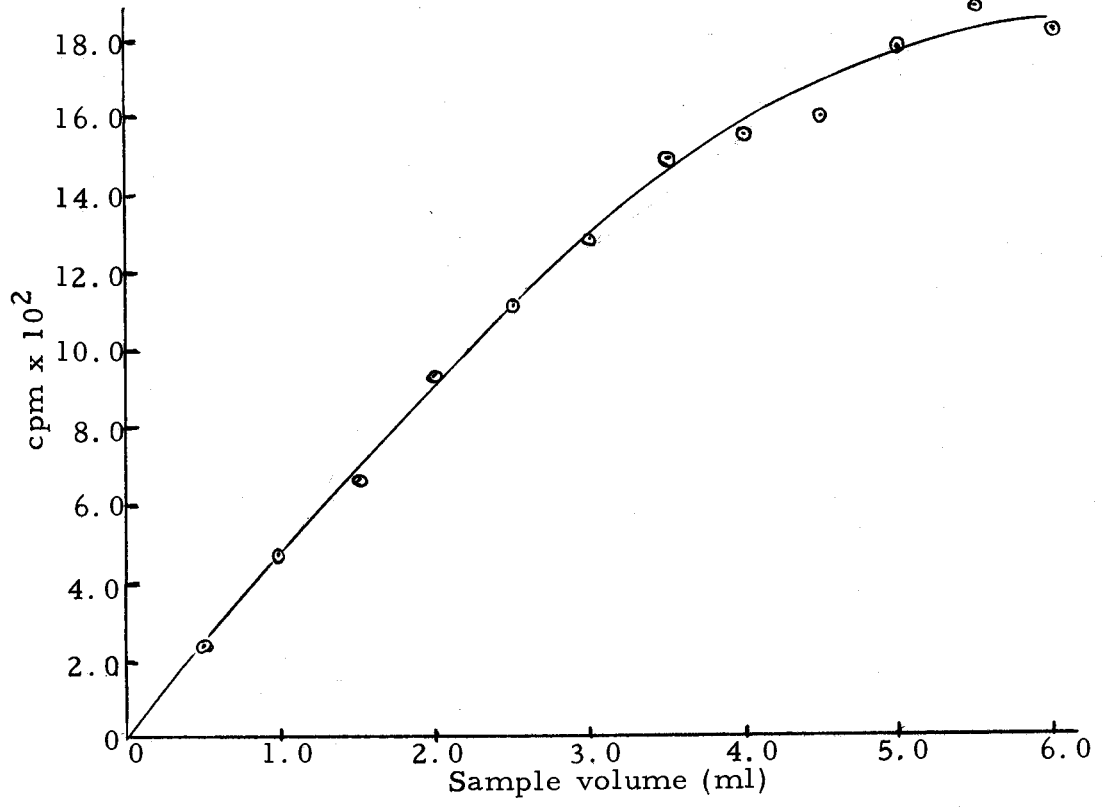


Figure 1. Activity of a radioactive Hg-203 solution, counted in a well-type solid scintillation gamma detector.

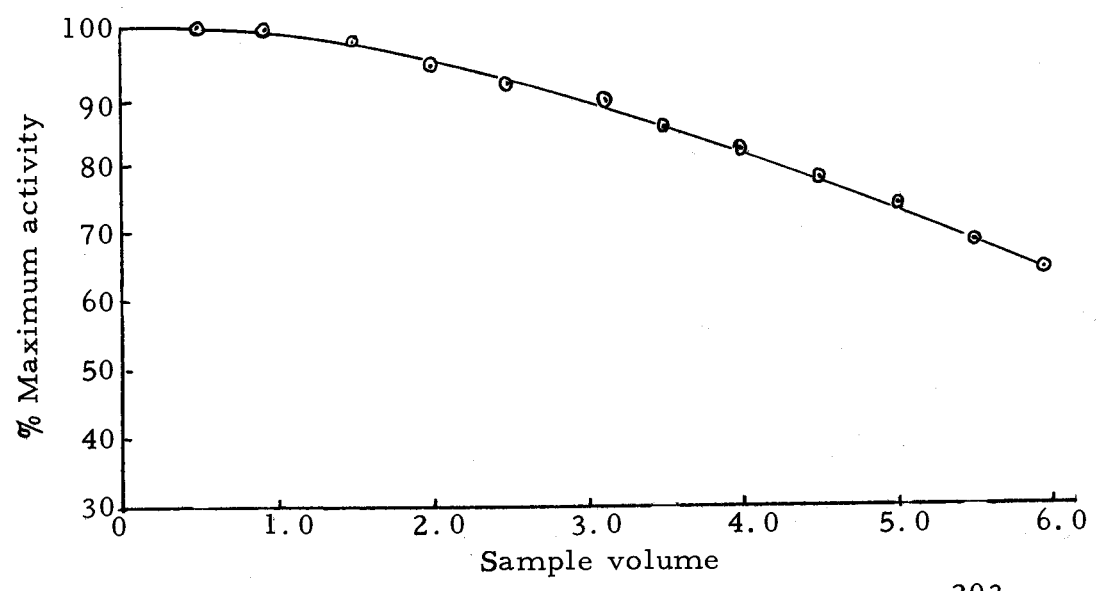


Figure 2. Correction curve for the sample volume of <sup>203</sup>Hg gamma activity counted on a well-type solid scintillation gamma detector.

The correction curve for self-absorption was obtained by plotting the relative specific activity against the weight of protein (Figure 4).

The specific activity of the labeled PMA and inorganic mercury was determined by pipetting 0.1 milliliter into 4 milliliters of liquiflour and 4 milliliters of methyl cellosolve (the methyl cellosolve contained 25 grams of naphthalene per 500 milliliters) and counting in the liquid scintillation counter.

Since the geometry for counting activity in a homogeneous solution is better than if the sample is in the shape of a disc and lying at the bottom of the vial, a correction factor was determined for the difference in counting efficiency. This was done by pipetting 0.1 milliliters of  $10^{-4}$  molar  $^{203}\text{Hg}(\text{oAc})_2$  into several liquid scintillation vials containing 4 milliliters of liquiflour and 4 milliliters of methylcellosolve, and the same amount into test tubes containing different amounts of soluble proteins. The protein solutions were precipitated, filtered, weighed, and corrected for weight loss and self-absorption as before. The ratio of the activity in the homogeneous solution divided by the activity in the precipitated proteins (the value was found to be 1.37) was multiplied times the inverse specific activity of the homogeneous solution (expressed as the millimicromoles of mercury per 100 counts per minute) to give the inverse specific activity of the precipitated protein sample. Reasoning will show that there has to be more radioactive mercury present



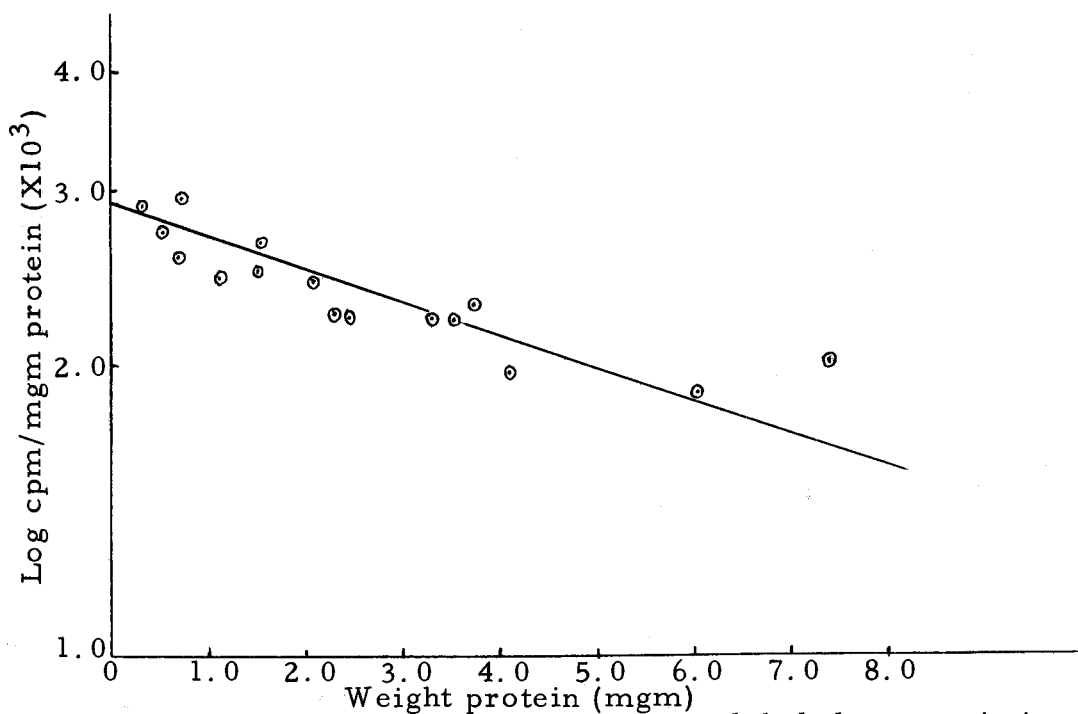


Figure 3. Beta activity from Hg-203 labeled mercuric ion bound to precipitated and filtered protein. Activity counted by liquid scintillation.

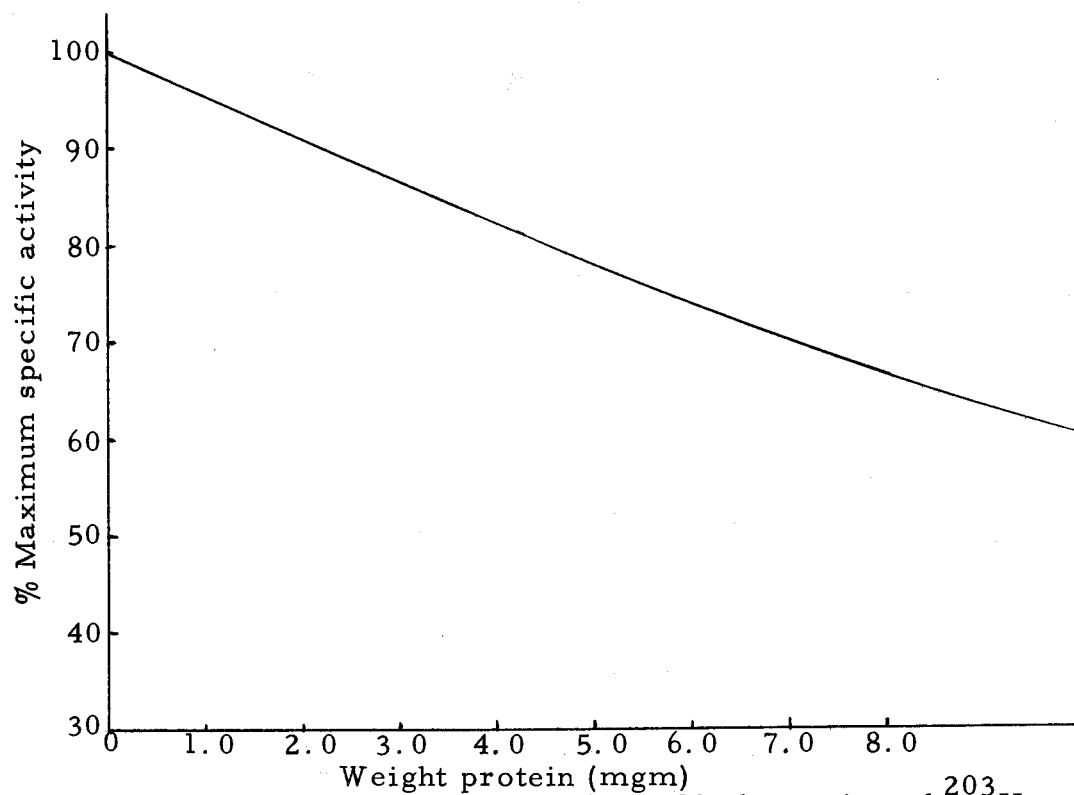


Figure 4. Correction curve for self-absorption of <sup>203</sup>Hg beta activity bound to precipitated and filtered protein. Activity counted by liquid scintillation.

when counting by the precipitated protein technique to give 100 counts per minute as compared to the homogeneous solution counting technique.

In this experiment, there was found to be the same activity in the precipitated proteins even though there were different amounts present. This result indicated that there was no loss of mercury in the washing and drying steps and that all remained bound to the protein throughout the procedure.

The activity of the elution fractions was converted to the amount of mercury present, and this amount was divided by the net wet weight of the incubation tissue slices and the volume of the fractions. The result of these calculations was then plotted as the millimicromoles of PMA or mercuric salt per gram-milliliter as a function of the elution volume.

The magnitude of the mercury binding or the specific binding in the proteins shown in the elution pattern was expressed as the millimicromoles of PMA or inorganic mercury per milliliter per O.D. in the experiments in which the optical density patterns were determined. For the protein precipitation experiments, the specific binding was expressed as the millimicromoles of the two mercurials per milligram protein. The specific binding was plotted as a function of the elution volume.

Depending on the experiment and the specific activity of the

PMA or  $\text{Hg}(\text{oAc})_2$  used, the activity in tissue slices was 1,000 to 5,000 counts per minute or better. The activity in the subcellular fractions varied from 500 to 3,000 counts per minute in the nuclear fraction to about 20 to 150 counts per minute in the soluble fraction on the Tracerlab gamma counter. The background on the Tracerlab gamma counter averaged about 250 counts per minute. All counting determinations were made over a ten-minute interval to insure enough accuracy.

When the Auto-Gamma Spectrometer was used to determine the activity in the soluble protein elution patterns, the counts per five minutes varied from 200 to 1,500 with a background of about 175. As the blanks (background), standard solutions, and samples were all counted for five minutes, it was decided to leave the data on the basis of five minutes. The activity in the incubation solution proteins varied from 200 to 1,300 counts per 5 minutes with a background of about 170.

For the precipitated proteins bound with radioactive mercury, the activity averaged about 100 counts per minute, with a range of 20 to 200. With a higher specific activity of inorganic mercury used in one experiment, the counts per minute ranged from 100 to 1,200. The background of the Tri-Carb Liquid Scintillation counter was about 16 counts per minute. The activity was determined over a five-minute interval and converted to counts per minute.

Method of Separation of the Soluble Proteins from Kidney Slices  
by Disc Polyacrylamide Gel Electrophoresis

Kidney slices were incubated, homogenized, and centrifuged as described in the section on Sephadex filtration of soluble proteins. The time of incubation was 1.5 hours. The soluble fraction was separated electrophoretically on polyacrylamide gel columns. The apparatus used in the experiments was constructed similar to a type commercially available from the Canalco company. The methods for the experimental procedure were based on a procedure described by Davis (9), with some modifications suggested by Morris (31).

The gel columns were prepared in six glass tubes (10 X 90 millimeters). The tops of the tubes were inserted through six holes drilled in a circle in the bottom of a plastic container, and they were ringed by rubber gaskets such that the seals between the dish and the tubes were watertight. The upper container held reservoir buffer solution. The upper reservoir, fitted snugly with the gel tubes, was suspended above the lower reservoir so that the bottom of the tubes were immersed below the lower reservoir buffer by about 1/4 of an inch. Fitted through a hole in the bottom of the lower reservoir was a single platinum electrode. The fitting was watertight and the electrode was placed in the center of the circle of the bottoms of the tubes so that the distance from each tube was about 3 to 4 centimeters, and each tube was the same distance from

the electrode. A similar electrode was suspended in the upper reservoir so that it was about the same distance from and centered in the middle of the tops of the tubes protruding through the bottom of the upper reservoir container.

The solutions used for the polyacrylamide gels were the following:

1. Reservoir Buffer: Tris-Glycine

Dissolved in 600 milliliters of water was 28.8 grams of glycine. The pH was adjusted to 8.3 with a strong solution of Tris (about 6 grams of trishydroxymethylamino methane). The solution was diluted to one liter.

For use the solution was diluted to 0.1 molar concentration.

2. Sample Buffer: Tris-Phosphate

Dissolved in about 25 milliliters of water was 5.7 grams of Tris. The pH was adjusted to 6.9 with 1 molar phosphoric acid and diluted to 100 milliliters. Because the soluble protein preparation was not buffered, the sample buffer in the volume of 1/10 was added.

3. Spacer Slurry:

To 10 milliliters of the sample buffer (diluted 1/10) 3.5 grams of sucrose was added and enough dry Bio-Rad P100 polyacrylamide gel particles to make a stiff gel.

4. Small Pore Acrylamide Solution:

To 100 milliliters of water was added 30 grams of acrylamide and 0.8 grams of N, N'-methylenebisacrylamide.

5. Large Pore Acrylamide Solution: Used for spacer gel.

To 100 milliliters of water was added 10 grams of acrylamide and 2.5 grams of methylenebisacrylamide.

6. Gel Buffer:

To 100 milliliters of water was added 183 grams of Tris and 1.15 grams of N, N, N', N'-Tetramethylethylenediamine. One molar HCl (about 240 milliliters) was added to bring the pH down to 8.9. Water was added to bring to a volume of 500 milliliters.

7. Ammonium Persulfate Solution:

To 100 milliliters of water was added 0.14 grams of ammonium persulfate. This solution must be made up fresh for each experiment.

8. Amido Black Staining Solution:

One gram of Amido Black was stirred into 200 milliliters of 10 percent (v/v) acetic acid. The solution was filtered.

All the solutions with the exception of the staining solution were stored at 2°C.

The tubes were placed in a test tube rack after capping the bottom with parafilm. The small pore gel solution was poured into these tubes to about an inch from the top. The gel was made up as follows:

Gel Buffer	5 ml
Water	5 ml
Small Pore Acrylamide Solution	10 ml
Ammonium persulfate	10 ml

The gel solution was overlaid with about 1/4 inch of water and polymerization was allowed to proceed for 30 minutes. The water prevents the formation of a curved boundary at the top of the gel solution and also prevents oxygen from reaching it. The presence of oxygen in the gel solution will inhibit polymerization.

After polymerization, the water is shaken out and the spacer gel solution is poured on top to a depth of 1/4 inch. Water was again added to 1/4 inch in depth. The spacer or large pore gel solution is made up as follows:

Gel Buffer	2.5 ml
Water	2.5 ml
Large Pore Acrylamide Solution	5.0 ml
Ammonium Persulfate	5.0 ml

After polymerization, the water was shaken out of the tubes and the spacer slurry was layered on top to a 1/4 inch depth. The sample (0.1 to 0.5 ml), containing enough sucrose to give a final

concentration of 0.75 molar, was added on top of the spacer slurry. Dry polyacrylamide powder was added to the sample to prevent convection. Over the sample was layered the sample buffer brought up to a concentration of sucrose of 0.5 molar. The rest of the tubes were then very carefully filled with the reservoir buffer. The use of a dropper is recommended for the layering of the sample and buffers.

The reservoir buffer was carefully added to the upper reservoir after inserting the tubes into the rubber-gasket-fitted holes in the bottom. After removing the parafilm from the bottom of the tubes, the reservoir and tubes were lowered until the bottoms of the tubes were immersed in the buffer in the lower reservoir. The same buffer was used in both the upper and lower reservoir.

A Heathkit Variable Voltage Regulated Power Supply, Model PS-3, was wired to the electrodes (anode below). A current density of 3 to 5 milliamperes per tube was maintained for 2 to 3 hours, until an adequate separation was completed. The buffer discontinuity can be seen in the gel due to the difference in the indices of refraction. The distance through which the discontinuity has moved is used to ascertain the extent of separation (usually about 5 centimeters).

The gels were removed from the tubes by rimming gently with water from a hypodermic syringe, and they were then placed in the staining solution overnight.



The gels were destained by inserting them back into the tubes and removing the dye electrophoretically. Ten percent acetic acid was used in both reservoirs, with the anode on top. The same current density used for the electrophoresis of the protein sample was used for the destaining.

#### Quantitative Determination of the Gel Electrophoresis Patterns of the Kidney Soluble Proteins

After destaining, the gels were sliced on the tissue slicer number 140 from the Harvard Apparatus Company. Slices along the longitudinal axis were made such that they were 2 to 5 millimeters in thickness. The initial slice on a new gel column had a flat and a round side. The first slice was discarded, and more slices were taken until one with flat smooth surfaces was obtained. Slices with different thicknesses were taken on different columns due to the amount of stained protein in the gel. If the sample introduced into the column was small, the amount of stained protein in the bands was faint. In this case a larger slice was taken to insure detectable colored protein bands. With any particular slice taken, it was important to insure that the thickness was the same throughout its length.

The gel slice was mounted between two glass slides by wrapping tape around both ends of the slides. The gel was squashed or

compressed slightly to remove any air bubbles, and care was taken to insure that the thickness of the gel was the same throughout its length.

The prepared gel slice was then mounted on a Photovolt Electronic Densitometer, Model 525, and the optical density pattern of the bands in the gel was determined. Since the bands in the gel were very thin, it was necessary to decrease the slit width over the light source. Also, a microcaliper was attached to the housing of the search unit so that it impinged on the movable platform on which the gel slice was mounted.

Since the stain of the proteins in the gel was blue, a yellow filter was mounted in front of the photomultiplier tube to increase the sensitivity. Readings of optical density were taken from the Electronic Photometer Model 501-A. The blank reading, to establish the zero optical density, was taken through the gel in front of the boundary where there were no protein bands.

The optical density patterns of the gel electrophoresis strips were plotted as the optical density against the number of revolutions of the microcaliper. Because of the fact that the sample of soluble proteins placed on the gel column varied (20 to 50 micrograms of nitrogen) and the fact that the slices of the gel used for the determination of the electrophoretic patterns were of varying thickness, the peak intensities varied from graph to graph. In order to be able

to compare the results for the mercury treated samples against the control, it was important to standardize the data.

Peak 2 (Figures 41 to 43) on the gel electrophoresis patterns was found to be present in all the experiments. Also its shape seemed to approximate the standard bell-shaped curve that would be expected from a pure protein. It was decided to use the peak intensity of peak 2 as a standard and to adjust its intensity to 1.0 optical density. From this adjustment the intensities of the other peaks were adjusted proportionally. The results of these calculations on two experiments are shown in Table 2, in which the intensity of peak 2 is 1.00 optical density.

The difference between the values of the intensity of the peaks for the control and either the PMA or mercuric ion treated samples was divided by the values of the control peaks. The result was two columns of figures representing the adjusted optical density readings of the control, PMA, and inorganic mercury treated samples and the percent difference, from the control, of the mercury treated samples. Whether the intensities of the peaks for PMA and mercuric ion treated samples were greater or lesser than those for the control is indicated by the plus or minus sign.

Method for the Determination of the Alkaline Phosphatase  
Content of the Microsomal and Soluble Fractions

The alkaline phosphatase activity was measured in the soluble fraction, isolated according to the method described in the section on Sephadex filtration of soluble proteins. The time of incubation was 1.5 hours. The analysis of the enzyme activity was based on a method described by Melani and Guerritore (29).

The substrate for the assay was p-nitrophenylphosphate (PNPP). Splitting of PNPP by phosphatase produces p-nitrophenol (yellow in basic media) and inorganic phosphate in a 1:1 ratio. Measurement of the increase of optical density at 405 millimicrons as a function of time gives the enzyme activity. The extinction coefficient of PNP is relatively constant above a pH of 8.5, but below this pH it drops rapidly. The use of PNPP as a substrate for the measurement of alkaline phosphatase is ideal, because the pH range for optimum activity of the enzyme is about 10.4 in rat kidney homogenate according to Melani and Guerritore (29).

The reaction mixture for the alkaline phosphatase assay is shown in Table 1.

The volume of enzyme solution and water was varied in duplicate or triplicate runs. However, the total volume of the reaction mixture was always three milliliters. The pH of the buffer was changed when determining the pH for optimum activity of the enzyme.

The glycine buffer was brought to the desired pH by addition of dilute NaOH solution.

Table 1. Reaction mixture for alkaline phosphatase assay.

	Volume (ml)	Final Concentration
0.2 M Glycine Buffer, pH 10.4	1.50	100
1.5 mM MgSO <sub>4</sub>	0.40	0.125
30.4 mM PNPP	0.50	5.06
Enzyme Solution	0.10	
Water	0.50	
Total volume (ml)	3.00	

Samples from the soluble fraction were used without further purification. The microsomal pellet was resuspended with the aid of the teflon homogenizer in 0.25 molar sucrose, with the same volume as its respective soluble fraction. The microsomal suspension was then diluted down to 1/10 the concentration, and an aliquot of this was taken for the assay.

A nitrogen analysis was done on each of the samples in the same manner as described in the section on the Johnson method for analysis of nitrogen.

The extinction coefficient of p-nitrophenol was determined in basic pH (9 to 11) and was used to calculate the millimicromoles of PNPP hydrolyzed per minute per milligram nitrogen.

## RESULTS

The Uptake of Phenylmercuric Acetate and Mercuric Acetate by Rat Kidney and Liver Slices

The in vitro binding of PMA and mercuric acetate in rat kidney slices as a function of time is similar for both compounds. The binding of the mercurials in liver slices as a function of time was much less than in the kidney. Figures 5 and 6 show the binding of the mercury compounds in the liver and kidney slices. The binding of PMA in the liver is almost double that of inorganic mercury. It is possible that the binding sites for inorganic mercury in liver slices are approaching saturation, because the uptake curve begins to level off at three hours. Binding sites for both the mercury compounds in the kidney are far from near becoming saturated, as both PMA and inorganic mercury continue to be taken up at a fast rate after three hours.

The first few experiments were done using the organs from male rats. Due to a shortage of male rats, females were used. There was found to be no difference in the binding of the mercury compounds with regard to sex in the kidney and liver slices and in the subcellular fractions. Heimburg and Schmidt have found that there was no significant difference in resistance to mercury toxicity in male and female rats (16).

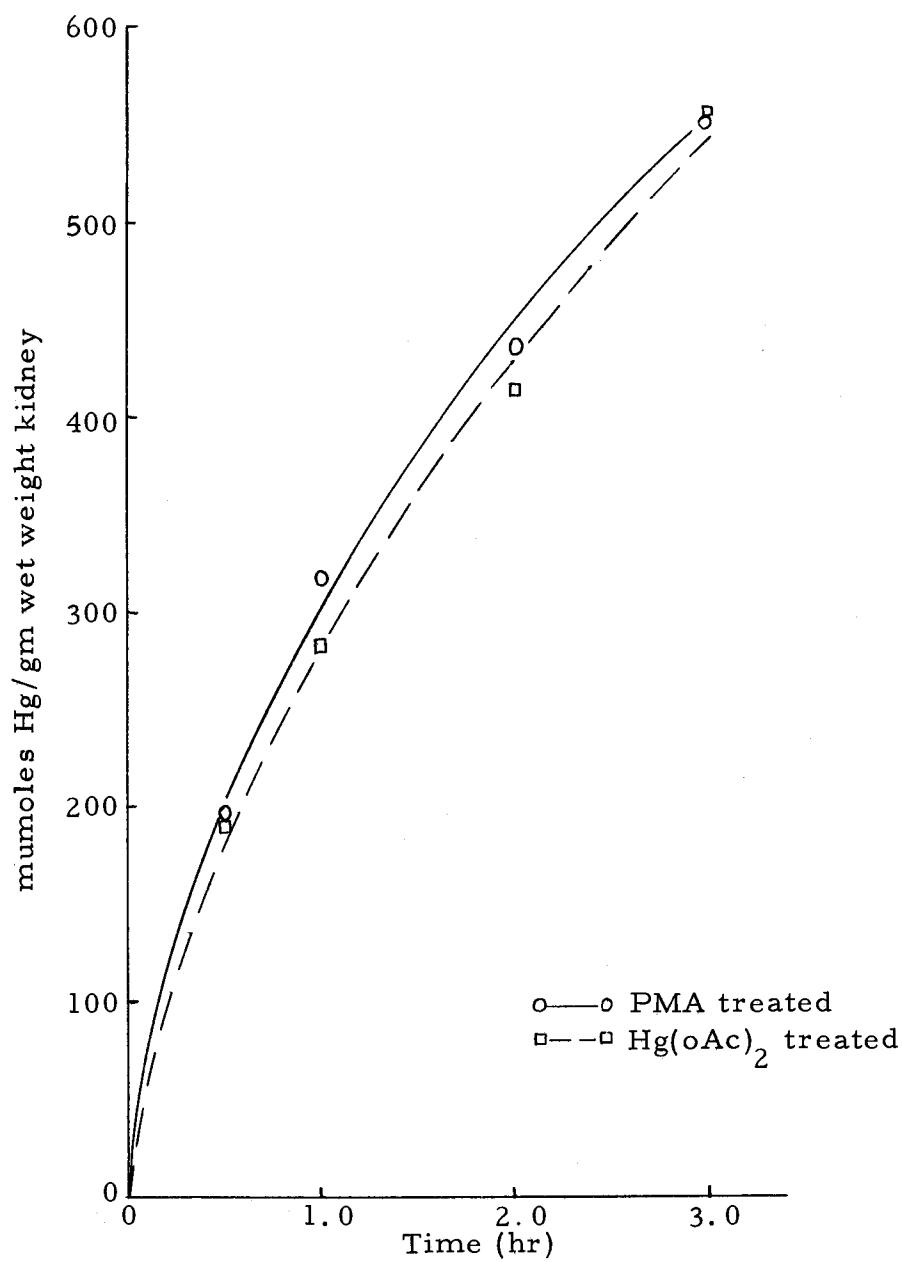


Figure 5. Uptake of mercury by rat kidney slices.

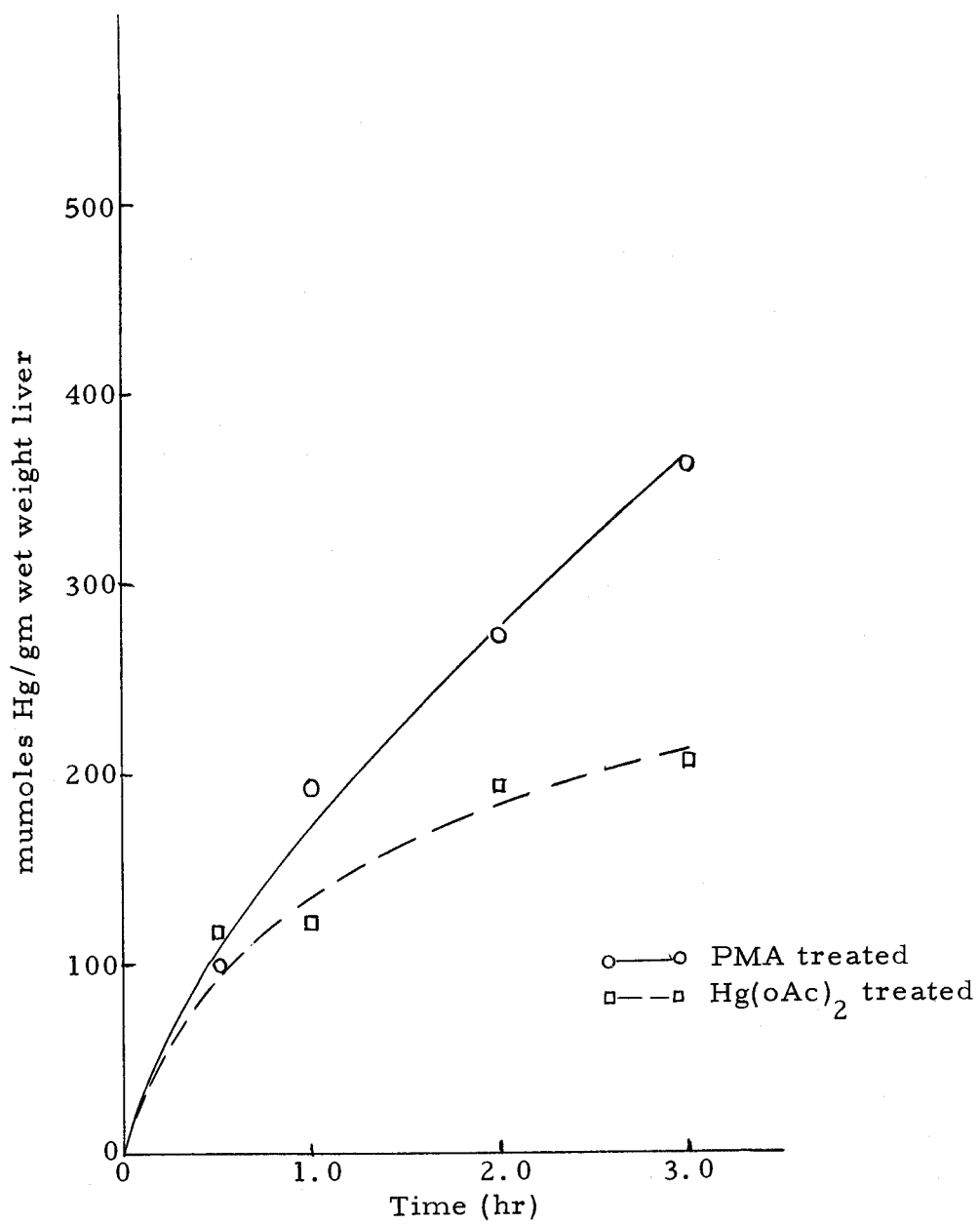


Figure 6. Uptake of mercury by rat liver slices.



The Incorporation of Phenylmercuric Acetate and Mercuric Acetate into the Subcellular Fractions of Rat Kidney and Liver Slices

Figures 7 and 8 show the binding of PMA and  $\text{Hg}(\text{oAc})_2$  in the subcellular fractions of kidney, and Figures 9 and 10 show the same for liver on the basis of the wet weight of the tissue slices. The percent binding of the two mercurials in the subcellular fractions in the kidney is shown in Figures 11 and 12. The same is shown for liver in Figures 13 and 14.

The mercury bound to the subcellular fractions on the basis of the nitrogen present is shown for kidney in Figures 15 and 16 and Figures 17 and 18 for liver.

From the percentage binding of PMA and mercuric ion in liver and kidney slices, it can be seen that the inorganic mercury binds much higher in the nuclear fraction than in the other fractions. This trend is observed in both kidney and liver. Although the highest percentage of PMA is also found in the nuclear fraction, it is not nearly so marked as compared to mercuric ion.

The percent  $\text{Hg}(\text{oAc})_2$  in the soluble proteins decreases with time and is evident in both kidney and liver. The percent of PMA in the soluble proteins drops only slightly in both kidney and liver.

The rate of increase of binding of PMA and  $\text{Hg}(\text{oAc})_2$ , on the basis of the milligram weight of nitrogen in the soluble fractions,

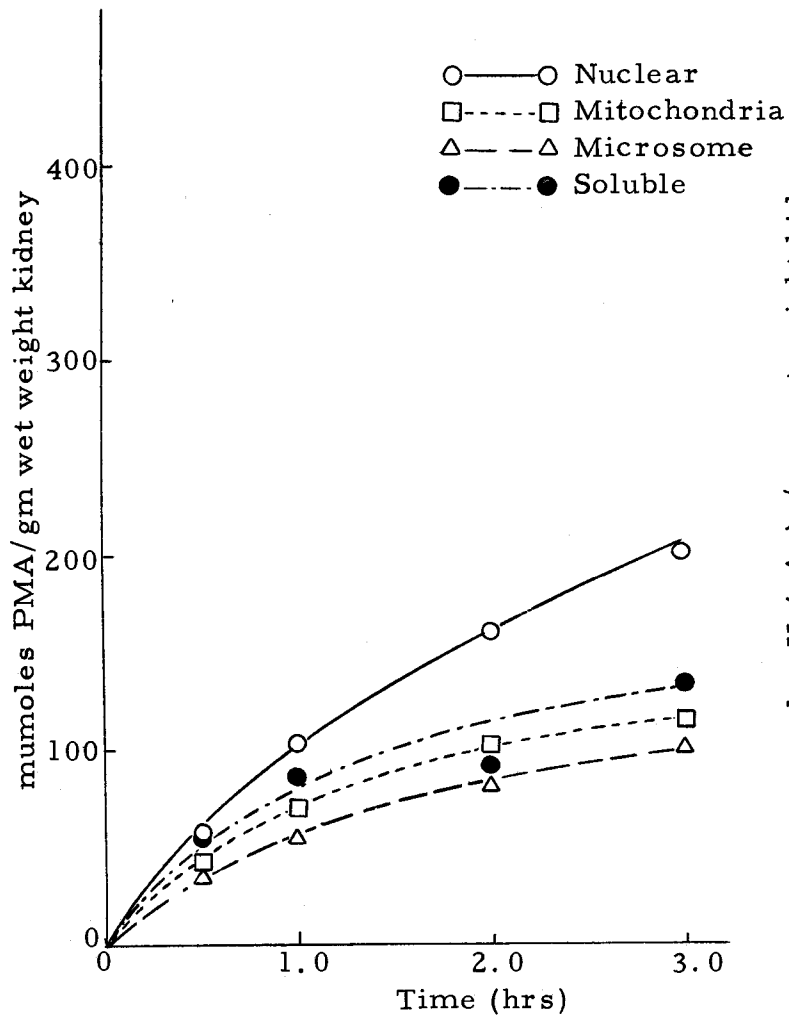


Figure 7. Uptake of PMA in subcellular fractions of rat kidney on the basis of wet weight of tissue.

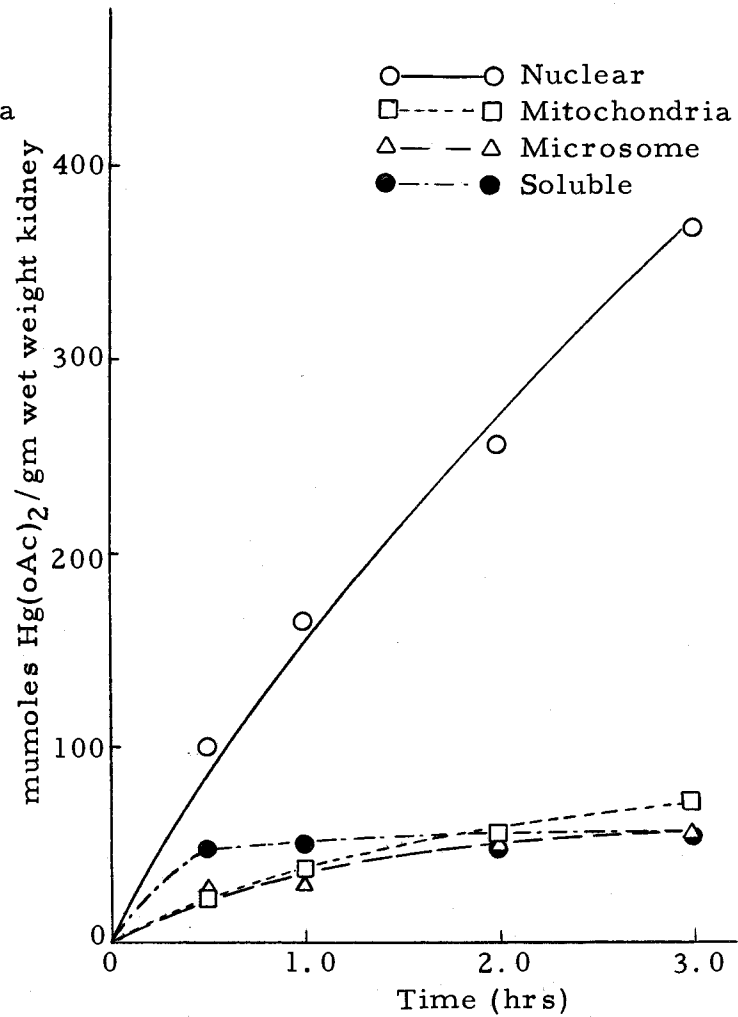


Figure 8. Uptake of inorganic mercury in subcellular fractions of rat kidney on the basis of wet weight of tissue.

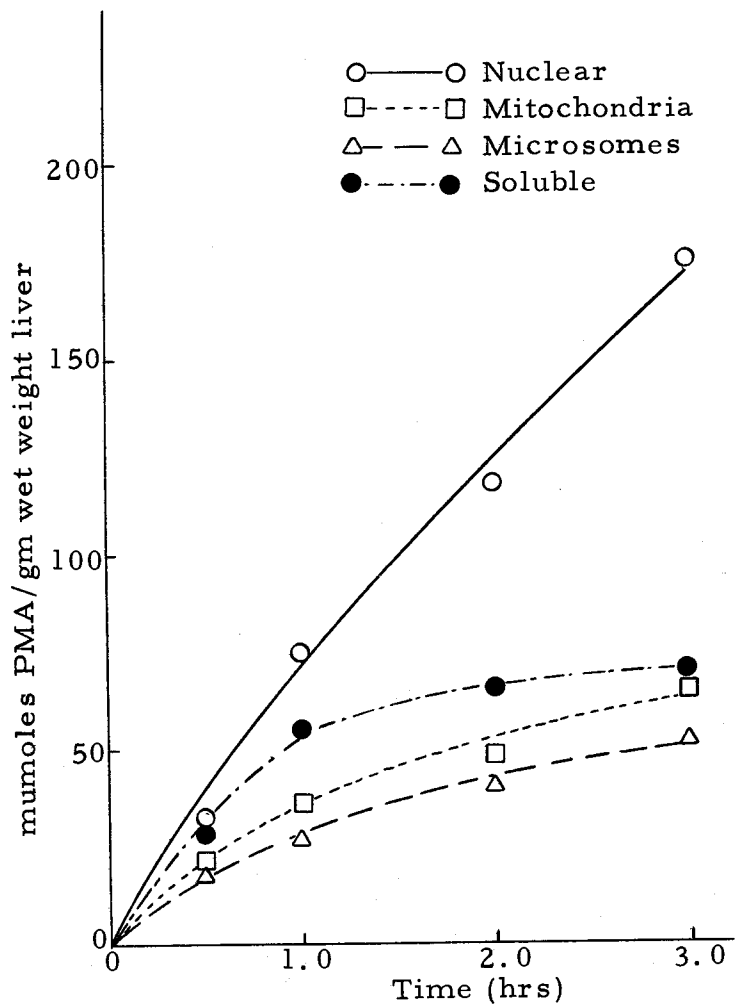


Figure 9. Uptake of PMA in subcellular fractions of rat liver on the basis of wet weight of tissue.

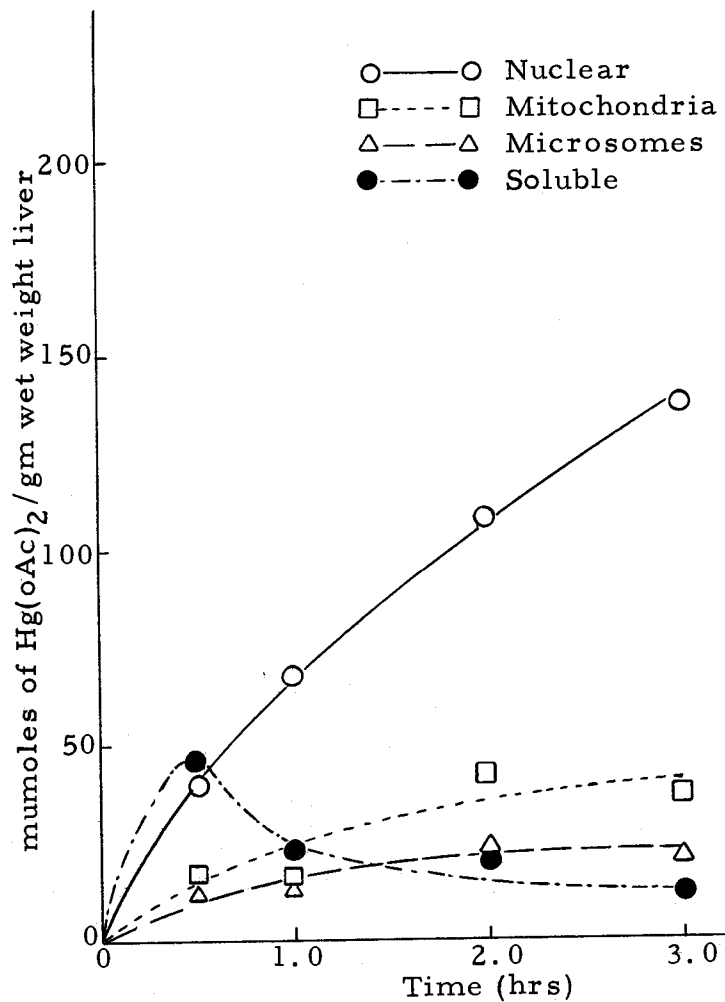


Figure 10. Uptake of inorganic mercury in subcellular fractions of rat liver on the basis of wet weight of tissue.

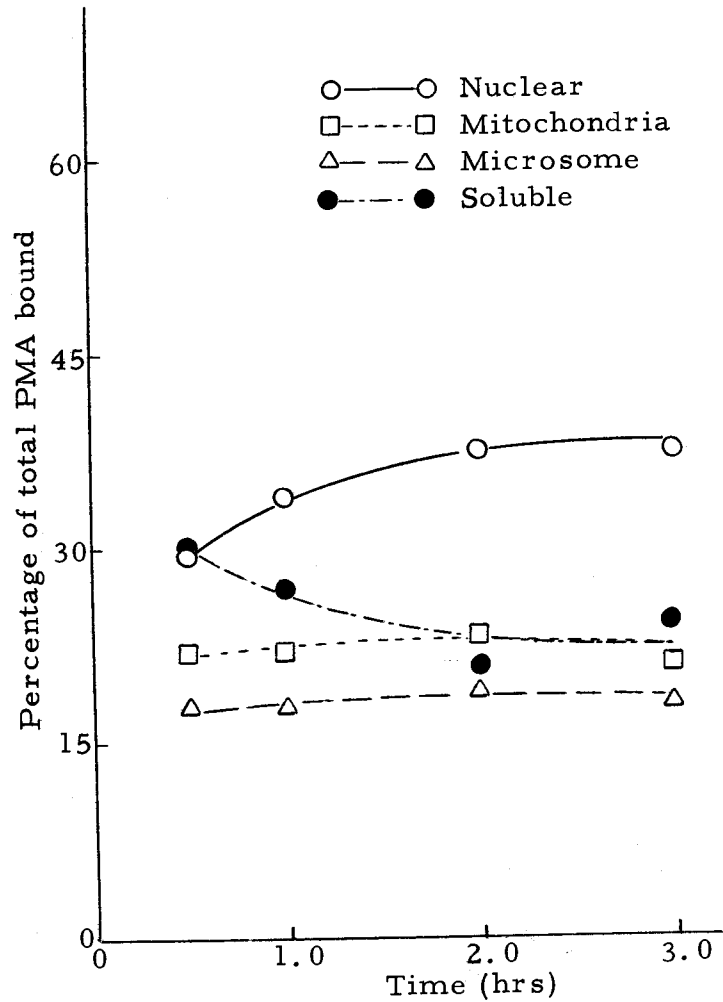


Figure 11. Subcellular binding of PMA in rat kidney slices as percent of total uptake.

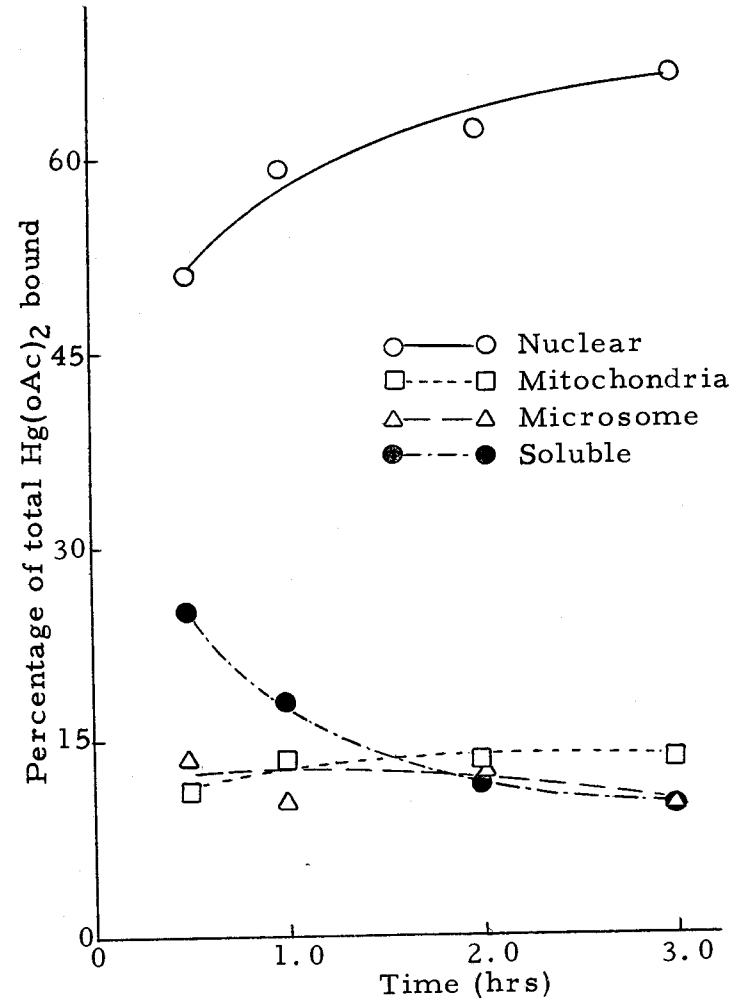


Figure 12. Subcellular binding of inorganic mercury in rat kidney slices as percent of total uptake.

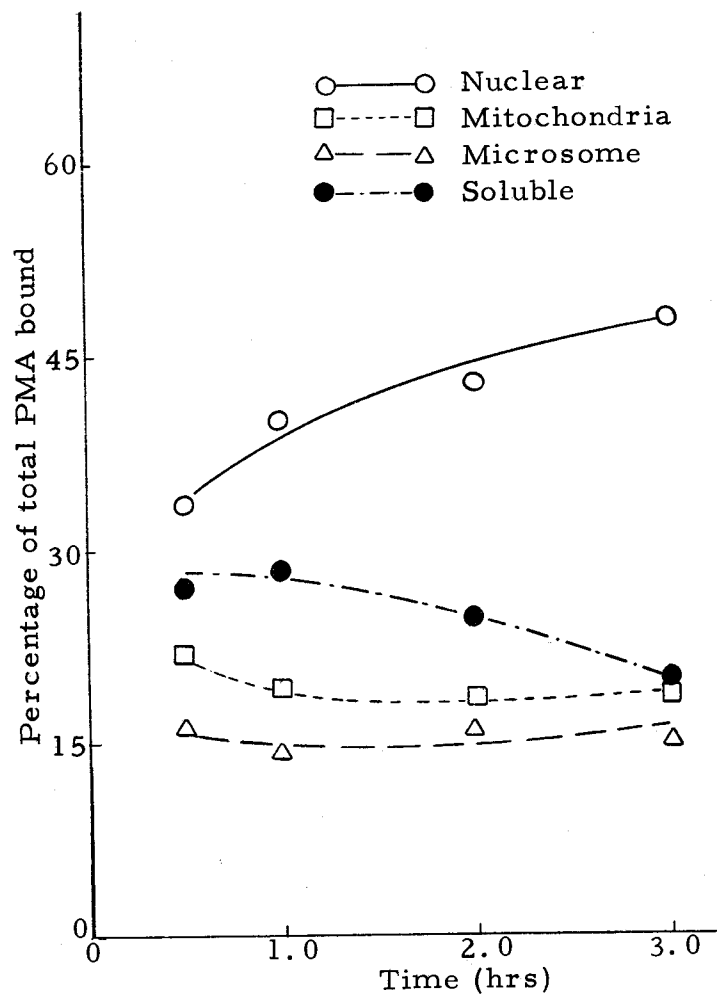


Figure 13. Subcellular binding of PMA in rat liver slices as percent of total uptake.

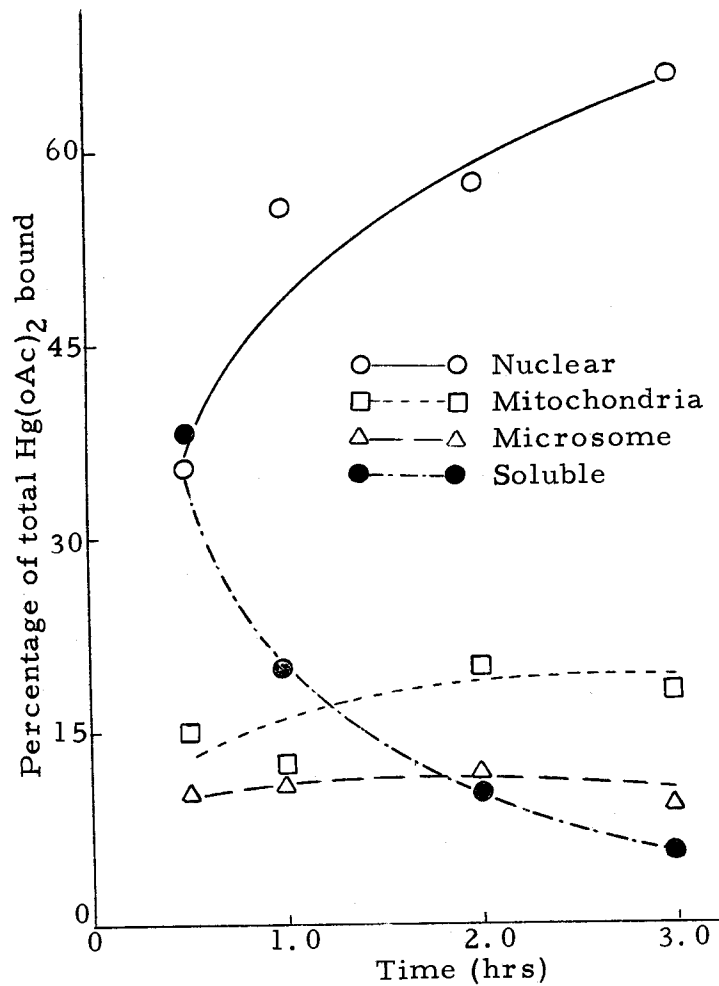


Figure 14. Subcellular binding of inorganic mercury in rat liver slices as percent of total uptake.

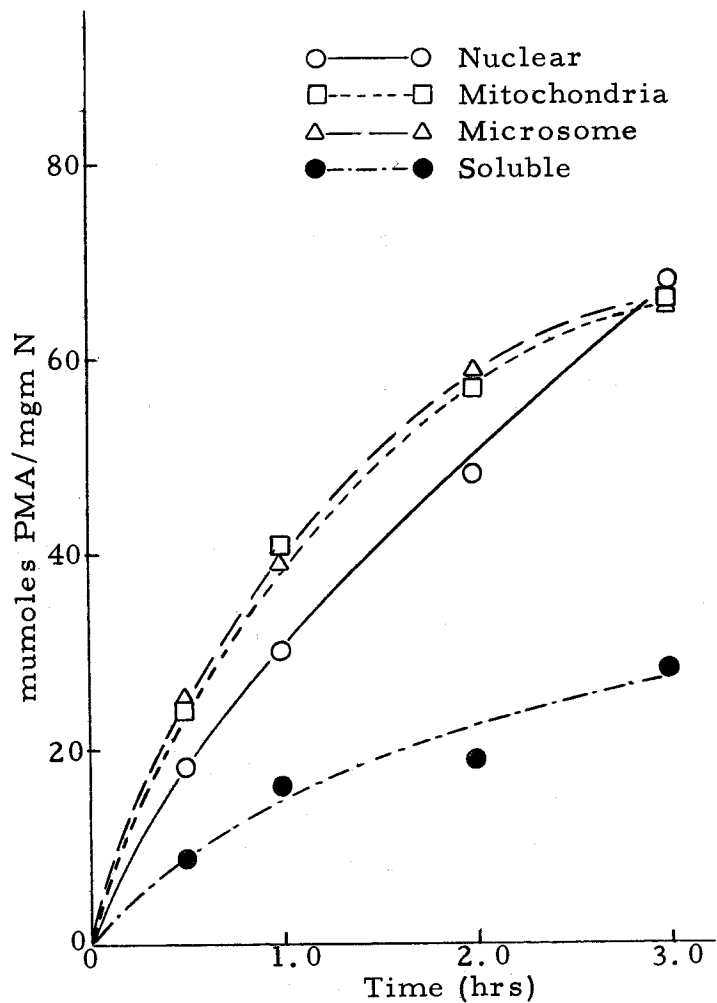


Figure 15. Subcellular binding of PMA in rat kidney slices on the basis of nitrogen weight.

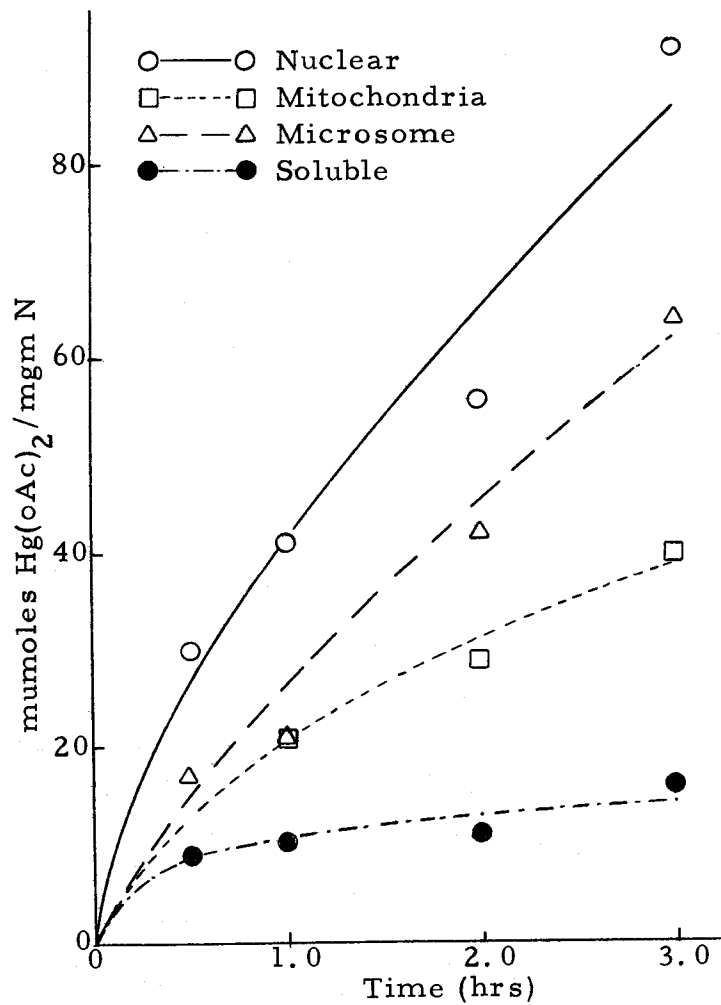


Figure 16. Subcellular binding of inorganic mercury in rat kidney slices on the basis of nitrogen weight.

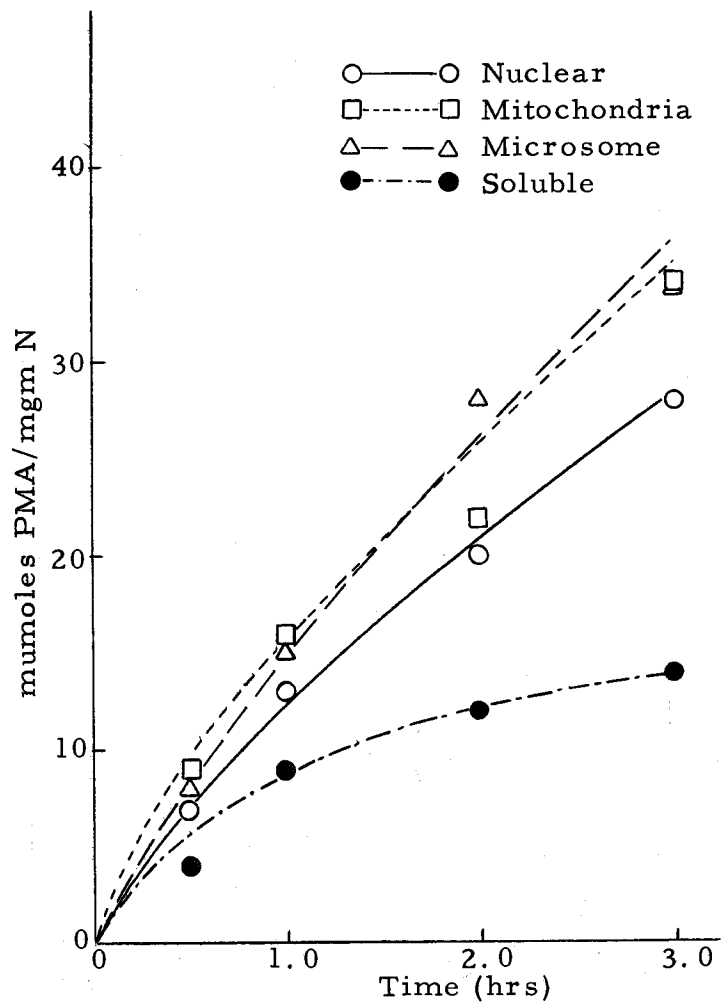


Figure 17. Subcellular binding of PMA in rat liver slices on the basis of nitrogen weight.

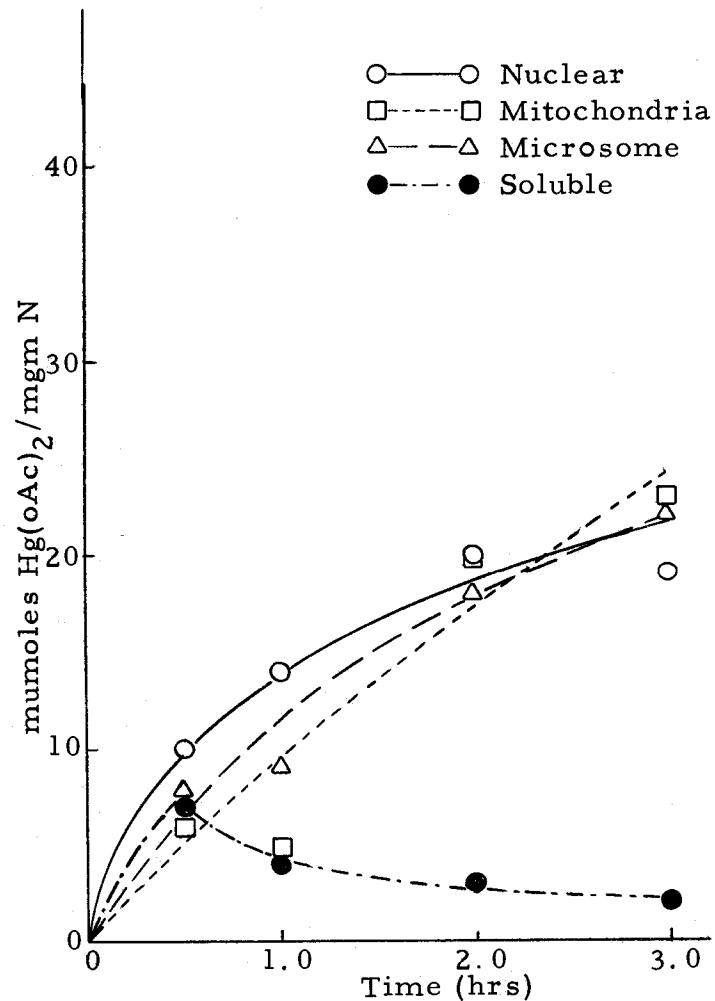


Figure 18. Subcellular binding of inorganic mercury in rat liver slices on the basis of nitrogen weight.

levels off after the first hour of incubation, except for mercuric ion in the liver soluble fraction, which decreases.

There is about three to four times as much PMA per milligram nitrogen as there is inorganic mercury in the liver soluble proteins, after two hours. In the kidney the PMA per milligram nitrogen is only twice that for mercuric ion, after two hours.

The percent of both PMA and mercuric ion in the mitochondria and microsomes of both kidney and liver remains fairly constant. The PMA in these fractions was slightly higher in both organs. In terms of mercury per milligram nitrogen PMA is nearly one and a half to twice that found for inorganic mercury in the 1 and 2 hour incubation periods for both the mitochondria and microsomes.

#### The Nitrogen Content of the Subcellular Fractions in Control and Mercury Treated Kidney and Liver Slices

The nitrogen content of the subcellular fractions from control incubated kidney and liver slices as a function of time is not significantly different from that after PMA or inorganic mercury incubation (Figures 19 to 24). The nitrogen content in the nuclear fraction increased with time while the soluble fraction shows a loss of nitrogen. However, the nitrogen content in the nuclear fraction of kidney slices when incubated in PMA remained constant throughout the time of incubation.



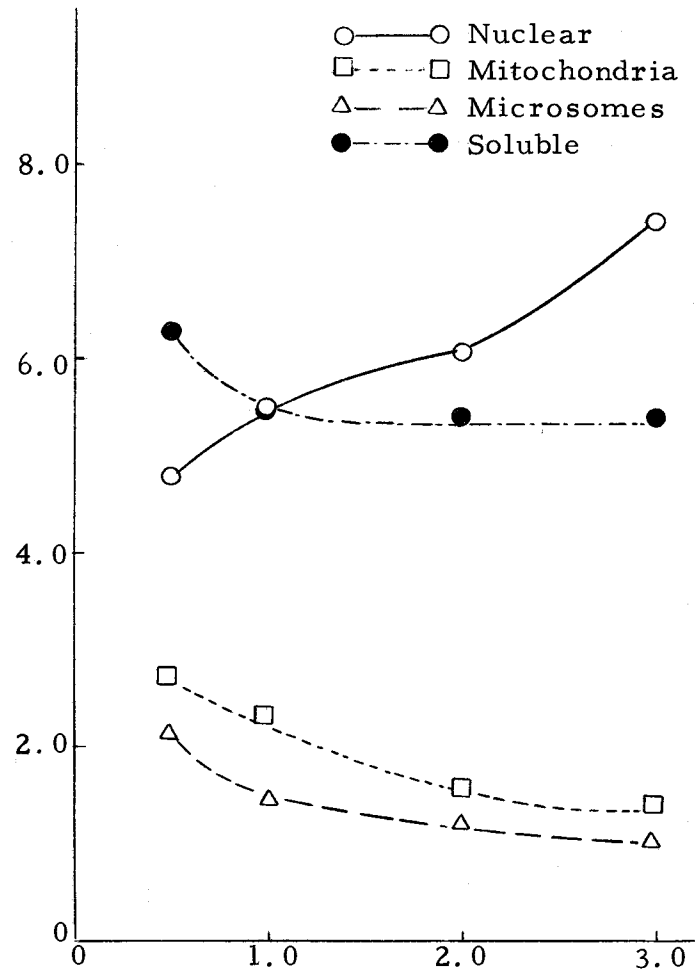


Figure 19. The nitrogen content in the subcellular fractions of control liver slices.

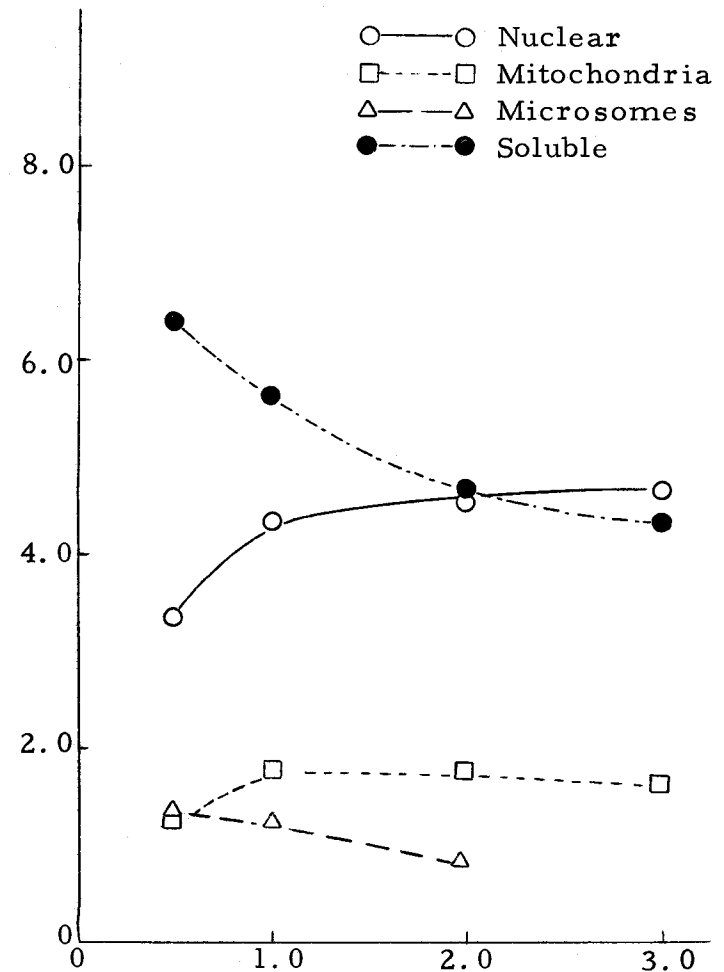


Figure 20. The nitrogen content in the subcellular fractions of control kidney slices.

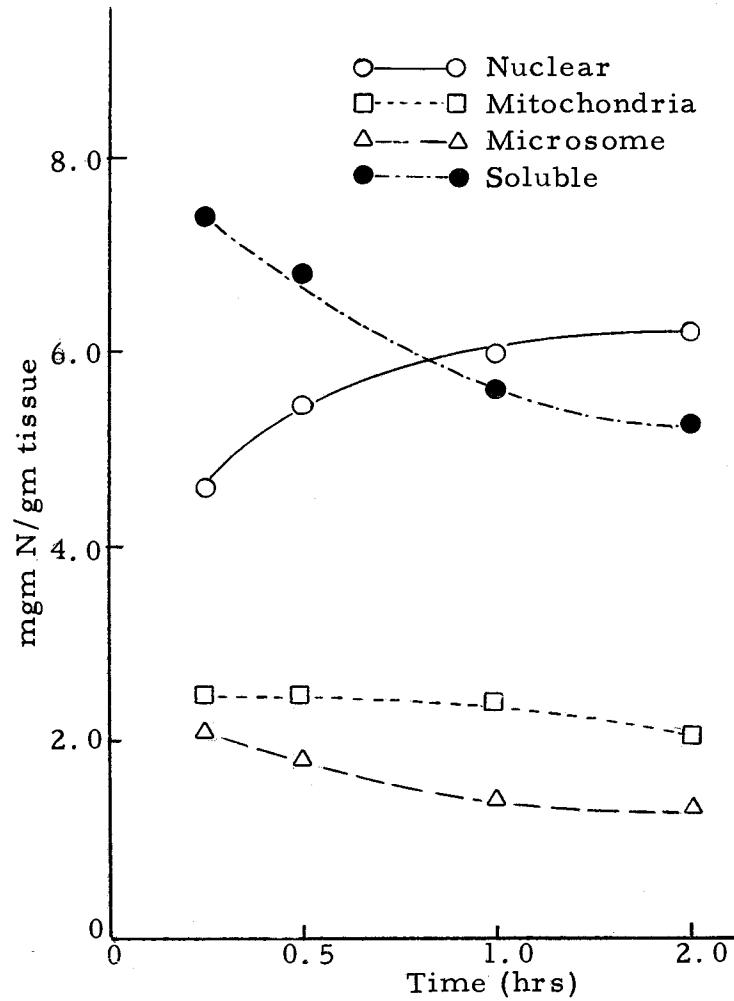


Figure 21. The nitrogen content in the sub-cellular fractions of PMA treated liver slices.

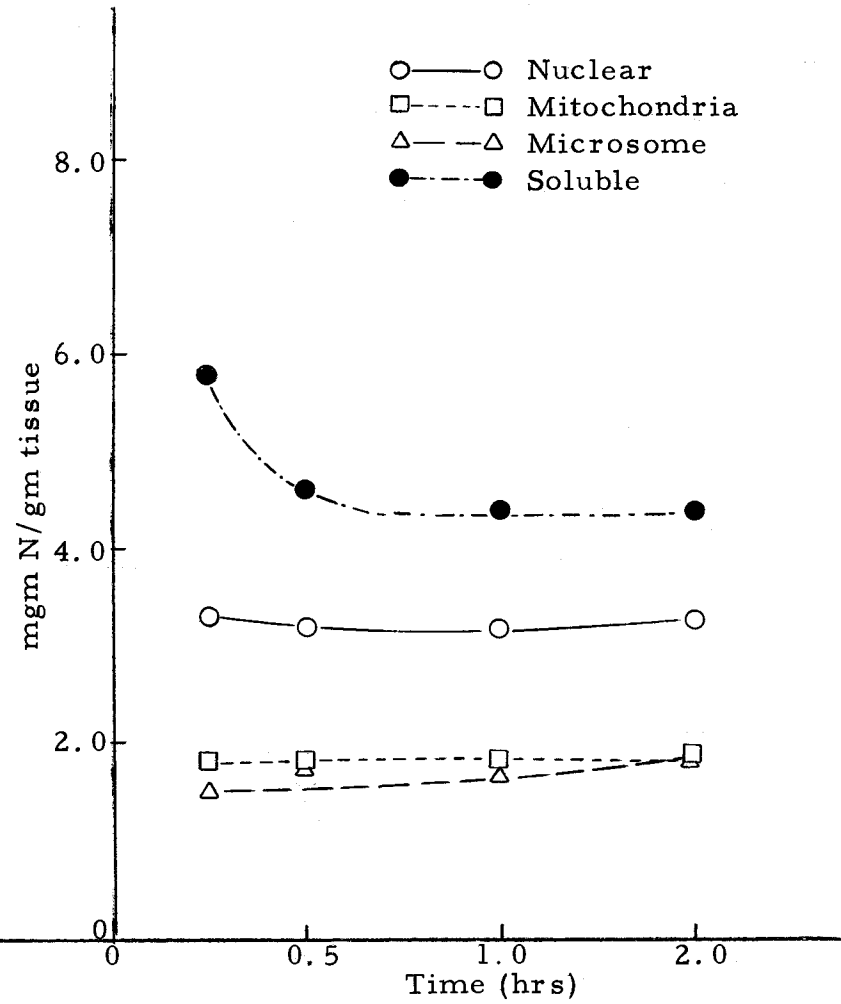


Figure 22. The nitrogen content in the sub-cellular fractions of PMA treated kidney slices.

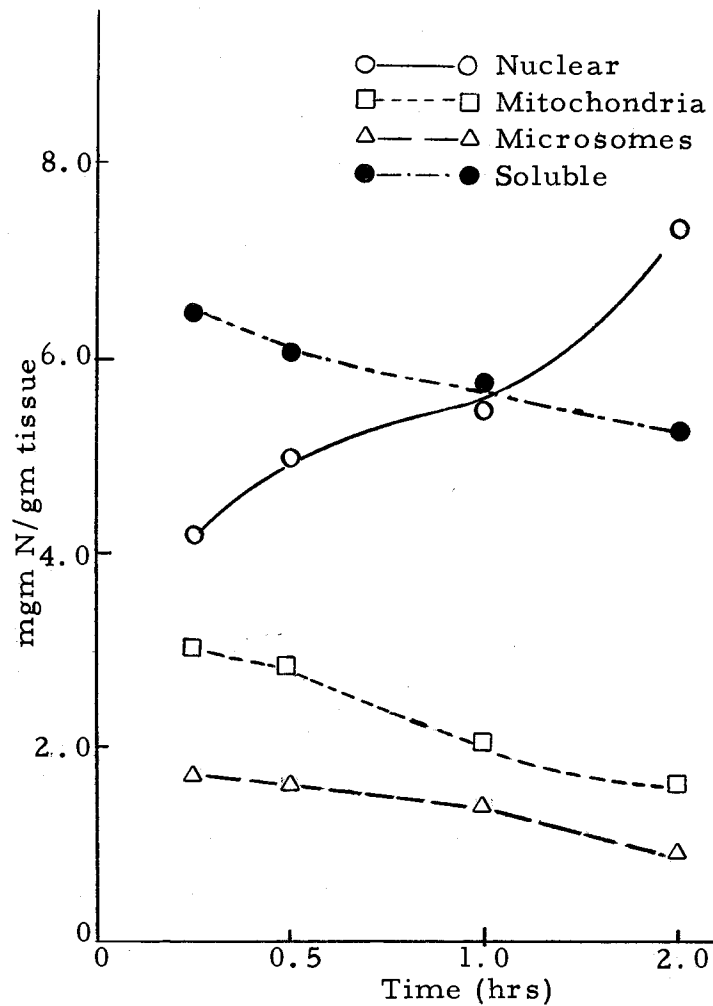


Figure 23. The nitrogen content in the sub-cellular fractions of inorganic mercury treated liver slices.

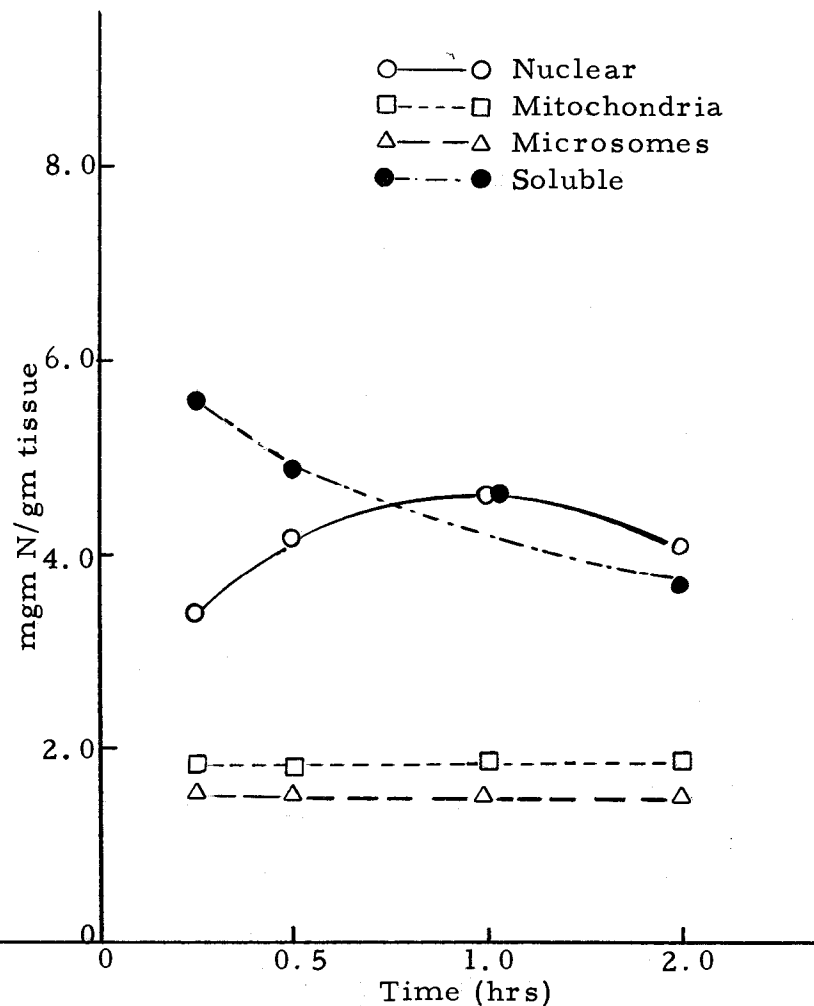


Figure 24. The nitrogen content in the sub-cellular fractions of inorganic mercury treated kidney slices.

Sephadex G-100 Elution Patterns and the Mercury Binding  
of the Soluble Proteins from Liver and Kidney Slices

The optical density elution patterns for liver soluble proteins from 60 centimeter Sephadex columns show a large peak at 50 to 60 milliliters elution volume (Figure 25). There was a second peak or plateau at 65 to 110 milliliters and a third peak at about 200 milliliters. No significant shift of peaks was found with binding of PMA and mercuric salts as shown in Figures 24 and 25.

The elution patterns of TCA and heat precipitable proteins also shows a large peak at 50 to 60 milliliters (Figure 29). The second peak was not resolved completely from the first but shows up as a shoulder in the range of 65 to 110 milliliters. The analysis was not carried out past the second peak. Figure 29 also compares a typical optical density elution pattern plotted with the pattern determined by the weight of the protein in the fractions. It can be seen that in the shoulder or second peak the extinction coefficient for 260 millimicron light is less than in the first peak. The optical density profiles are used because they are easy to determine and reproduce, but they are not a true representation of the amount of protein present in any particular area of the pattern.

The elution pattern of the kidney soluble proteins was determined only by the method of optical density. The elution curves for kidney were similar to those of liver except for a much higher peak

at 205 milliliters elution volume (Figure 33).

There is a difference in the degree of binding of PMA and mercuric ion in the liver soluble proteins. Figure 26, 27, 30, and 31 show that there were also differences in binding of the same mercury compound in different areas of the elution pattern. In the area of the first peak PMA is bound one and a half to two times the amount of inorganic mercury. In the second peak PMA is bound 2.5 to five times the amount of inorganic mercury.

Figures 28 and 32 show the binding per unit amount of protein or the specific binding of PMA and  $\text{Hg}(\text{oAc})_2$ . The high differential binding of PMA in the proteins of the second peak is clear. Figure 28 shows a marked specific binding of both PMA and mercuric salts from 125 to 170 milliliters in the elution pattern. Some binding is seen at 190 milliliters, which does not coincide with the protein peak in this area.

The specific binding of the mercurials on the basis of protein weight (Figure 32) shows that the binding of PMA in the area of the second peak is the same when the liver slices were incubated in  $10^{-4}$  and  $2 \times 10^{-4}$  molar PMA. However, the binding of inorganic mercury increases in the liver soluble proteins when the liver slices were incubated in twice the concentration of mercuric acetate solution. Also, both PMA and mercuric ion increase their specific binding in the first peak when incubated in  $2 \times 10^{-4}$  molar solutions.

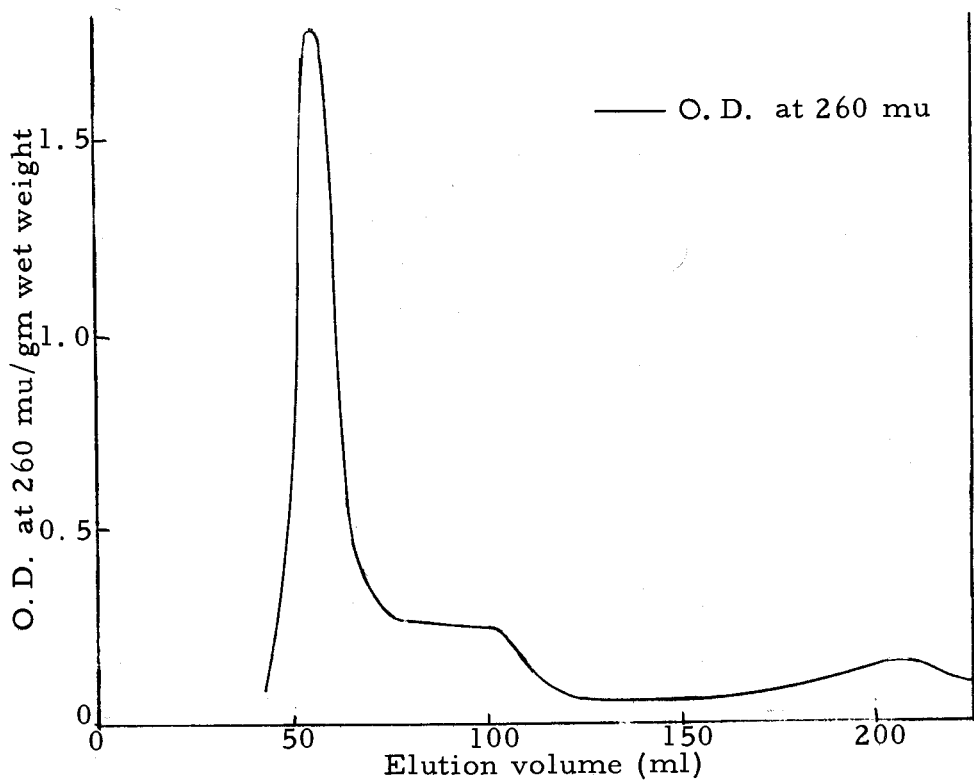


Figure 25. Sephadex G-100 O.D. elution pattern of control rat liver soluble proteins.

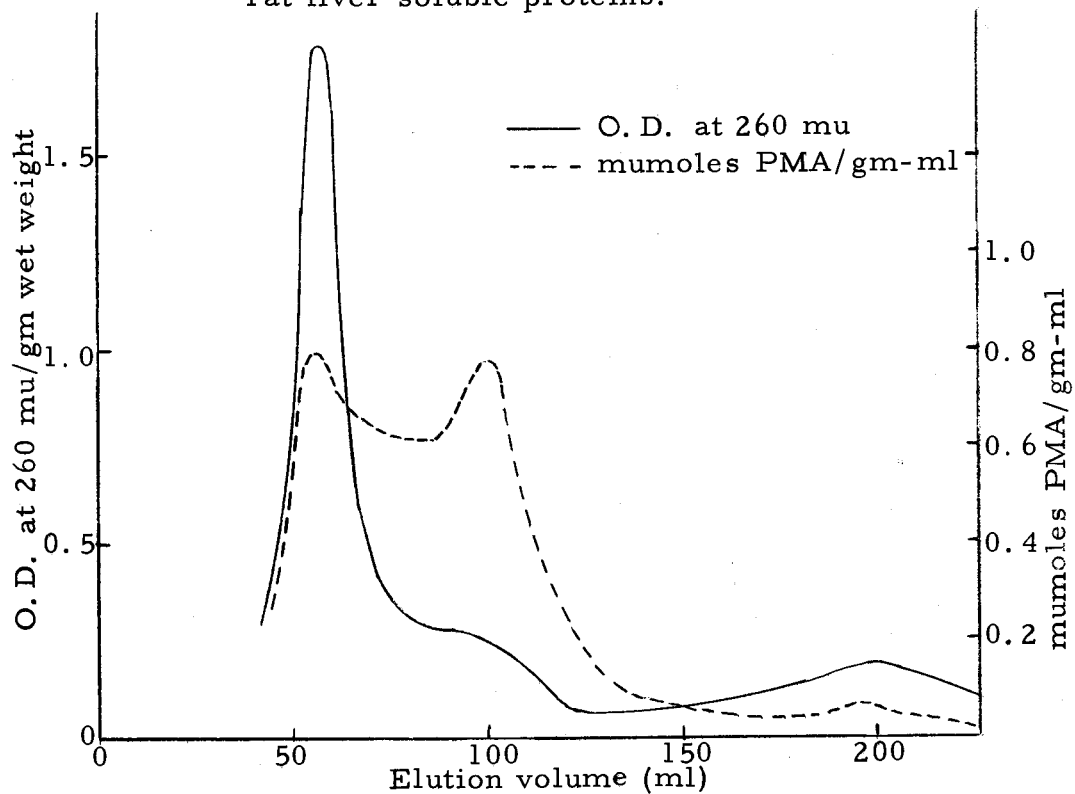


Figure 26. Sephadex G-100 O.D. elution pattern of PMA bound rat liver soluble proteins.

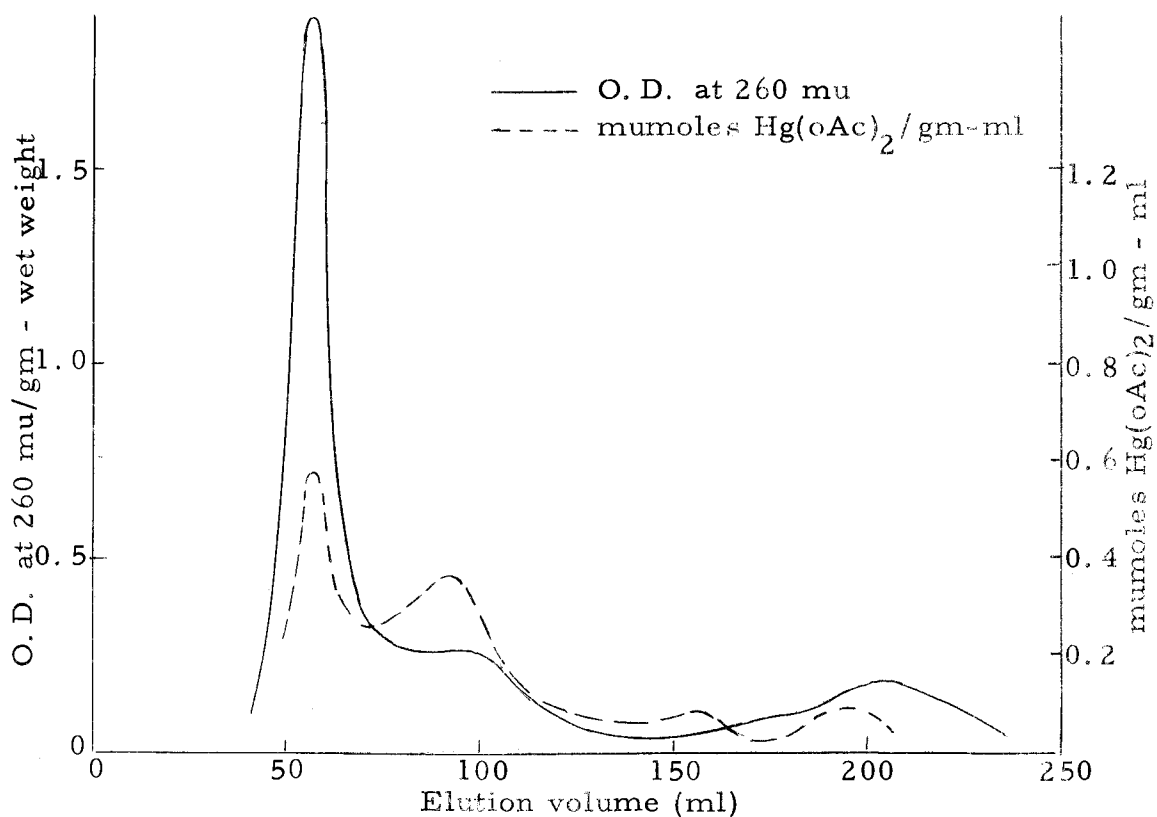


Figure 27. Sephadex G-100 O. D. elution pattern of inorganic mercury bound rat liver soluble proteins.

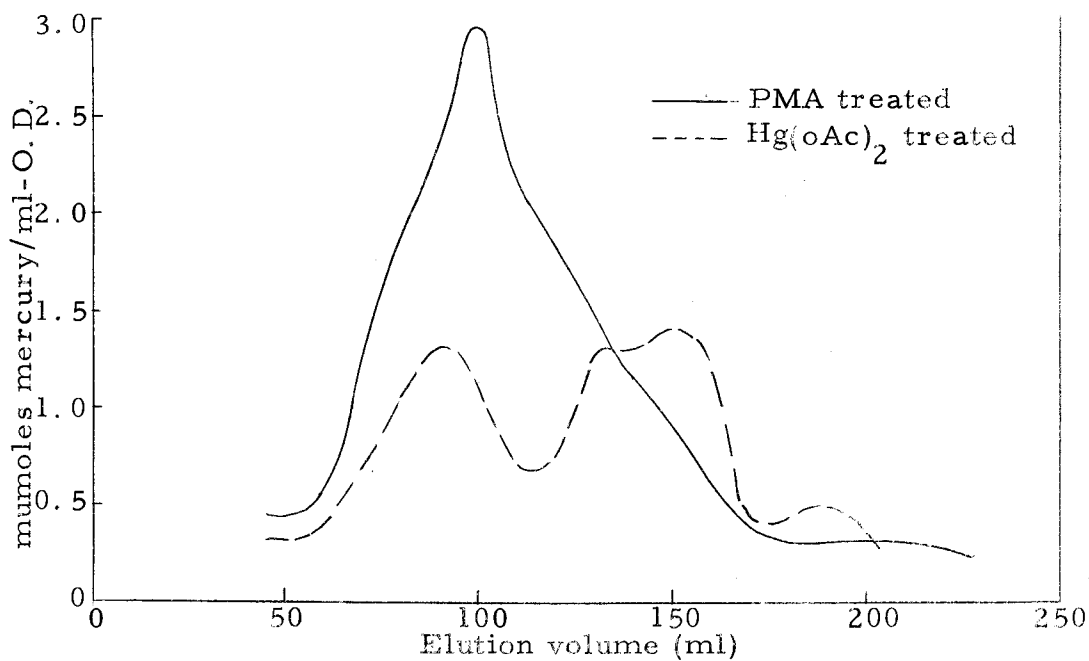


Figure 28. The O. D. specific binding of PMA and inorganic mercury in rat liver soluble proteins.

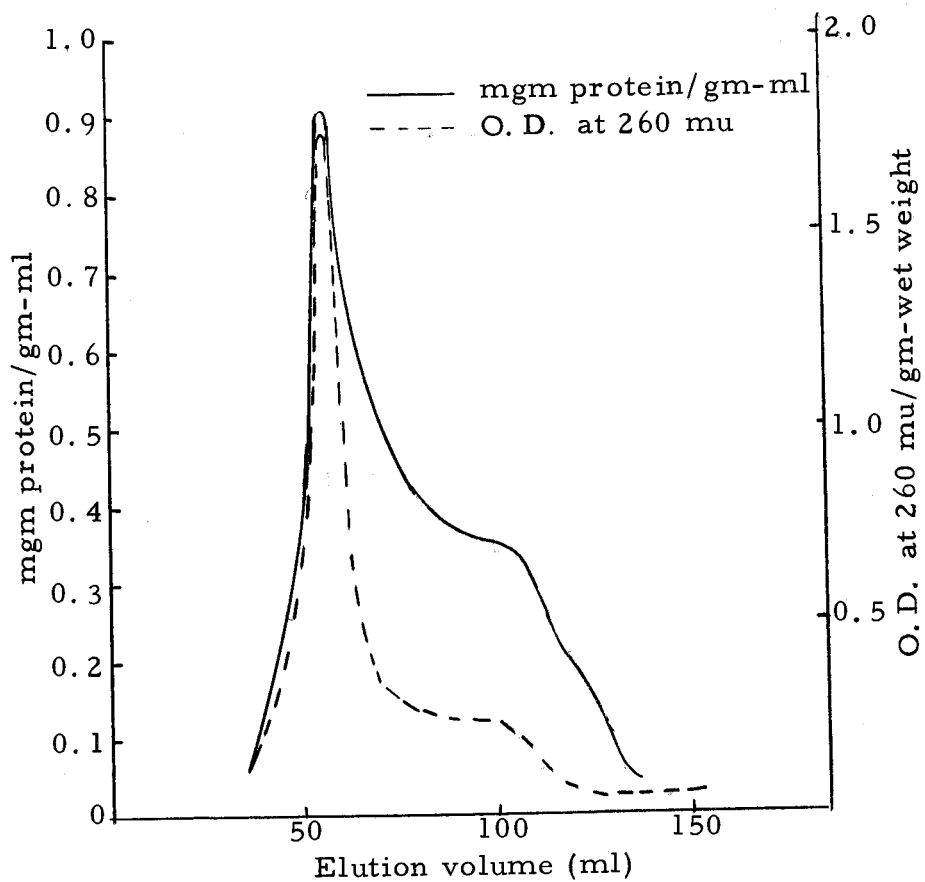


Figure 29. Sephadex G-100 precipitable protein elution pattern of control rat liver soluble proteins.



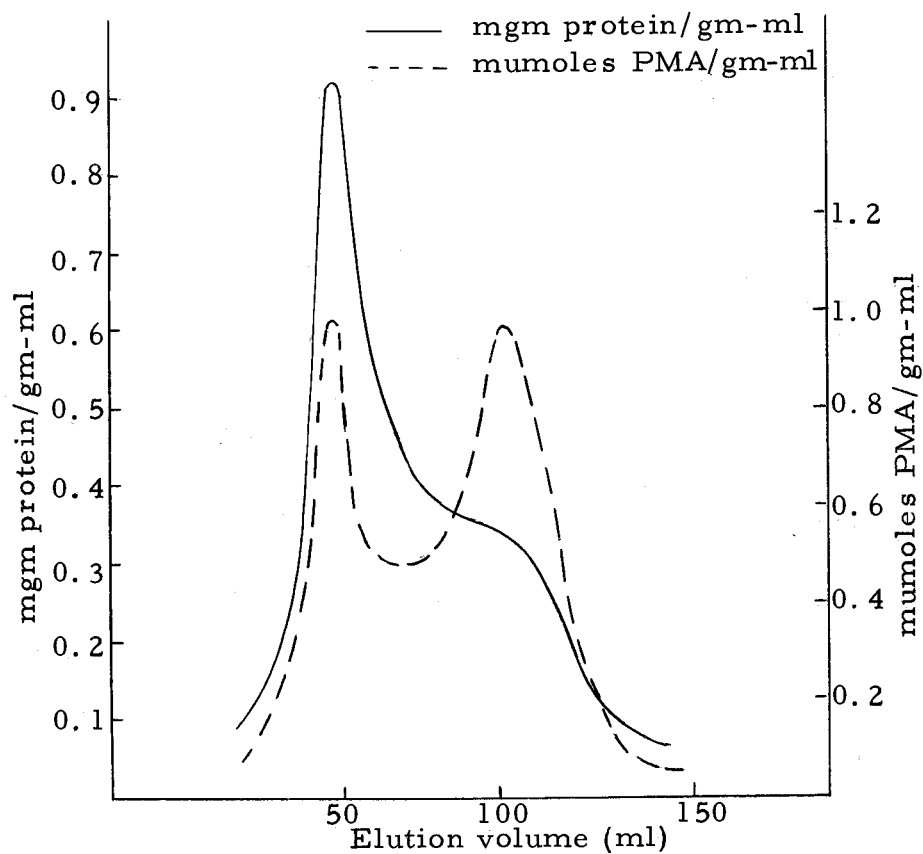


Figure 30. Sephadex G-100 precipitable protein, elution pattern of PMA bound rat liver soluble proteins.

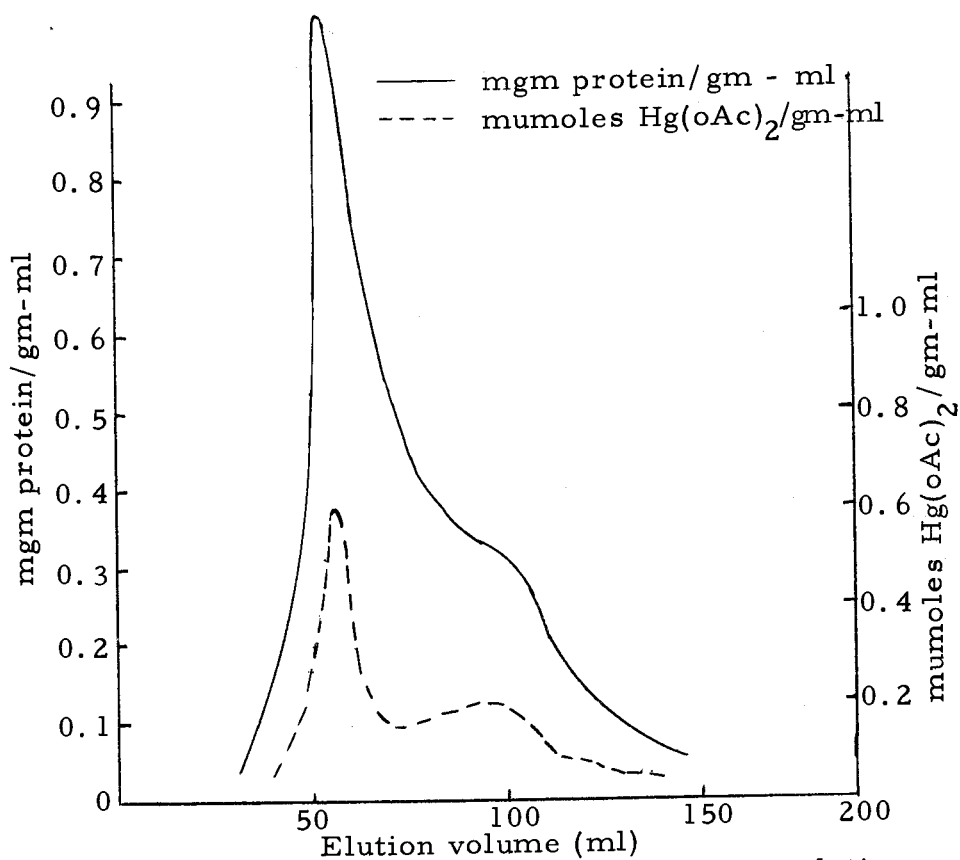


Figure 31. Sephadex G-100 precipitable protein elution pattern of inorganic mercury bound rat liver soluble proteins.

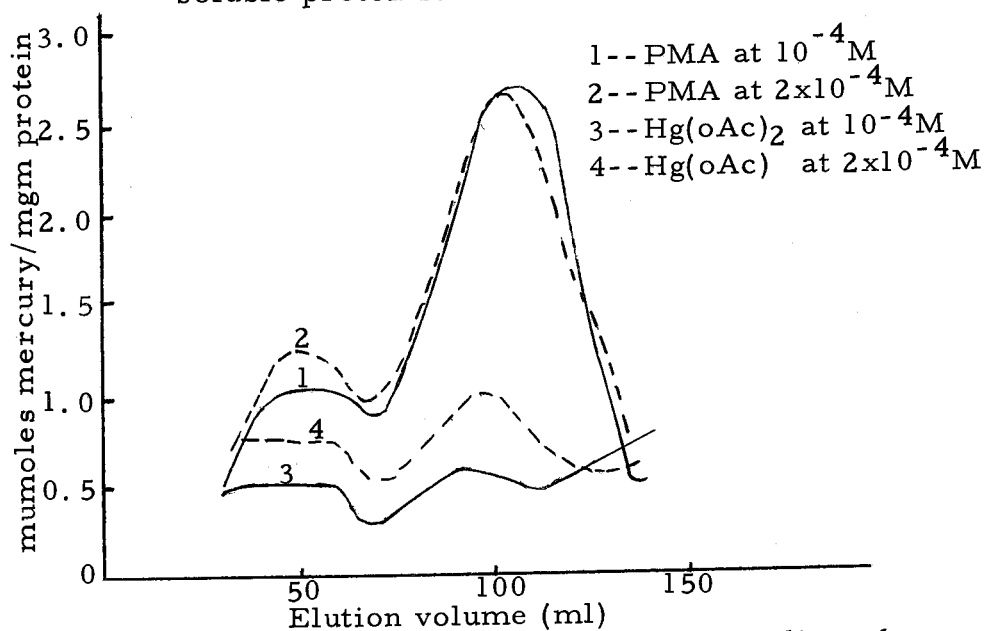


Figure 32. The precipitable protein specific binding of PMA and inorganic mercury in rat liver soluble proteins.

The specific binding of PMA is about double that of inorganic mercury in the first peak at both concentrations.

The binding of PMA and  $\text{Hg}(\text{oAc})_2$  in the kidney soluble proteins is shown in Figures 34 and 35. The proteins in the second peak bind approximately twice the amount of PMA as compared to inorganic mercury. At the elution volume of 150 milliliters there is a marked binding of both PMA and  $\text{Hg}(\text{oAc})_2$  and to about the same extent.

The specific binding curves of PMA and mercuric ion for kidney soluble proteins also show that twice the amount of PMA was bound to protein in the second peak than that of inorganic mercury. There is a very high specific binding of both mercurials at 150 milliliters, with the inorganic mercury being slightly higher.

According to Whitaker (51) the molecular weights of the proteins in the first peak of the elution pattern for the soluble proteins are of the order of 100,000 or greater. The composition of the first peak may be small microsomes that were not sedimented at 35,000 X G or large protein complexes, both of which have been completely excluded from the Sephadex G-100 gel particles. A decreasing order of molecular weight occurs with increasing elution volume. The proteins in the area of the shoulder or second peak are of the order of 15,000 to 30,000 molecular weight. The last peak represents peptides and amino acids (elution volume of 180 to 220 milliliters.) The trough in the elution pattern, between the second and the last

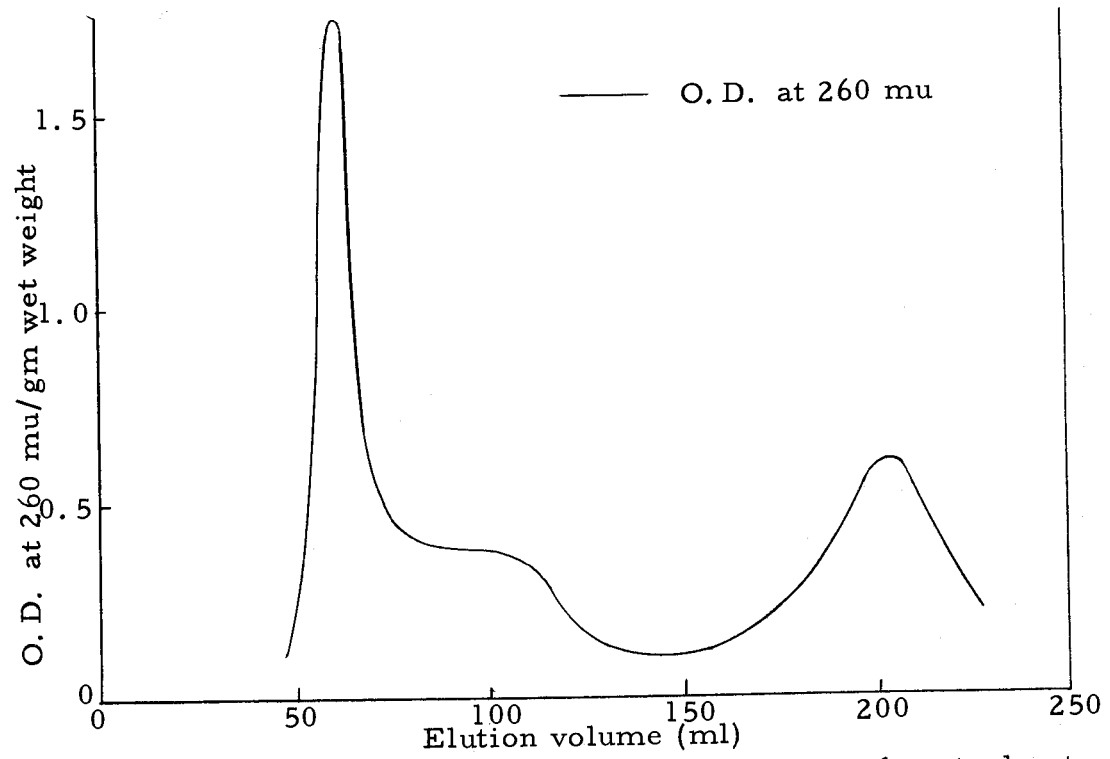


Figure 33. Sephadex G-100 O.D. elution pattern of control rat kidney soluble proteins.

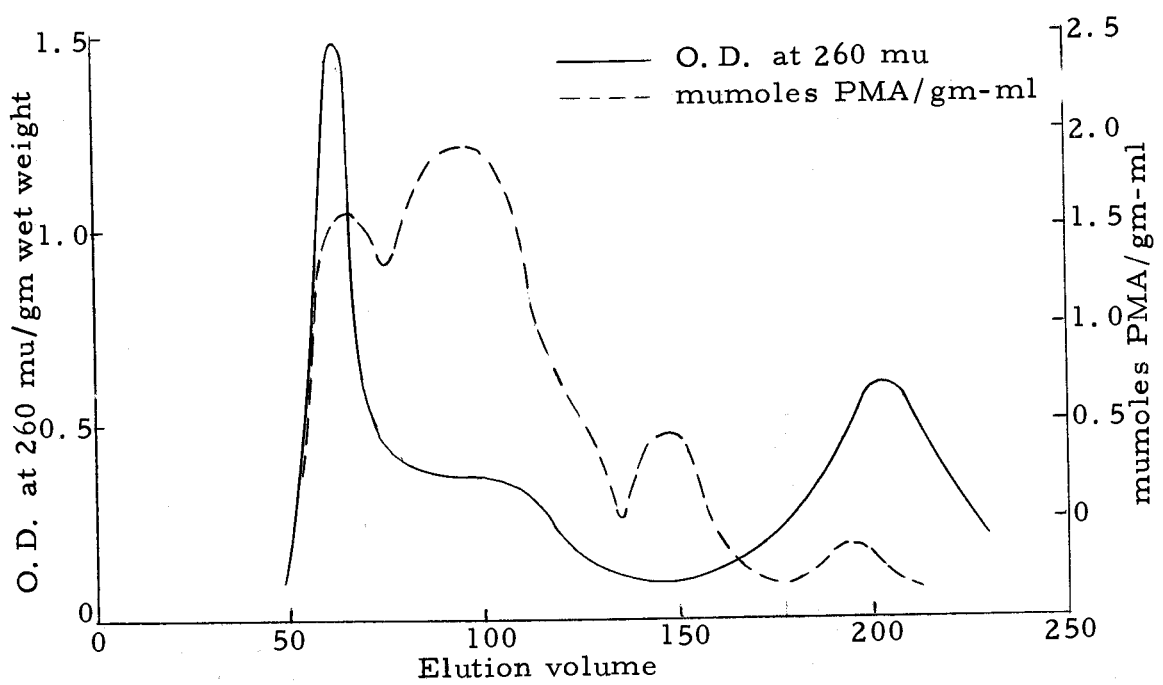


Figure 34. Sephadex G-100 O.D. elution pattern of PMA bound rat kidney soluble proteins.

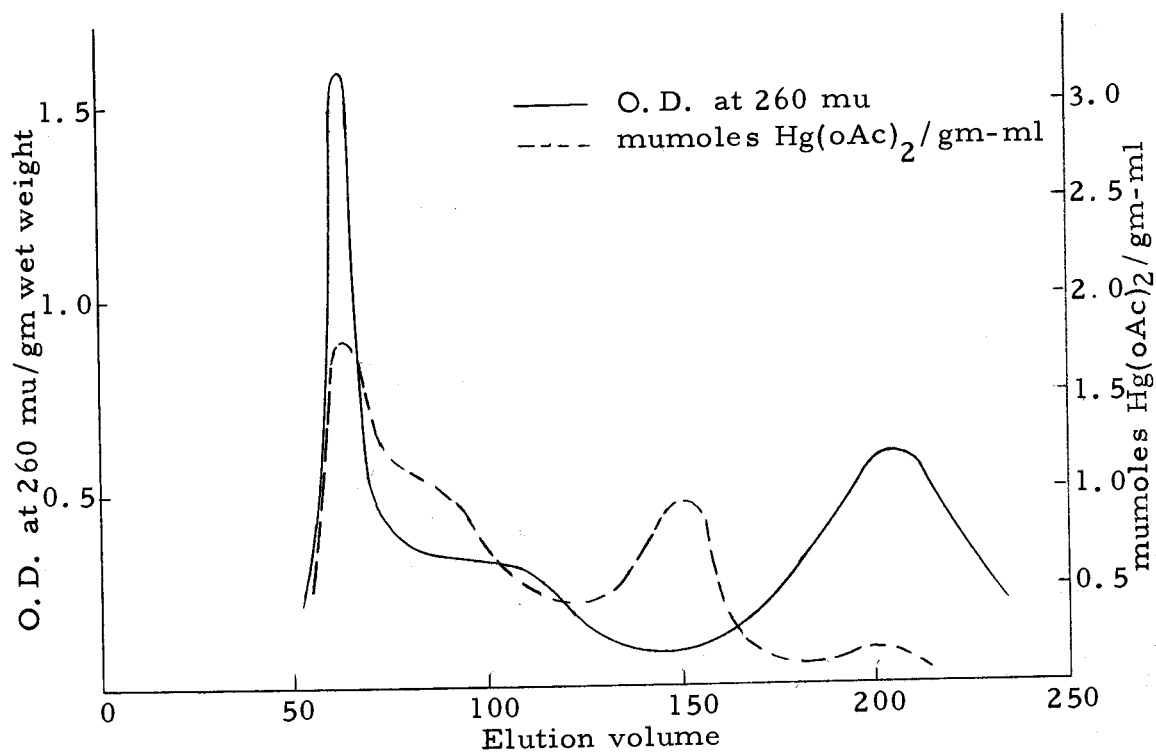


Figure 35. Sephadex G-100 O.D. elution pattern of inorganic mercury bound rat kidney soluble proteins.

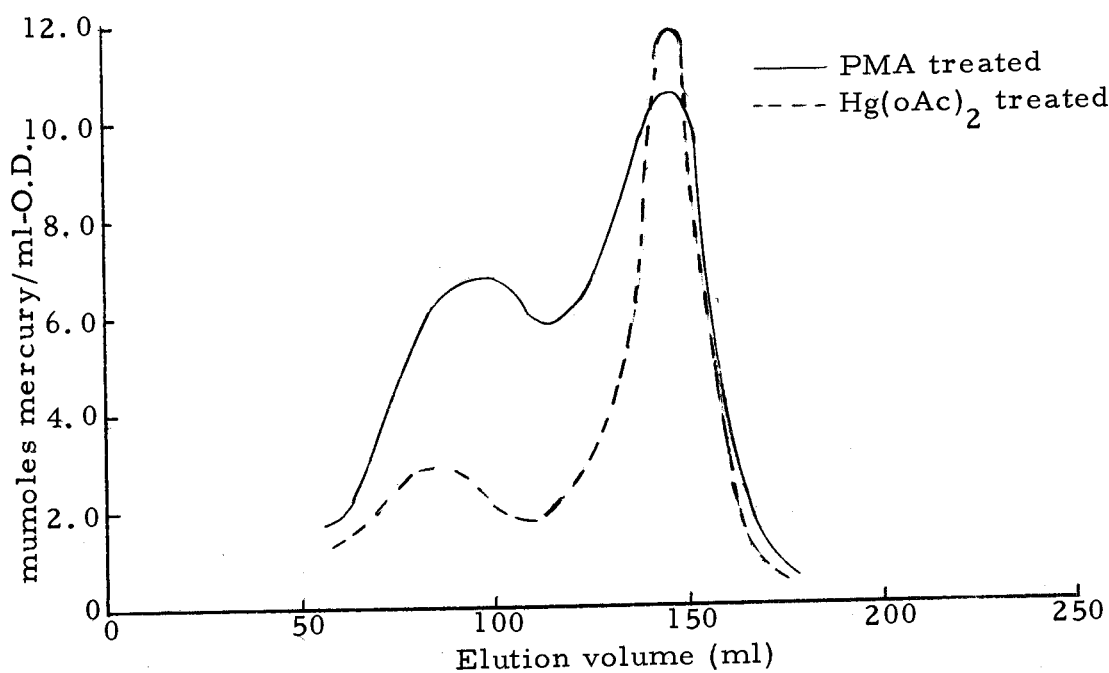


Figure 36. The O.D. specific binding of PMA and inorganic mercury in rat kidney soluble proteins.

peak corresponds to polypeptides with molecular weights of about 1,000.

Sephadex G-100 Elution Patterns and the Mercury Binding of the Incubation Solution Proteins Leached from Liver Slices

The optical density elution patterns for the incubation solution proteins shows a peak between 50 and 60 milliliters and corresponds to that found in the soluble proteins (Figures 37 to 40). There was some indication of a second peak or shoulder in the range of 80 to 90 milliliters comparable to that found in the soluble protein patterns, but this was not obvious as the optical density begins to rise immediately with an indication of a peak at 150 to 180 milliliters. The optical density keeps rising until it reaches the peak found at the 210 to 220 milliliter area. It is believed that this last peak corresponds to that found in the soluble protein elution patterns.

It is interesting to note that the first peak for protein leached from the PMA incubated liver slices is much higher than for protein leached from liver slices incubated in control or inorganic mercury solutions. The optical density in the range of 95 to 135 milliliters rises slightly for the PMA and mercuric ion treated slices, whereas the optical density for the control incubation solution proteins keeps falling and rises sharply from 135 to 145 milliliters.

The mercury binding curves for PMA and mercuric ion are

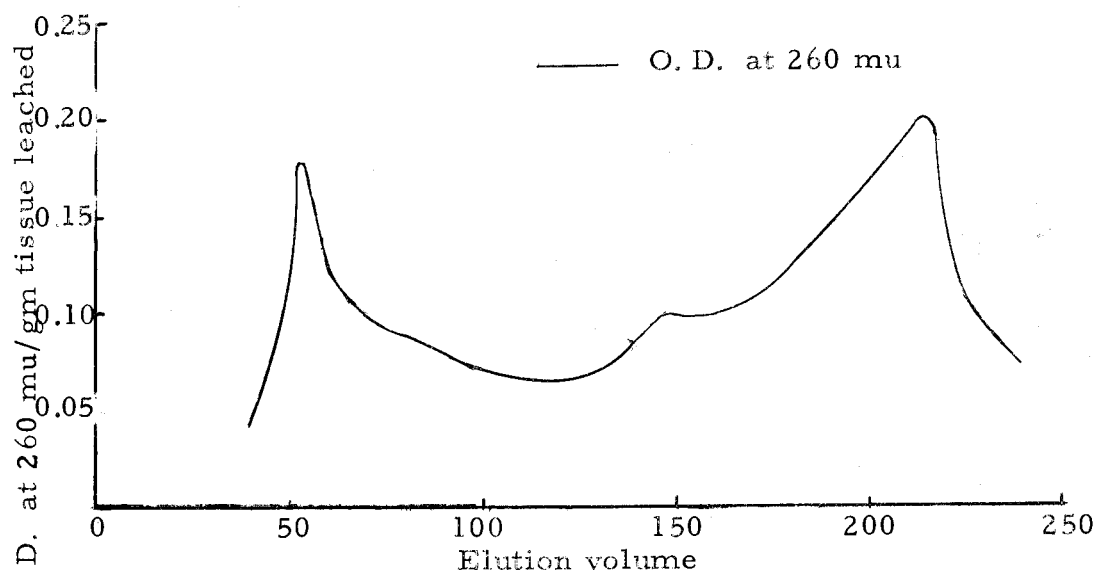


Figure 37. Sephadex G-100 O. D. elution pattern of control proteins leached from rat liver slices.

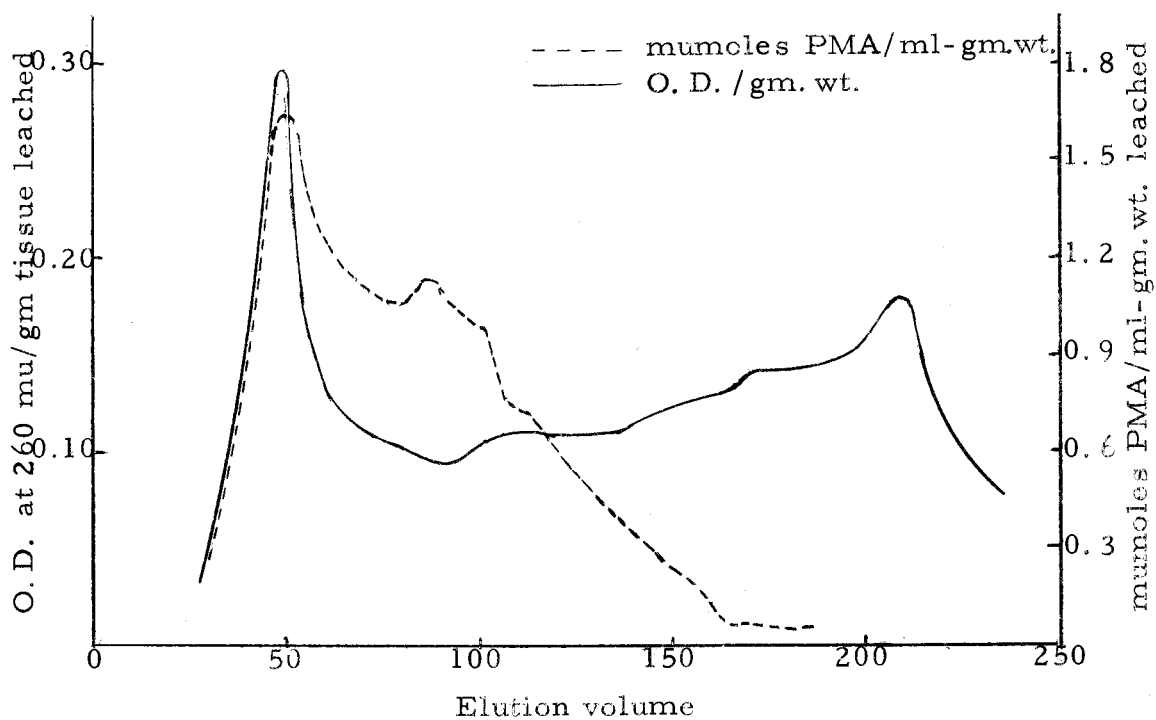


Figure 38. Sephadex G-100 O. D. elution pattern of PMA bound proteins leached from rat liver slices.

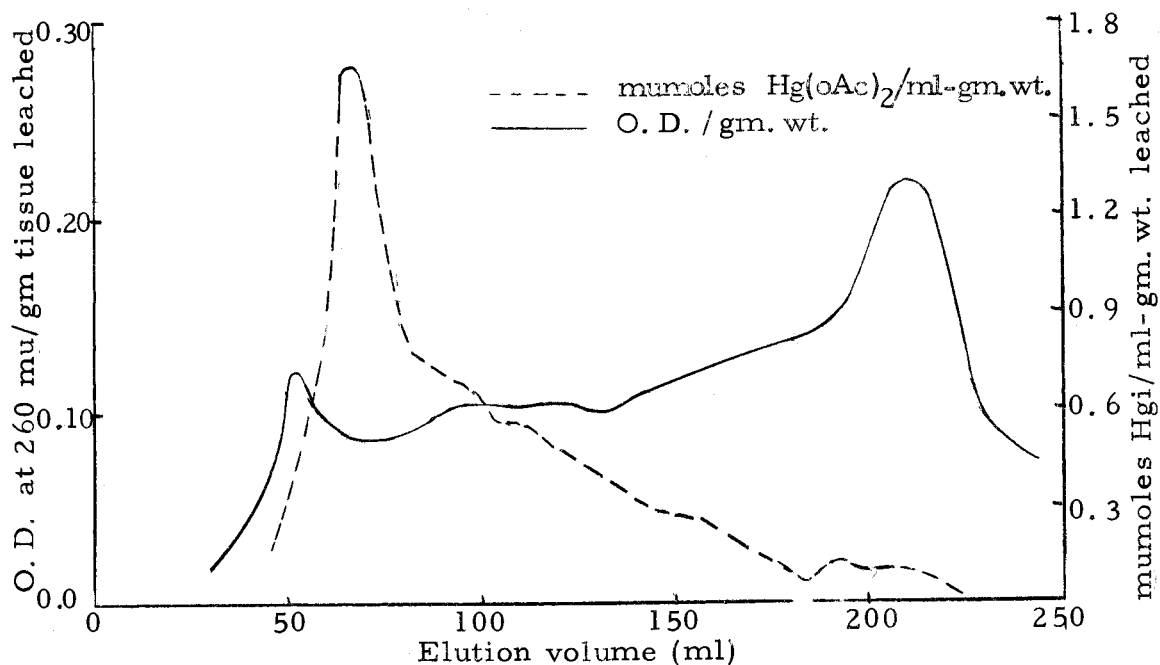


Figure 39. Sephadex G-100 O. D. elution pattern of inorganic mercury bound proteins leached from rat liver slices.

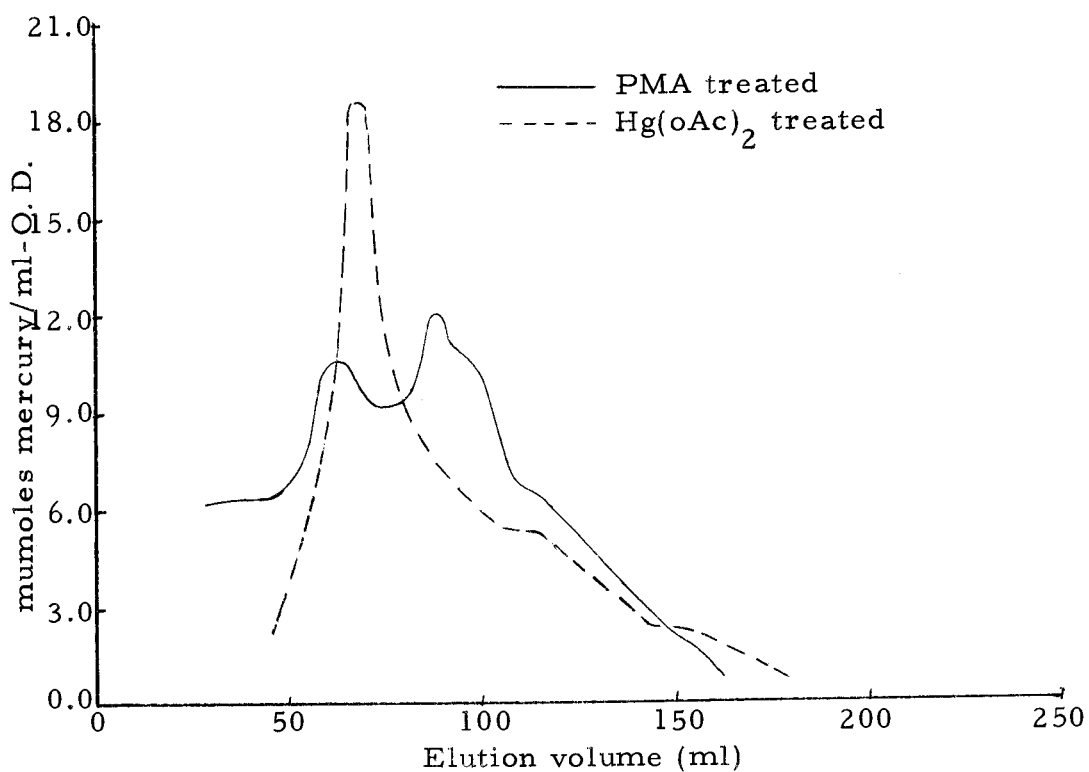


Figure 40. The O. D. specific binding of PMA and inorganic mercury in proteins leached from rat liver slices.



fairly similar except for a peak appearing at 80 to 120 ml for the PMA incubation solution. Also, it is interesting that, for one gram of liver slices incubated there is almost the same amount of mercury per milliliter present in the first peak, whether the slices were incubated in PMA or mercuric ion.

The specific binding of mercuric salts in the first peak (Figure 40) is nearly double that of PMA. In the region of 80 to 100 milliliters PMA has a specific binding of the protein almost double that found for mercuric ion and forms a separate specific binding peak. It is assumed that the high specific binding of PMA in the 80 to 100 milliliter range corresponds to its high specific binding in the soluble proteins in the 85 to 110 milliliter area.

The results indicate that there is a greater permeability of the cell membranes to large molecular weight proteins of 100,000 or greater (seen in the first peak of the elution profile) after PMA incubation than after control or mercuric acetate incubation. The amino acids and small peptides seem to be able to leach out whether the liver slices were incubated in the mercurial or control solutions.

#### Polyacrylamide Gel Electrophoresis Patterns of the Soluble Proteins from Control and Mercury Incubated Kidney Slices

It can be seen that, after standardizing the peak intensities of the electrophoresis patterns to the intensity of peak 2, there is a

definite decrease in the peak intensities for the PMA incubated samples. Peaks 5 through 8 in the soluble protein pattern from PMA treatment show about a 20 percent decrease in intensity as compared to the respective peaks in the control patterns. Peak 9 shows an even greater loss of intensity, about 30 percent (Table 2).

Values for the intensities of the peaks are different in the two experiments. The reasons for this difference are not clear but can possibly be attributed to a lack of complete destaining of the samples in Experiment 1. However, regardless of the error involved in the procedure, it is assumed that the results obtained for the peak intensities of one of the samples in either experiment are comparable to the results from other samples in the same experiment.

The spacer slurry and the spacer gel are used purely as an anti-convectant in which the concentration of the sample takes place electrophoretically. The small-pore gel acts not only as an anti-convectant but serves as a molecular sieve (41). If the assumption is made that for a homogeneous solution of a variety of proteins in a specified pH, there will be, on the average, the same specific charge (number of ionized groups per unit length of peptide), then the gel electrophoresis procedure must separate the proteins out on the basis of molecular weight, as well as total charge on the protein. It therefore can be assumed that the molecular weights of the proteins in the area of the peaks 7 to 9 are probably of a higher molecular

Table 2. Major peak intensities, relative to peak no. 2, of the disc polyacrylamide gel electrophoresis patterns for control and mercury treated kidney soluble proteins.

Peak	Control Intensity	Hg(oAc) <sub>2</sub> Intensity	Percent Difference	PMA Intensity	Percent Difference
<u>(Experiment No. 1)</u>					
1	0.66	0.56	-15	0.58	-14
2	1.00	1.00	---	1.00	---
3	1.01	0.97	- 4	0.85	-16
4	1.56	1.39	-11	1.25	-19
5	1.36	1.22	-10	1.15	-12
6	1.65	1.77	+ 7	1.34	-19
7	1.95	2.00	+ 3	1.68	-14
8	2.11	2.32	+ 9	1.74	-18
9	4.18	4.15	- 1	3.05	-27
<u>(Experiment No. 2)</u>					
1	0.61	0.60	- 2	0.59	- 3
2	1.00	1.00	---	1.00	---
3	0.87	0.94	+ 8	0.81	- 7
4	1.67	1.75	+ 5	1.43	-14
5	1.53	1.52	+ 1	1.23	-20
6	1.97	1.91	- 3	1.59	-19
7	2.08	1.89	- 5	1.57	-24
8	1.78	1.76	- 1	1.23	-31
9	2.18	2.22	+ 5	1.33	-39

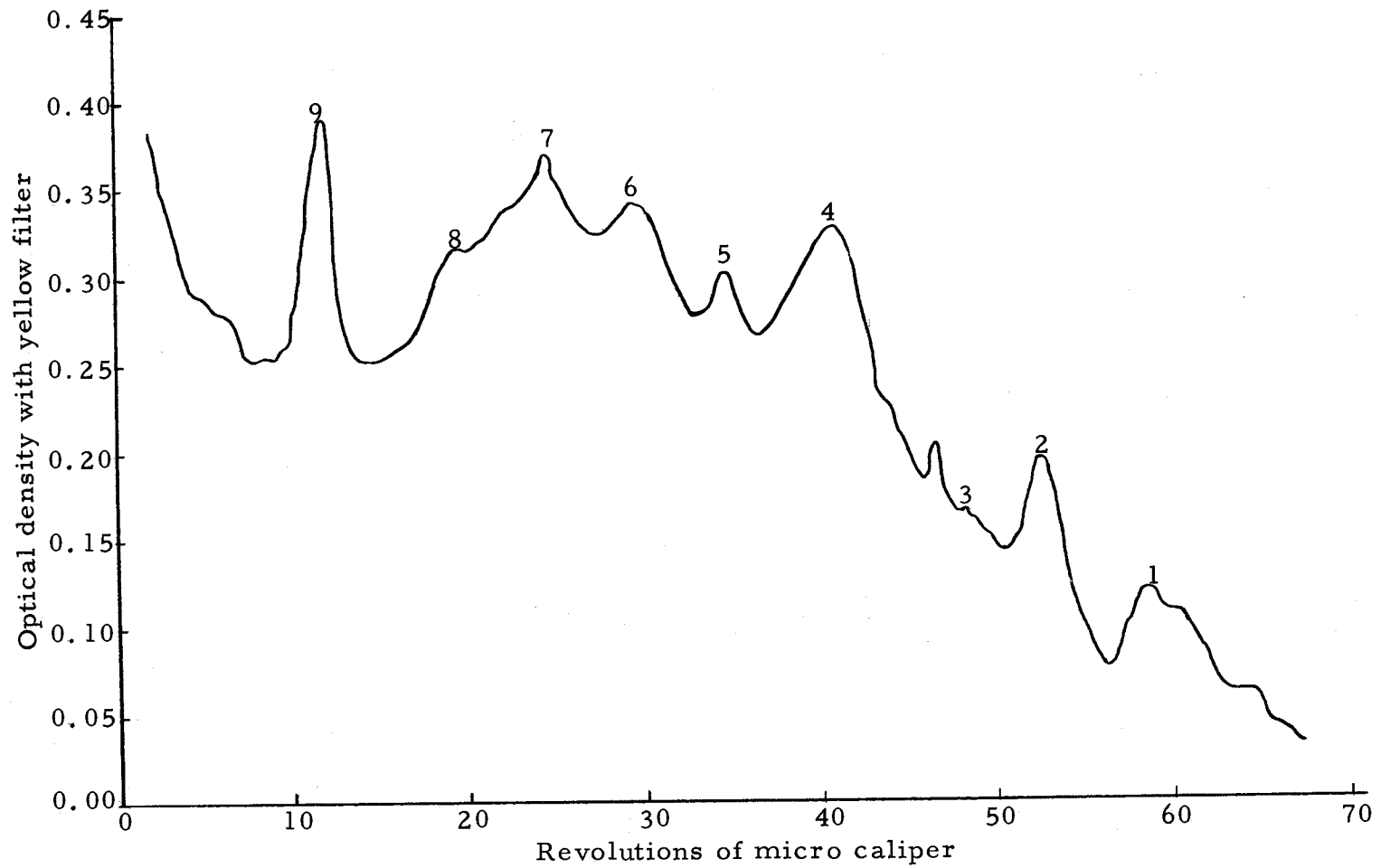


Figure 41. Disc polyacrylamide gel electrophoresis pattern of soluble proteins from control treated kidney slices.

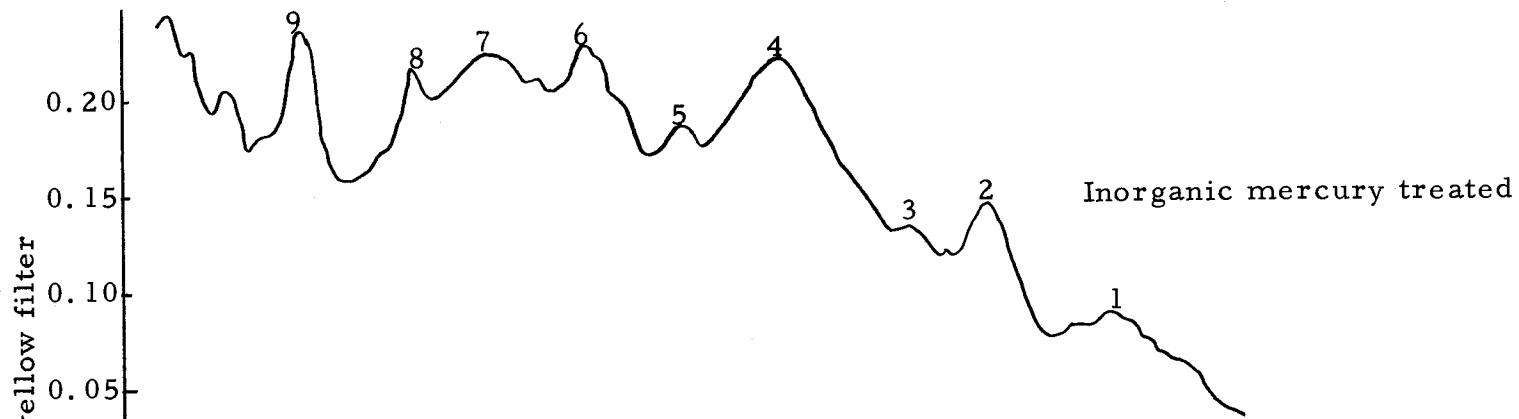


Figure 42

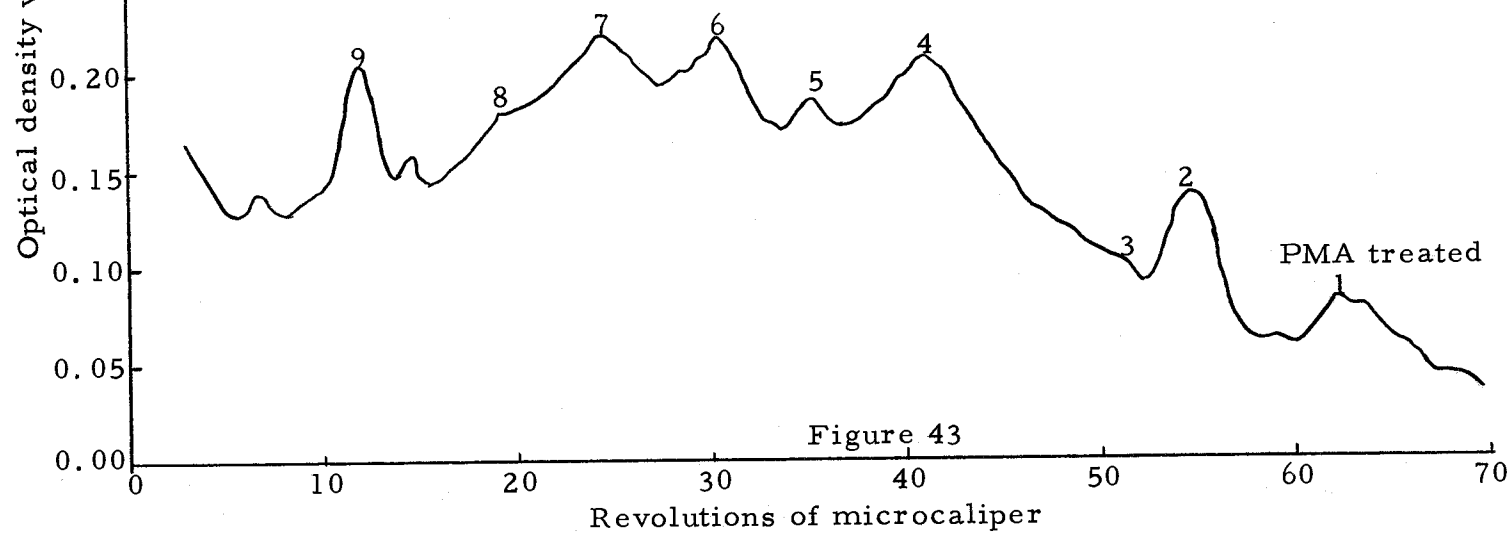


Figure 43

Figure 42 and Figure 43. Disc electrophoresis patterns of soluble proteins from mercury treated kidney slices.

weight than those in the area of peaks 1 and 2.

The continuous smear of a vast number of different types of proteins, each species of which is in a low enough concentration not to be resolvable in the electrophoretic pattern, has resulted in increasing the background optical density, the net effect of which is to increase the optical density of the peaks that were resolvable in the pattern. On the basis of these assumptions, the decrease in the peak intensities (peaks 5 through 9) for the PMA treated samples is interpreted as a general decrease in the concentration of the proteins making up the background optical density and not as a decrease in concentration of the proteins comprising the observable peaks.

The data from the gel electrophoresis patterns indicate a general loss of large molecular weight proteins from the kidney slices incubated in PMA as compared to the results for the control and inorganic mercury incubated kidney slices.

The Effect of Incubation of Kidney Slices in Phenylmercuric Acetate and Mercuric Acetate on the Alkaline Phosphatase Activity in the Microsomal and Soluble Fractions

The extinction coefficient for p-nitrophenol in basic <sup>SOLUTION</sup> pH was determined as 66.6 micromolar per 1.0 optical density. The volume of the reaction mixture being three milliliters, the amount of p-nitrophenolphosphate hydrolyzed per minute per milligram nitrogen was calculated as the product of the extinction coefficient, 3 milliliters,

and the change of optical density per minute-per milligram nitrogen.

The results of the alkaline phosphatase assay on the soluble and microsomal fractions are given in Table 3.

Table 3. Alkaline phosphatase activity of soluble and microsomal fractions from control and mercury treated kidney slices.

Experi- ment	Treatment	mumoles PNP/ min/mg N		Percent different from control	
		Soluble fraction	Microsomal fraction	Soluble fraction	Microsomal fraction
1	Control	73		---	
	PMA	77		6	
	Mercuric ion	120		66	
2	Control	96	3,560	---	---
	PMA	143	3,300	49	- 7
	Mercuric ion	229	3,050	138	-14
3	Control	70	5,450	---	---
	PMA	99	5,150	40	- 6
	Mercuric ion	98	4,880	40	-11
4	Control	43	2,820	---	---
	PMA	66	2,240	53	-21
	Mercuric ion	78	2,070	81	-28
4A*	Control	29	17	---	---
	PMA	51	22	76	
	Mercuric ion	56	20	94	

\* The soluble fraction from the experiment 4 was centrifuged at 150,000 X G for one hour. Activity shown for resulting fractions.

A definite trend is observed in all the experiments. There is an apparent activation of the enzyme in the soluble fraction and an observed inhibition in the microsomes. The inorganic mercury-treated slices produced a more pronounced effect than did PMA.

Figure 45 shows the effect of PMA and inorganic mercury added to the reaction mixture. The addition of PMA in concentrations of  $10^{-3}$  and  $10^{-4}$  molar resulted in no significant effect on the activity of alkaline phosphatase; however, one assay did show some stimulation at a concentration of  $6 \times 10^{-5}$  molar. Inorganic mercury showed a marked inhibition at concentrations higher than  $10^{-6}$  molar. Concentrations higher than  $10^{-4}$  molar resulted in nearly 100 percent inhibition.

Besides determining the pH at which optimum activity of alkaline phosphatase occurred as a routine procedure, it was questioned whether possible binding of mercury (PMA or mercuric ion) to the enzyme would change the pH optimum. There was found to be no change in the pH optimum for the enzyme after incubation of the kidney slices in the mercury solutions, even with the observed activation. The pH optimum curve for a control sample is shown in Figure 44.

As a result of the fact that addition of PMA or inorganic mercury to the reaction mixture did not give the same results as the incubation of the kidney slices with respect to the observed activation phenomenon, the question arose as to whether the observed stimulation was only apparent and that possibly it was a result of a solubilization of the enzyme or that it was bound to a particle that would not sediment at 35,000 X G.



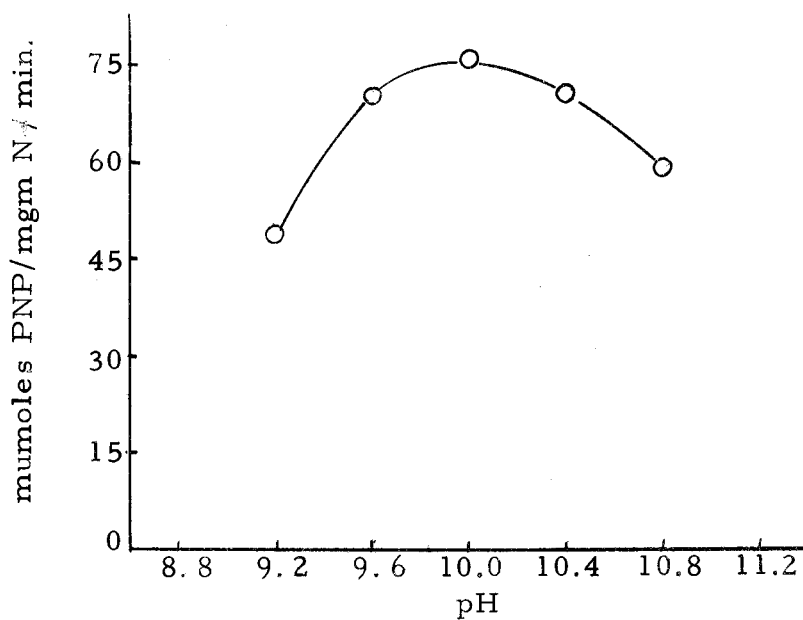


Figure 44. The effect of pH on the activity of alkaline phosphatase from rat liver soluble proteins.

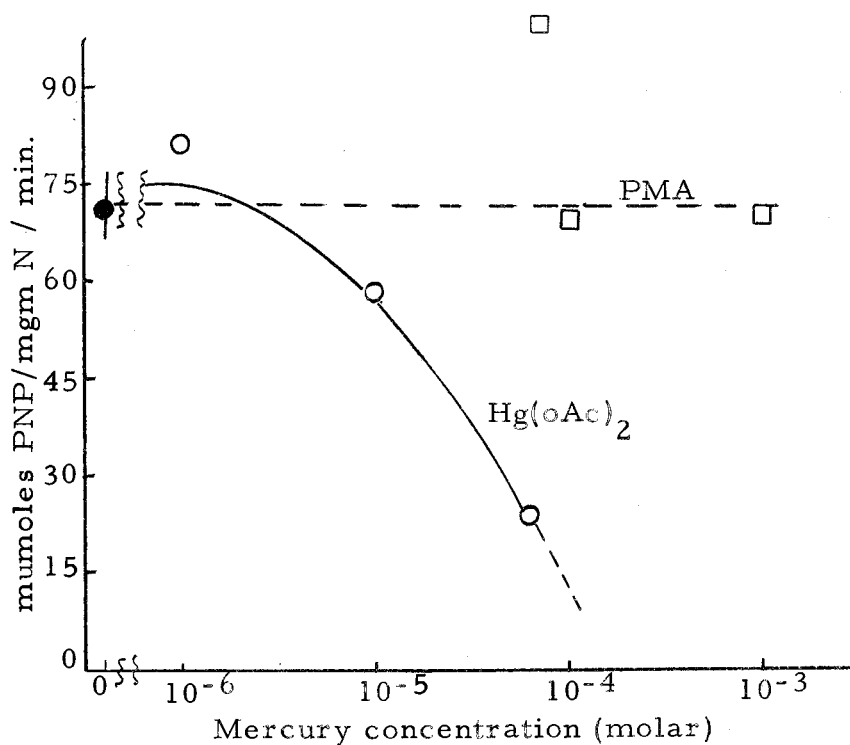


Figure 45. The effect of PMA and inorganic mercury at various concentrations in the reaction mixture on the activity of alkaline phosphatase in the soluble proteins of rat kidney.

The last two experiments, 4 and 4A, seem to indicate that at least some of the activity is soluble. The 35,000 X G soluble fraction was placed in a Beckman Model L-2-50 ultracentrifuge and centrifuged for one hour at 150,000 X G (average). The material sedimented in the form of a pellet was very red in color as compared to the 35,000 X G microsomal pellet which was pale reddish-brown. The 150,000 X G pellet was resuspended in 0.25 molar sucrose and the activity was again determined on both fractions. It can be seen that only about 20 to 30 percent of the activity was sedimented at 150,000 X G for the control as well as for the PMA and mercuric ion samples.

A complete inventory of the alkaline phosphatase in all the subcellular fractions was not carried out.

An analysis of the alkaline phosphatase activity was carried out on the elution fractions of Sephadex G-100 filtration of kidney soluble proteins. The kidney soluble fraction and the elution fractions were prepared as outlined in the section on Sephadex G-100 filtration of liver and kidney soluble proteins.

Figure 46 shows the optical density pattern of kidney soluble proteins and the alkaline phosphatase activity. There was found to be no significant difference in the area of the activity of the enzyme with regard to treatment of the kidney slices with the mercurials. About 15 percent of the total activity of alkaline phosphatase

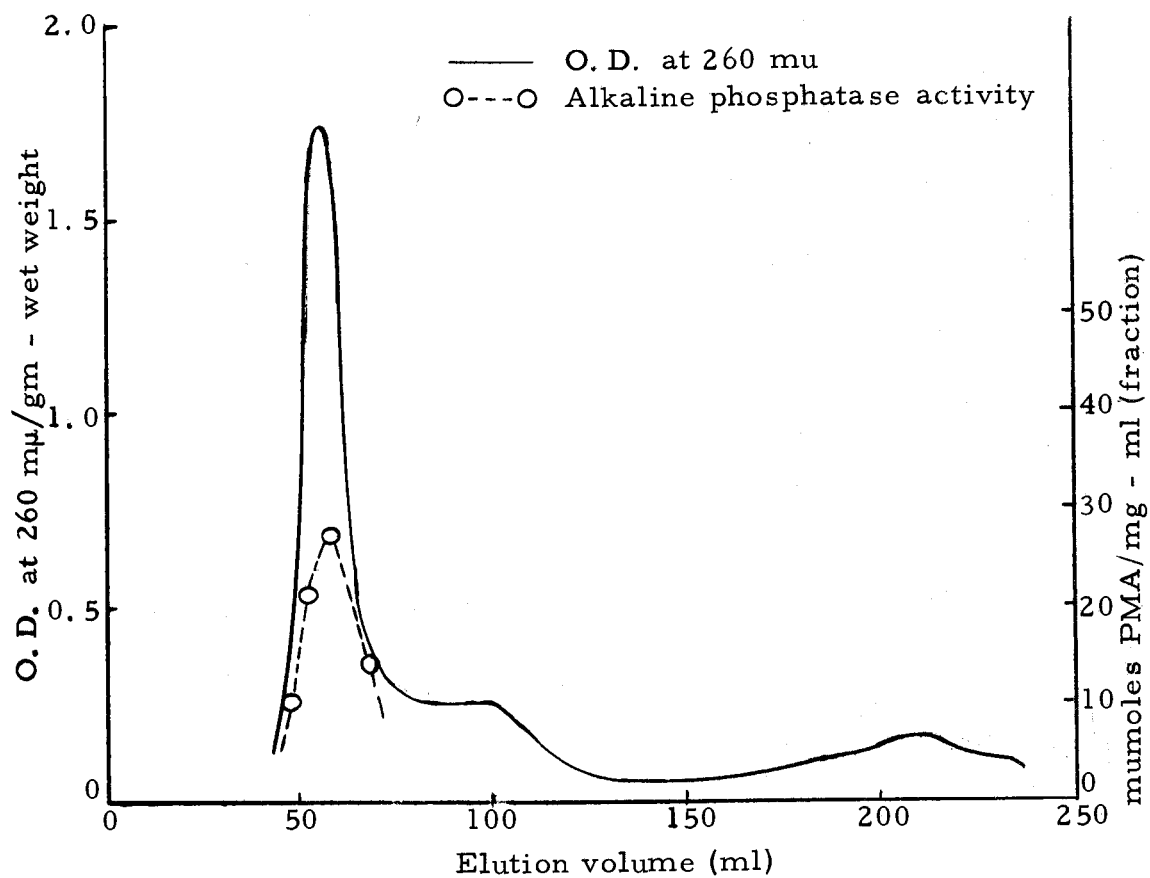


Figure 46. Sephadex G-100 O. D. elution pattern and the distribution of alkaline phosphatase activity after Sephadex G-100 filtration of soluble proteins from control kidney slices.

phosphatase introduced into the column (as the soluble fraction) was recovered in the elution fractions. Addition of solution from the last peak in the pattern did not cause any change in the activity determined from the fractions in the first peak proteins. Because of the low recovery of activity from the Sephadex column, further experiments were not carried out.

## SUMMARY AND CONCLUSIONS

It is apparent that phenylmercuric acetate definitely has the ability to penetrate the cell barriers and to bind to the intracellular particles better than has inorganic mercury. The binding data in the whole tissue slices (Figures 3 and 4) indicate that there is definitely a difference in rate of binding of the mercurials for the case of liver. PMA seems to bind to the mitochondria and microsomes almost twice as much as inorganic mercury for both kidney and liver.

It is seen that for both PMA and inorganic mercury, the highest intracellular binding is in the nuclear fractions (on the basis of tissue weight). It is well known that the nuclear fraction isolated according to the procedure described in the materials and methods section contains cell debris which includes cell membranes and some connective tissue. Therefore, the possibility cannot be eliminated that part of the mercury bound in the nuclear fraction is, in reality, bound to cell membranes and other debris.

It is shown in Figures 9 to 12 that inorganic mercury exhibits a very high binding in the nuclear fraction (percentage of the total mercury bound to the slices) with relatively little in the mitochondria, microsome, and soluble fractions. The question can be raised: why does inorganic mercury have such a tremendous affinity for the nuclei? The answer is, possibly, that much of the bound mercury

is really located in the cell membranes.

Another important trend observed in the subcellular mercury binding curves (Figures 5 to 16) is the initial high values for mercuric ion binding in the soluble fraction. This phenomenon is especially apparent in the subcellular fractions of liver. Demis and Rothstein (10) have found that incubation of rat diaphragm in  $2 \times 10^{-4}$  molar mercuric chloride showed a fast rate of uptake in the first 20 to 25 minutes, after which there was a sharp lessening in rate. They suggested that the diffusion of mercury into the extracellular spaces took place in the first 20 to 25 minutes and that the fixation of mercury to the surface of the cells followed by slow diffusion into the interior explained the second rate of accumulation.

It is therefore possible that the 30 minute and the one hour figures for the mercury binding in the nuclear and the soluble fractions are, to a certain extent, measurements of the mercury content in structures outside of the cell.

The mercury binding data plotted on the basis of nitrogen content show definitely that PMA has a much higher affinity for all the subcellular fractions except the nuclear as compared to inorganic mercury, sometimes as much as twofold. Also, the binding of PMA in the soluble fraction on a basis of nitrogen is 2.5 to 3 times the binding of inorganic mercury.

This stoichiometry ratio of two PMA molecules to one inorganic

mercury ion can be understood on the basis of the fact that PMA carries only one positive charge, whereas the mercuric ion carries two. It is possible that, if the binding sites of PMA and inorganic mercury are the same, it will take twice as much PMA as it would mercuric ion to bind the same number of sites. On the other hand, if the binding sites for mercury in the subcellular fractions other than the nuclear fractions are not saturated at the end of one hour-- as one might so conclude by noticing that the slopes for the rate of mercury binding are nowhere near approaching a plateau when the binding data is plotted on the basis of nitrogen--then it could also be concluded that PMA has gained entrance into the cell much faster than mercuric salts.

In Figures 17 to 22 the nitrogen content of the subcellular components is shown. The most apparent trend observed is the loss of nitrogen in the soluble fraction from the control slices, as well as those incubated in mercury. This phenomenon may be caused by a leaching of proteins from the extracellular fluid causing an apparent loss from the isolated soluble fraction. The reason for the increase (with time) of the nitrogen content of the nuclear fraction is unexplained.

The Sephadex G-100 elution patterns of the soluble proteins of liver show no significant difference for the control samples as compared to those treated with the mercurials. It can be seen, however,

that the specific binding of PMA, in the first peak proteins, is twice as great as that for inorganic mercury for the elution patterns determined by the method of heat and acid precipitation of the proteins. The PMA binding is only slightly greater than inorganic mercury when determined in the optical density patterns. The two methods do not give too close an agreement, but they do show that PMA does bind to a greater extent in the first peak proteins.

The specific binding of the two mercurials in the shoulder of the elution patterns for liver demonstrates the very high specific binding of PMA as compared to mercuric ion. It is also important to note that the proteins in the second peak are saturated by PMA. Incubation of the liver slices in  $10^{-4}$  and  $2 \times 10^{-4}$  molar PMA resulted in nearly the same specific binding. The amount of PMA and inorganic mercury in the first peak proteins was seen to increase with incubation in a double strength solution. Also, the inorganic mercury in the second peak area increased its specific binding. These higher specific binding data for PMA in the elution patterns substantiate the results of the soluble fraction binding in the sub-cellular fraction analysis.

The binding data of the mercurials in the soluble protein elution patterns of kidney (Figures 31 to 34) show essentially similar results for the first and second peak areas. The interesting difference between liver and kidney specific binding of the mercurials is



that there is a very high peak in the area of the optical density pattern showing the least amount of protein and that the specific binding of the two mercurials is essentially the same. The stoichiometry of two PMA molecules to one mercuric ion required to bind the same number of sites does not seem to hold true.

The elution patterns for the proteins leached into the incubation solutions for liver slices indicate that even without treatment with the mercury compounds, there is a considerable loss of protein, the preponderate of which has a small molecular weight (15,000 or less).

This evidence gives support to the results obtained for the nitrogen content of the soluble fractions in Figures 17 to 22. It is interesting that inorganic mercury does not cause a significant change in the nitrogen loss as compared to the control, but PMA does cause an extra loss of some large molecular weight proteins.

The results obtained with the gel electrophoresis patterns of the soluble proteins of kidney slices also seem to indicate that there is a possible loss of large molecular weight proteins due to treatment with PMA as compared to the control or inorganic mercury treatments.

The results obtained for the alkaline phosphatase activity in the soluble and microsomal fractions, after treatment with PMA and inorganic mercury, do not correlate with the specific binding

of the mercurials. The effect of inorganic mercury on the activity of alkaline phosphatase in the soluble fractions is greater than for PMA, but the binding of inorganic mercury is only one-half that for PMA. The same thing can be said about the microsomal fraction. Inorganic mercury, which binds much less than PMA, causes a much greater inhibitory effect in the alkaline phosphatase activity.

Ernster, Siekevitz, and Palade (12) describe the process of formation of microsomes in rat liver homogenates. The microsomes consist of vesicular and tubular fragments of the endoplasmic reticulum that were formed during homogenization. The endoplasmic network breaks down by a pinching-off process into separate vesicles. Each vesicle contains a "quantum" of the soluble material contained inside the reticulum surrounded by a membrane with a set of attached ribonucleo-protein particles. They demonstrated that some microsomal enzymes (NADH-cytochrome reductase, NADH diaphorase, magnesium-activated ATPase, and glucose-6-phosphatase) were either part of the microsomal membranes or bound tightly to them, after treatment of the microsomes with 0.26 percent deoxycholate. After sedimenting the deoxycholate treated microsomes and diluting the deoxycholate concentration in the supernatant, there appeared more sedimentable vesicles which contained NADH-cytochrome c reductase and glucose-6-phosphatase activities. They postulate that these particles arise from aggregation of small micells and individual molecules.

Griffin and Cox (15) found that alkaline phosphatase was bound to light microsomal membranes and was sedimentable after treatment with 0.26 percent deoxycholate. The specific activity of the enzyme in this fraction was the highest of any subcellular fraction.

In this report ultracentrifugation of the supernatants obtained at 150,000 X G formed a pellet that contained a very low specific activity of the enzyme as compared to the pellet from the 35,000 X G centrifugation. The supernatant after ultracentrifugation showed about a 20 percent decrease in the specific activity of alkaline phosphatase. It seems that there is a true solubilization of the enzyme with the mercury compounds causing an increased effect.

It is possible that the pinching-off process of the endoplasmic reticulum during homogenization is not complete and some of the soluble material in the lumina of the reticulum is lost to the supernatant. Both inorganic mercury and PMA would have an effect on the reticulum membranes, the pinching-off process being slightly impaired and resulting in an enhanced alkaline phosphatase activity in the supernatant.

The essence of this work can be summarized by saying that just as phenylmercuric acetate has a somewhat greater ability to distribute itself in the animal body as compared to mercuric ion (cited extensively in the literature review), it also has a better ability to penetrate cell membranes and distribute itself more evenly

throughout the subcellular structures.

Phenylmercuric acetate also has an ability to increase the membrane permeability of cell membranes to large molecular weight proteins, whereas mercuric ion exhibits no such effect. This enhanced loss of protein nitrogen was described by Kleinzeller and Cort (22) for both p-chloromercuribenzoate and mercuric chloride incubation of kidney slices. The results of this report indicate that inorganic mercury does not have an effect on the membrane permeability of cells to protein, which are in disagreement with the results of Kleinzeller and Cort.

Both phenylmercuric acetate and mercuric acetate possibly have an effect on the membranes of the endoplasmic network that slightly inhibits the pinching-off process of the reticulum and allows more of the intralumina fluid to be released into the soluble fraction, the net result of which is an apparent activation of alkaline phosphatase. The trend of an increased activity of alkaline phosphatase in the soluble fraction in the order of control, PMA, and mercuric ion treated samples is directly proportional to the decrease of the enzyme activity in the microsome fractions in the same order. It should be pointed out that the activity of alkaline phosphatase in the whole homogenate, the nuclear fraction, and the mitochondria fraction was not determined and that there is the possibility of the enzyme activity having its genesis in some subcellular fraction other than the microsomes.

## BIBLIOGRAPHY

1. Agus, Saul G., Rody P. Cox and Martin J. Griffin. Inhibition of alkaline phosphatase by cysteine and its analogues. *Biochimica et Biophysica Acta* 118:363-370. 1966.
2. Battigelli, M. C. Mercury toxicity from industrial exposure. A critical review of the literature. Part I. *Journal of Occupational Medicine* 2:337-344. 1960.
3. Berlin, Maths. Renal uptake, excretion, and retention of mercury. II. A study in the rabbit during infusion of methyl- and phenyl-mercuric compounds. *Archives of Environmental Health* 6:626-633. 1963.
4. Berlin, Maths and Sten Gibson. Renal uptake, excretion, and retention of mercury. I. A study in the rabbit during infusion of mercuric chloride. *Archives of Environmental Health* 6:617-625. 1963.
5. Clarkson, T. W. and L. Magos. Studies on the binding of mercury in tissue homogenates. *Biochemical Journal* 99:62-70. 1966.
6. Clarkson, T. W., A. Rothstein and R. Sutherland. The mechanism of action of mercurial diuretics in rats; the metabolism of  $^{203}\text{Hg}$ -labeled chlormerodrin. *British Journal of Pharmacology and Chemotherapy* 24:1-13. 1965. (Abstracted in *Chemical Abstracts* 62:10999a. 1965)
7. Cohen, E. M. Further experiments on the mechanism of action of mercurial diuretics. *Acta Physiologica et Pharmacologica Neerlandica* 3:59-71. 1953.
8. Cotten, L. H. Hazards of phenylmercuric salts. *Journal of Occupational Medicine* 4:305-309. 1947. (Abstracted in *Chemical Abstracts* 42:3506e. 1948)
9. Davis, Baruch J. Disc electrophoresis. II. Method and application to human serum proteins. *Annals of the New York Academy of Sciences* 121:404-427. 1964.
10. Demis, Dermot J. and Aser Rothstein. Relationship of the cell surface to metabolism. XII. Effect of mercury and copper on glucose uptake and respiration of rat diaphragm. *American Journal of Physiology* 180:566-574. 1955.

11. Dzurik, R. and B. Krajci-Lazary. Mechanism of action of mercury compounds in the kidneys. *Archives Internationales de Pharmacodynamie et de Therapie* 135:1-8. 1962. (Abstracted from *Chemical Abstracts* 56:12229d. 1962)
12. Ernster, Lars, Philip Siekevitz and George E. Palade. Enzyme-structure relationships in the endoplasmic reticulum of rat liver. *Journal of Cell Biology* 15:541-562.
13. Farah, A. and F. Koda. Action of mercurial diuretics on urinary sodium concentration and urine volume. *Journal of Pharmacology and Experimental Therapeutics* 113:256-261. 1955.
14. Frisell, Wilhelm R. and Leslie Hellerman. Sulfhydryl character of d-amino acid oxidase. *Journal of Biological Chemistry* 225:53-62. 1957.
15. Griffin, Martin J. and Rody P. Cox. Sub-cellular localization of rat kidney alkaline phosphatase. *Nature* 204:476-478. 1964.
16. Heimbürg, A. V. and L. Schmidt. The difference of resistance in male and female rats against chronic mercury poisoning. *Arzneimittel-Forschung* 9:321-324. 1959.
17. Hirade, Junkichirō. The inhibitory effect of some -SH reagents on the oxidative phosphorylation in the succinate system. *Journal of Biochemistry (Japan)* 39:165-174. 1952. (Abstracted in *Chemical Abstracts* 46:9140i. 1952)
18. Hughes, Walter L. A physicochemical rationale for the biological activity of mercury and its compounds. *Annals of the New York Academy of Sciences* 65:454-460. 1957.
19. Hunter, F. R. Permeability of erythrocytes to sugars. I. Effects of butyl alcohol and related studies. *Journal of Cellular and Comparative Physiology* 60:243-262. 1962.
20. Iannaccone, Angelo and Dario Gremigni. Alkaline phosphatase of the serum in chronic occupational mercury poisoning. *Riforma Medica* 74:1116-1118. 1960. (Abstracted in *Chemical Abstracts* 55:2938A. 1961)
21. Johnson, M. J. Isolation and properties of a pure yeast polypeptidase. *Journal of Biological Chemistry* 137:575-586. 1941.

22. Kleinzeller, A. and J. H. Cort. Mechanism of action of mercurial preparations on transport processes and the role of thiol groups in the cell membrane of renal tubular cells. *Biochemical Journal* 67:15-24. 1957.
23. Kosmider, S., A. Zurkowski and A. Wegiel. The effect of  $\text{HgCl}_2$ , KCN, and CO on alkaline phosphatase of granulocytes. *Polskie Archiwum Medycyny Wewnetrznej* 35:477-81. 1965. (Abstracted in *Chemical Abstracts* 64:13039g. 1966)
24. Lehman, Arnold J. Chemicals in foods: A report to the association of food and drug officials on current developments. II. Pesticides. Dermal toxicity. *Associated Food and Drug Officials U. S. Quarterly Bulletin* 15:122-133. 1951. (Abstracted from *Chemical Abstracts* 46:2703g. 1952)
25. Lundgren, K. D. and A. Swensson. Some organic mercury compounds used as fungicides. *Journal of the American Industrial Hygiene Association* 21:308-311. 1960.
26. Maizels, M. and Mary Remington. The effects of mercaptomerin on the water and cation exchanges in slices of rat tissue. *Journal of Physiology* 143:283-299. 1958.
27. Martin, Howard F. and Newton H. Reid. Hypoproteinemia as protection in mercuric chloride poisoning. *Proceedings of the Society for Experimental Biology and Medicine* 78:863-865. 1951.
28. Mathies, James C. Preparation and properties of highly purified alkaline phosphatase from swine kidneys. *Journal of Biological Chemistry* 233:1121-1127. 1958.
29. Melani, F. and A. Guerritore. Continuous optical determination of alkaline phosphatase. *Experientia* 20:464-66. 1964.
30. Miller, V. L., P. A. Klavano and Elizabeth Csonka. Absorption, distribution, and excretion of phenylmercuric acetate. *Toxicology and Applied Pharmacology* 2:344-352. 1960.
31. Morris, Roy O. Unpublished research on disc polyacrylamide gel electrophoresis techniques. Corvallis, Oregon, Agricultural Experiment Station, Dept. of Agricultural Chemistry, 1965.

32. Mudge, Gilbert H. Electrolyte and water metabolism of rabbit kidney slices: Effect of metabolic inhibitors. *American Journal of Physiology* 167:206-223. 1951.
33. Nygaard, Agnar P. Essential groups in DPN-linked lactic dehydrogenase. *Acta Chemica Scandinavica* 10:397-407. 1956.
34. Pershin, G. N. and L. I. Shcherbakova. Mechanism of antibacterial action of mercurials. *Farmakologiya i Toksikologiya* 21:51-56. 1958. (Abstracted from *Chemical Abstracts* 52:20405d. 1958)
35. Piedrafeta, F. Ponz, M. Lluch Trull and I. Alemany. Inhibition of intestinal absorption of sugars by mercuric ion. *Revista Espanola de Fisiologia* 13:265-274. 1957. (Abstracted in *Chemical Abstracts* 52:16619g. 1958)
36. Prickett, C. S., Edwin P. Laug and Frieda M. Kunze. Distribution of mercury in rats following oral and intravenous administration of mercuric acetate and phenylmercuric acetate. *Proceedings of the Society for Experimental Biology and Medicine* 73:585-588. 1950.
37. Sachs, Hans Wolfgang and Antanas Dulskas. Kidney alkaline phosphatase in some types of poisoning. *Virchows Archiv fuer Pathologische Anatomie und Physiologie* 329:466-485. 1956. (Abstracted in *Chemical Abstracts* 51:5143h. 1957)
38. Schaechter, M. and Katherine A. Santomassino. Lysis of Escherichia coli by sulfhydryl-binding reagents. *Journal of Bacteriology* 84:318-325. 1962.
39. Shaw, William H. R. The inhibition of urease by various metal ions. *Journal of the American Chemical Society* 76:2160-2163. 1954.
40. Smalt, Sister Marie Augustine, Cornelius W. Kreke and Elton S. Cook. Inhibition of enzymes by phenylmercury compounds. *Journal of Biological Chemistry* 224:999-1004. 1957.
41. Smithies, O. Zone electrophoresis in starch gels and its application to studies on serum proteins. *Advances in Protein Chemistry* 14:65-113. 1959.



42. Stock, Alfred. Chemische Beiträge zur Kenntnis der Quecksilbervergiftung. Berichte der Deutschen Chemischen Gesellschaft 75: 1530-1535. 1942.
43. Surtshin, A. and Koichi Yagi. Distribution in renal cell fractions on sulfhydryl groups in rats on normal and sucrose diets and its relation to renal mercury distribution after mercuric chloride injection. American Journal of Physiology 192: 405-409. 1958.
44. Suzuki, Tsuguyoshi, Tomoyo Miyama, and Haruo Katsunuma. A comparative study on the distribution and excretion of several mercuric compounds in rat. Nisshin Igaku 48: 716-722. 1961. (Abstracted in Chemical Abstracts 57: 2536a. 1962)
45. Swensson, Ake, Kark David Lundgren and Olle Lindström. Distribution and excretion of mercury compounds after a single injection. A. M. A. Archives of Industrial Health 20: 432-443. 1959.
46. Tadatomo, Atsuo. Mercury poisoning studied with  $\text{Hg}^{203}(\text{NO}_2)_3$ . II. Distribution of mercury combined with proteins in the intracellular particulates. Okayama Igakkai Zasshi 74: 701-712. 1962. (Abstracted in Chemical Abstracts 59: 13255h. 1963)
47. Taylor, C.B. The effect of mercurial diuretics on adenosine-triphosphatase of rabbit kidney in vitro. Biochemical Pharmacology 12: 539-550. 1963.
48. Tucci, G., C. Cenacchi and A. Lodi. Serial enzyme variation and histological aspects in rats experimentally intoxicated. II. Action of mercuric chloride. Bologna Medica 5: 609-619. 1959. (Abstracted in Chemical Abstracts 56: 1717b. 1962)
49. Umbriet, W.W., R.H. Burris and J.F. Stauffer. Manometric techniques. Rev. ed. Minneapolis, Burgess Publ. Co., 1957. 338 p.
50. Wang, C.H. and D.E. Jones. Liquid scintillation counting of paper chromatograms. Biochemical and Biophysical Research Communications 1: 203-205. 1959.
51. Whitaker, John R. Determination of molecular weights of proteins by gel filtration on sephadex. Analytical Chemistry 35: 1950-1953. 1963.